

University of Mississippi

eGrove

Open-File Reports

Mississippi Mineral Resources Institute

1984

Petrology and Genesis of Clinoptilolite in the Tallhatta Formation of Lauderdale and Clarke Counties, Mississippi

W. R. Reynolds

Follow this and additional works at: https://egrove.olemiss.edu/mmri_ofr

Recommended Citation

Reynolds, W. R., "Petrology and Genesis of Clinoptilolite in the Tallhatta Formation of Lauderdale and Clarke Counties, Mississippi" (1984). *Open-File Reports*. 78.
https://egrove.olemiss.edu/mmri_ofr/78

This Report is brought to you for free and open access by the Mississippi Mineral Resources Institute at eGrove. It has been accepted for inclusion in Open-File Reports by an authorized administrator of eGrove. For more information, please contact egrove@olemiss.edu.

Open-File Report 84-9F

Petrology and Genesis of Clinoptilolite in the Tallahatta
Formation of Lauderdale and Clarke Counties, Mississippi

W. R. Reynolds

1984

The Mississippi Mineral Resources Institute
University, Mississippi 38677

PETROLOGY AND GENESIS OF
CLINOPTILOLITE IN THE
TALLAHATTA FORMATION OF LAUDERDALE
AND CLARKE COUNTIES, MISSISSIPPI

BY
WILLIAM R. REYNOLDS, Ph.D.
DEPARTMENT OF GEOLOGY AND
GEOLOGICAL ENGINEERING
THE UNIVERSITY OF MISSISSIPPI

Final Report for
MMRI Project 84+9F
(including MMRI Project
83-5F)
Submitted 21 December 1984
to James R. Woolsey, Ph.D.
Director, Mississippi Mineral
Resources Institute
(Bureau of Mines Grant# G 1134128)

INTRODUCTION

The purpose of MMRI Project 84-9F combined with the results obtained through a previous field investigation supported by MMRI project 83-5F was to research the mining potential of sedimentary zeolites contained in strata of the Tallahatta Formation that is exposed in the vicinity of Meridian, Mississippi. The zeolite mineral found in this area which is used in a variety of industrial applications is clinoptilolite. Principle applications of clinoptilolite to mention only a few include its use as an agricultural food supplement in sewerage and waste water treatment, as a radio active waste containment, as a heavy metal extractant, as a paint extender, and as a whitener.

Sedimentary zeolites, by definition, are microcrystalline hydrated alumina silicates of alkali and alkaline earth cations. They are the product of diagenetic alterations or authigenic deposition in both open or closed marine and alkaline or ground-water sedimentary systems. Structurally zeolites are tectosilicates constructed of three dimensional totally polymerized alumina and silica tetrahedra. Such structural arrangement gives rise to numerous types of interstructural channel and cage configurations of varying sizes. Cations incorporated within these configurations through mainly hydroryl bonding are most commonly sodium, potassium, magnesium, calcium, and rarely strontium and barium. Clinoptilolite, one of the more common sedimentary zeolites, is a monoclinic silica-rich variety with potassium, sodium, and rarely calcium as dominant interchannel corporate cations.

Clinoptilolite occurring in Gulf Coastal Plain strata of southeastern U.S. was first found in Lower Eocene strata of Alabama (Reynolds, 1966) and Middle Eocene strata of Mississippi (Wermond and Moiola, 1966). Later investigation in Alabama revealed clinoptilolite to be most abundant in the Middle Eocene Tallahatta Formation but also occurring in lesser quantities in the Lower Eocene Nanafalie Formation and the Paleocene Porters Creek Formation (Reynolds, 1970).

Clinoptilolite has also been found in the middle phase of the Porters Formation of Mississippi (Raybon, 1982) and in the lower mud facies of the Porters Creek Formation of Tennessee (Sims, 1972). It was not until 1981 that clinoptilolite was discovered in strata of the Tallahatta Formation that is exposed in the vicinity of Meridian Mississippi (Reynolds, 1983).

Preliminary investigation of the Tallahatta Formation in the vicinity of Meridian, Mississippi supported by MMRI Project 83-5F involved lithologic description and measurement, sampling, and mineral determination of surface exposures of Tallahatta strata. This preliminary investigation provided substantial data by which an initial facies analysis was made, and it also revealed varying concentrations of clinoptilolite throughout the Tallahatta Formation.

The preliminary and field investigation showed that typically, within the study area (Figure 1), the Tallahatta Formation consists of three lithologic or sedimentation units (Figure 2). At the base, immediately above an unconformity between the Meridian and the Tallahatta Formations is, on the average, 15 feet (4.6 m) of transitional bioturbated glauconitic wackes and muds usually capped by two to eight feet of zeolitic clay (unit A). Lenticular to wavy bedding is most notable in both the mud and wacke strata of this unit and the surface between the lower unit and the upward succeeding unit is disconformable. The overlying unit (unit B) is what typically has been described as the Basic Shale even though it is not a shale but rather, for the most part, a massive soft to hard opal-Ct claystone (Lundegard and Samuals, 1982). This unit is, on the average, 45 feet (14 m) thick and contains thin lenses of zeolitic clay, however the massive claystone is often interrupted by upwards to 10 feet (3m) beds of mud and zeolitic clay. The uppermost unit (unit C) begins with either a mud facies or a glauconitic bioturbate opaline cemented wacke, and the average thickness of the entire upper unit is 44 feet (13 m). This unit consists also

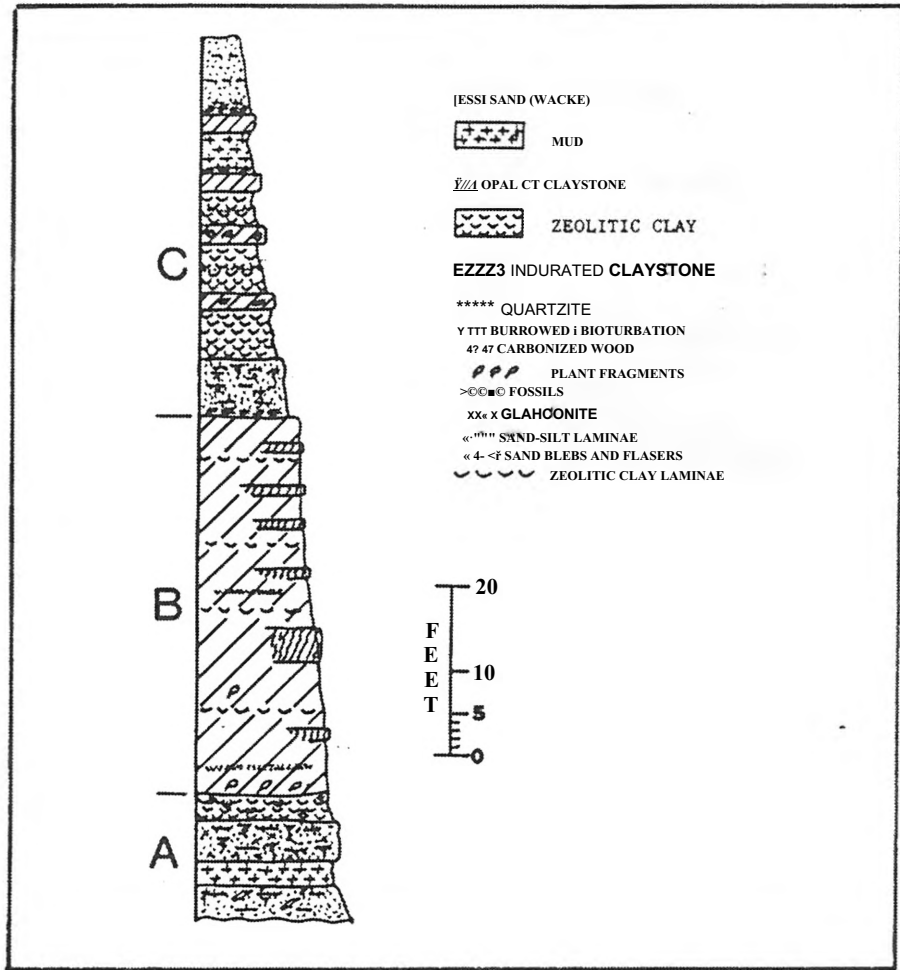


Figure 2a: Average lithologic composition of the Tallahatta Formation in the vicinity of Meridian, Mississippi.



Figure 2b: Exposure of Tallahatta outcrop seven miles south of Meridian on Valley Road. Units A, B and part of C are exposed overlying the Meridian Sand (M-lower right corner).

of alternating thin to massive, hard to soft opal-Ct claystone and zeolitic clay beds plus muds and wackes. Furthermore, it is usually capped by a thin often bioturbated arenaceous sand or sandstone.

The three lithologic units of the Tallahatta Formation, as described above, may vary in thickness and even arrangement but are fairly constant in content and can be traced throughout the study area (Roquemore, 1984).

One of the principal tasks designated as MMRI Project 84-9F is the description and mineral content analysis of eight cores taken with total penetration of Tallahatta strata at selected locations along the Tallahatta outcrop in Lauderdale and Clarke Counties, Mississippi. Drill site location (Figure 1) was based on outcrop exposure information. Data obtained from core analysis was coupled with exposure data in the effort to reconstruct the lithofacies of various depositional environments and subenvironments. Ultimately, when combined with mineral analysis, this would enable the derivation of a genetic model for clinoptilolite deposition.

Core description and measurement (Appendix A) added information on lithologies and lithologic sequence within the Tallahatta Formation compatible with data obtained from outcrop exposure. Study of the cores provided the extra stratigraphic control for lithofacies reconstruction. At each drill site approximately 150 feet of core was taken in 10 foot lengths starting in the Winona Sand, totally penetrating the Tallahatta and ending in the top of the Meridian Sand. Each 10 foot length was measured and described as it was pulled (Figure 3), then boxed and shipped to the University of Mississippi for further analysis. Elevation control for each measured section was maintained during field work by levelling from elevation monuments to the base of each exposed section to be measured and described. The position of each exposure section was also plotted on 7 1/2 minute quadrangles which allowed the qualification of subsequent adjustment of each basal elevation "brought" from various bench



Figure 3a: Describing core during coring operation at MCH 6.

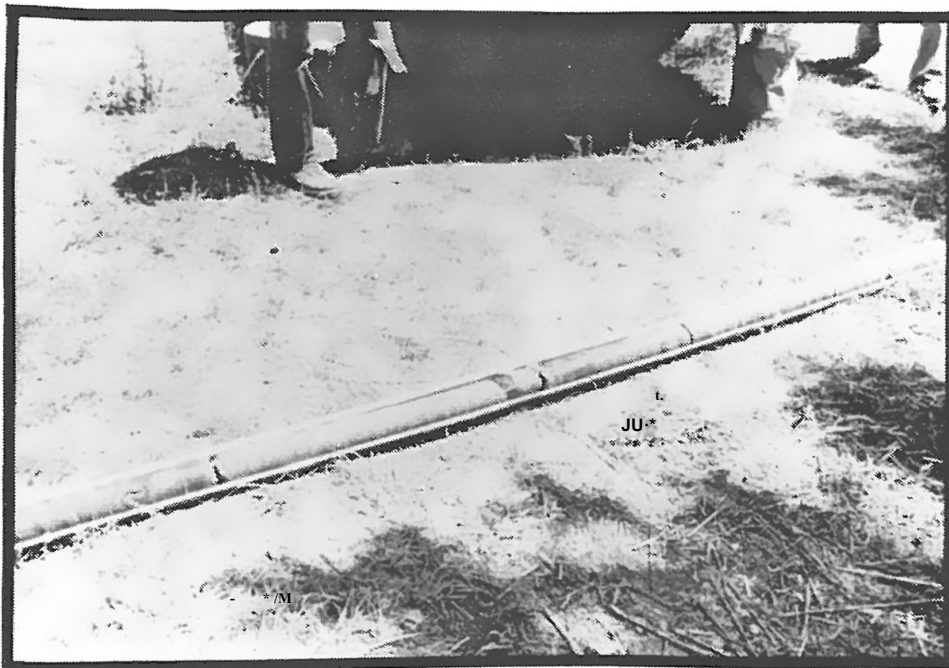


Figure 3b: Ten feet of fresh core ready to be measured and described at core site MCH 6.

marks. This also allowed short sections (Figure 4) which represented scattered integral portions of a singular section to be brought together as a composite section. Each drill site was positioned by triangulation using a compass and the field vehicle tripometer. Drill site elevations were determined by using a pocket altimeter along with 7 1/2 minute, quadrangles for refinement and adjustment.

STRUCTURE

An initial stratigraphic section was constructed by "hanging" core and exposure logs from a common datum of 500 feet above mean sea level along two cross-section traverses. One cross-section, AA, ¹ is essentially along strike, and the other, BB, is down dip (Figure 5). The tectonic elements in the study area turned out to be mainly a series of normal down-to-the-South faults (Figure 6) the movement of which involved the entire Tallahatta section with throws of 15 to 60 feet. The faulting events are not thought to be syndepositional but rather thought to have occurred post Tallahatta, deposition. Only one fold feature, the Lost Gap Monocline, was ascertained (figures 4 and 6) as dips measured east to west along 120 from Meridian went from 0° to 15° and finally increased to 34° (Figure 4). More fold features probably exist in the study area but were not evident. Two of the faults can be seen visually in the field. One, between sections 51A and 49 is quite obvious as these sections are only 200 feet apart and the Meridian Sand in section 51A is juxtaposed to unit B claystone in section 49, which is a throw of about 45 feet. The second fault can be seen as a fault-line through unit B at the Basic City type section; a cut along the Illinois Central Gulf railroad one-half mile north of Basic City.

STRATIGRAPHY

Two palinspastic cross sections were constructed from the initial structural cross sections for the purpose of facies reconstruction (Figures 7 and 8).

These cross sections essentially summarize the stratigraphy of the study area.

Even though the Meridian Sand was not considered a part of the operational unit of this study it has a few notable lithofacie characteristics pertinent to this study. The Meridian Sand is no longer the lower member of the Tallahatta but now is a separate formal unit (Dockery, 1981). It is quite evident that there is a distinct period of nondeposition of marine sediments between the arenaceous sands of the Meridian and the transitional muds and wackes of what is now the Lower Tallahatta. Throughout the study area the Meridian Sand for the most part is a clean medium-to fine-grained quartz arenite ranging from 100 feet (30 m) to 3 feet (0.9 m) in thickness. Weathered Meridian is either white or orange whereas fresh material is usually gray or brown where it contains organic material and is locally lignitic. The upper part of the Meridian is marked by a zone of intense burrowing with the unique cork-screw (*Gyrolithes*) and boxwork (*ophiomorpha*) burrows that are more resistant to erosion than the enclosing sand, and weather in relief.

Channel samples of the Meridian Sand were taken from exposures and cores for the purpose of grain-size distribution analysis. Probability plots indicate a polymodal grain-size distribution with an average phi mean of 1.75 and a strong predominance of the saltation population over a traction population (Appendix B). Most of the probability plots indicate a foreshore to nearshore intertidal beach as a general environment for the deposition of the Meridian Sand. However some plots along with cross-stratification data indicate very localized environments such as esturine, delta-plain fluvial and backshore subarea i beach (Visher, 1969; Roquemore, 1984 and Toulmin, 1966).

The lithologies of the Tallahatta Formation can be segregated into three lithofacies groups, and as previously discussed designated as units basically because each group is a distinct sedimentation unit. Unit A, the lowermost unit, consists of transitional wackes and muds and at least one distinct

zeolitic clay bed. Unit B, the middle unit, consists of massive to thin bedded opal-Ct claystone. Occasionally, this unit will contain beds of zeolitized mud and zeolitic clay. Furthermore, the more massive claystone beds will often contain laminae (1/2" to 3") of zeolitic-opaline clay. The uppermost unit, unit C, consists of wackes, occasionally arenites, muds, silts and often thick beds of zeolitic clay.

Unit A (Figures 7 and 8) is thickest due South of Meridian (Section E45, Valley Road) but thins immediately to the West (E51, Basic City Type Section) then thickens to 35 (11 m) feet further west, and (MCH5, MCH7, C55) north-west, and thins again to the extreme north-west (MCH1). East of the Valley Road Section unit A thins to an average 10 feet (3m). Downdip this unit thins to a thickness of less than 10 feet (3m). Extensive bioturbation is a very characteristic aspect of this unit often halmarked by burrow mottling (Figure 9). Both vertical and horizontal, simple to complex burrows are plentiful in the wackes and muds of this unit especially if these beds are at the top (Figure 9). The common trace fossils include Ophiomorpha, Thalassinoides sp. and Teeichichnus sp. of the Cruziana association (Chamberline, 1978). Zeolitic clay beds in this unit are also heavily burrowed with individual burrows often preserved as opaline casts (Figure 9). Also notable within these beds are small segregated concentrations of sand usually circular or flaser-like in appearance (Figure 9). The wackes and muds are always glauconitic and micaceous. Channel samples were also taken in the lower unit A Sands for grain-size distribution analysis. Probability plots based on these analyses using dry sieve data indicate a mixture of depositional conditions, mainly deposition from suspension which is most common along barred coasts (Visher, 1969). Unit A is for the most part nonfossiliferous however occasionally a shell layer can be observed in the agillaceous sand near the top of the unit. Most common in this unit are plant fragments including large pieces of carbonized wood plus lenticular and wavy

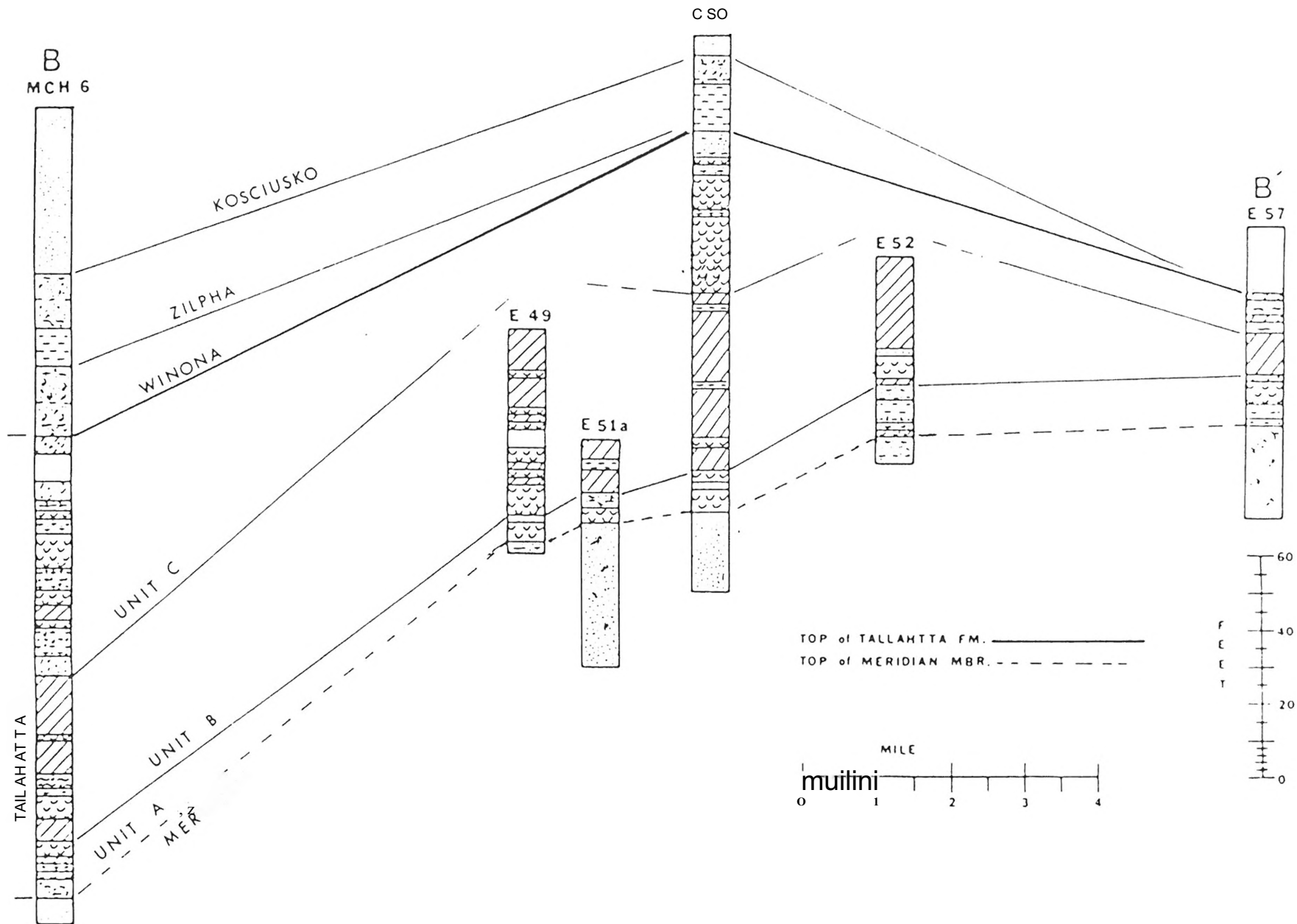
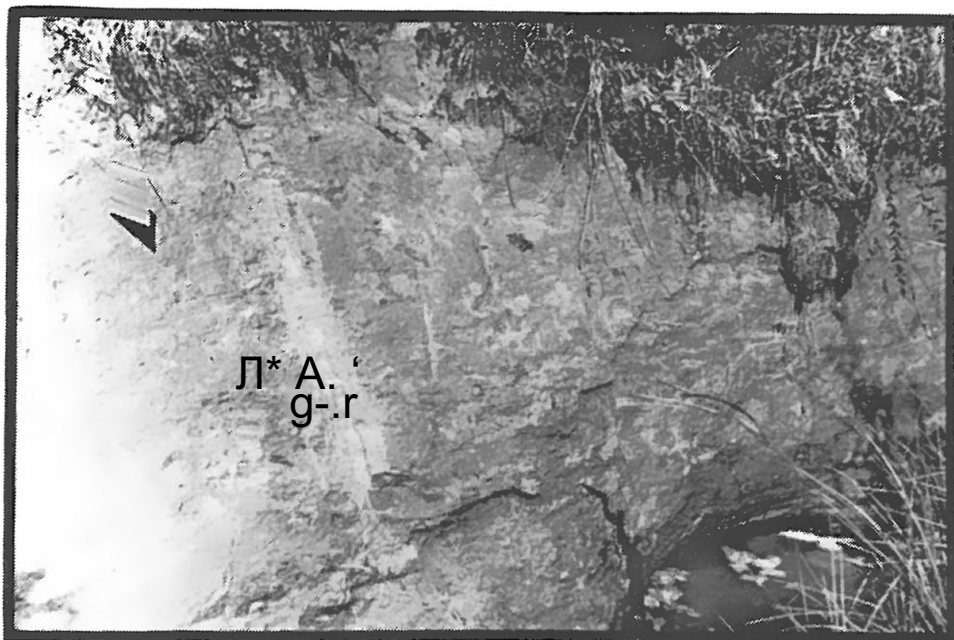


Figure 8: Stratigraphic section BB' down dip of the Tallahatta Formation showing facies units A, B and C plus the underlying upper Meridian Sand and the overlying Winona and Zilpha Formations. Refer to Figure 7 for lithologic key .



Figure 9 : Unit A exposed in Valley
Road section, section 45.
Left: Wacke with opaline
burrow casts and burrows of
Ophiomorpha and Thalassinoid
Lower: Burrow mottling in
unit C mud.



bedding (Figure 10).

The principle lithology of unit B is a siliceous claystone composed of microcrystalline opal-Ct (Carver, 1980). The opaline strata appear to be massive but upon close examination they are in part laminar. Some of the strata however are thin bedded and have the appearance of a brick pile. Furthermore, some of the beds of unit B are soft and could be referred to as an opaline clay while others are highly indurated and form ledges. A few of the indurated ledges are highly fossiliferous with a dominance of the bivalves Nucula, Nuculana, and Venericardia. Also notable in this unit, especially in core sections, are numerous thin layers (1^m to 6^m) of extremely brittle, sharp opaline chert.

Occasionally, wacke, mud and zeolitic clay strata are found in unit B. If any of these strata were found lithified the cement was either opal-Ct or clinoptilolite or both.

Throughout the study area unit B varies little in thickness ranging from 30 feet (9m) to 45 feet (14m). It is at its thinnest in the Valley Road Section (E45) where it is 30 feet but immediately thickens to the East and the West.

The clays and claystones of unit B are olive-green to gray-green when fresh, but will bleach to a buff-gray or white when exposed. These clays and claystones have a distinct conchoidal to subconchoidal fracture, however the beds of pure opal-Ct are laminar the opaline material is extremely brittle and sharp. Surface exposures of this unit are quite distinctive, often forming steep cliff faces, vertical walls and pronounced ledges in road and stream cuts.

Primary structures found in unit B claystone include mainly small-scale cross-lamination, hummocky cross-lamination and stratification, lenticular and wavy bedding. Flaser bedding is often found in the wackes and muds along with small-scale cross-stratification. Lebensspuren are common throughout the unit, mainly in the wackes, and consists of unidentifiable horizontal tubes, and the ichnofossil Chondrites sp. (Chamberline, 1978) was identified in several cores.

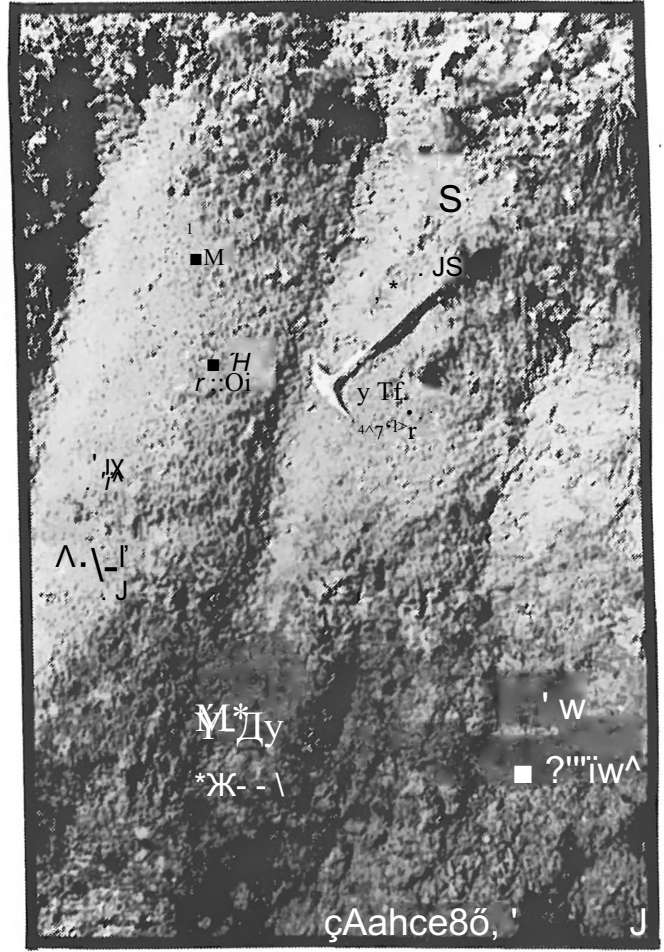
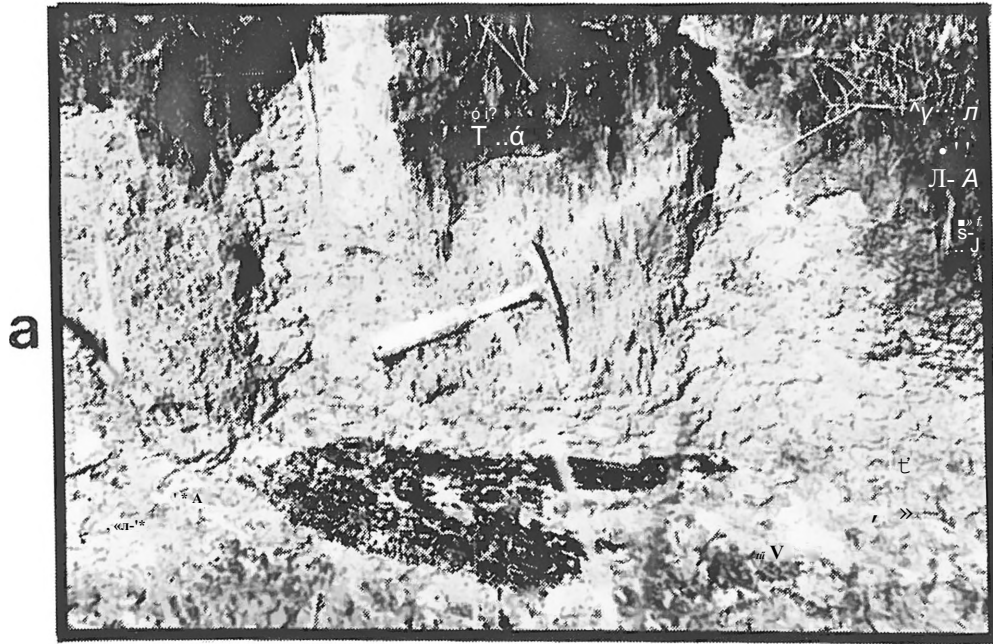


Figure 10: Unit A exposures along Savoy Road Section 50:

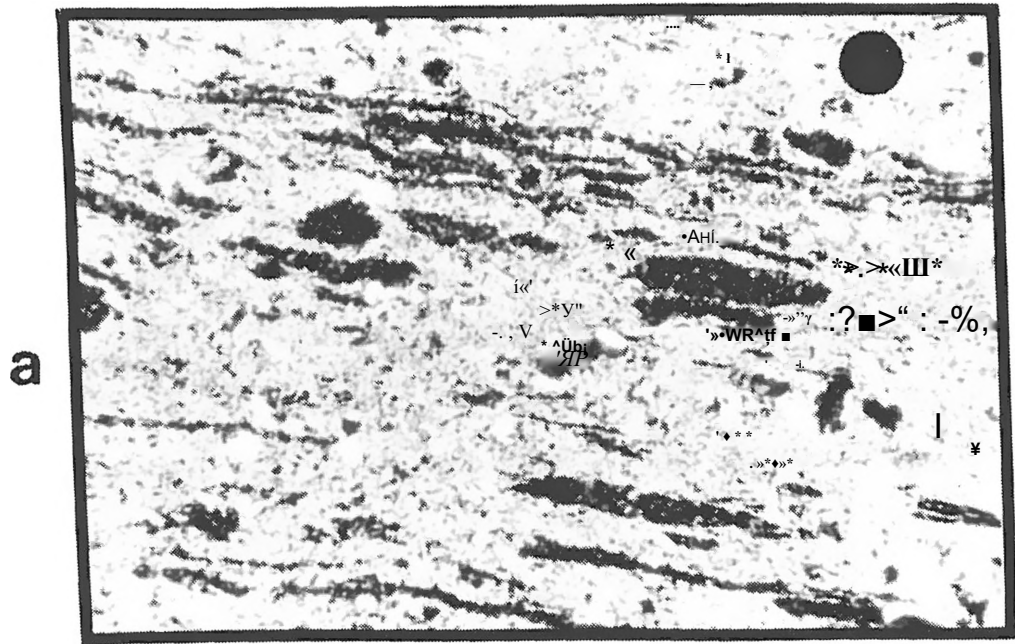
- a) Carbonized wood in wacke
- b) Wavy bedding
- c) Storm surge bedding

A secondary structure, quite unique and most diagnostic in the more massive siliceous claystones, the zeolitic clays and some of the muds of unit B is that produced by sheet dewatering (Collinson and Thompson, 1982) (Figure 11).

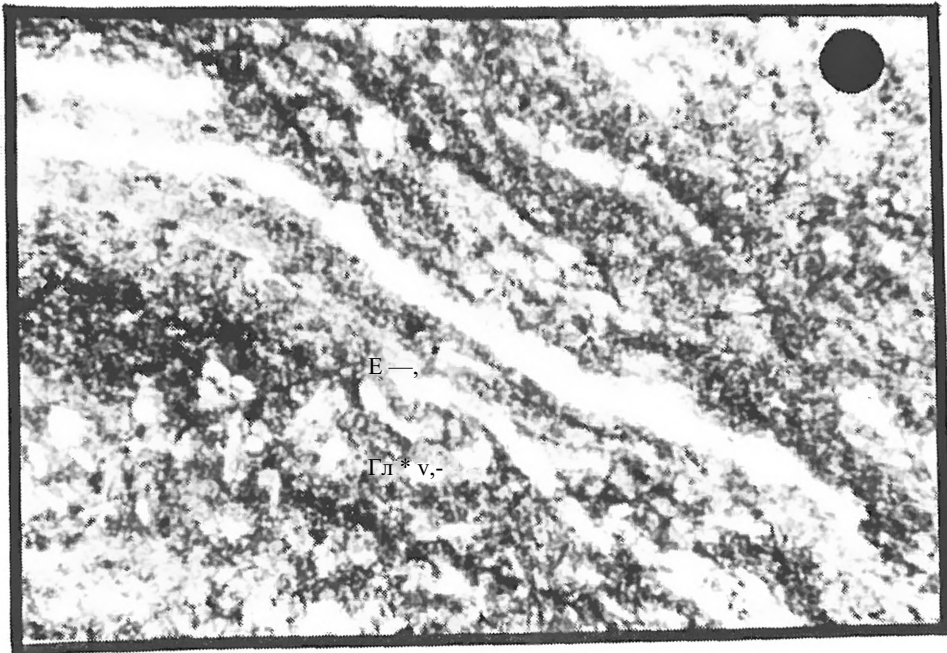
The upper unit, unit C, is similar in lithology to unit A. However, it is thicker than unit A being at its 20 feet (6m) thinnest in the northwest sector of the study area (MCHI) and thickest, 80 feet (24m), in the south west portion. This unit is not exactly a mirror image of unit A even though it contains similar type muds, wackes and zeolitic clays. There are some clay beds in unit C that are not zeolitic but are rather opaline smectites. On the other hand the zeolitic clay beds are thicker and more abundant in this unit than in unit A. Also, in unit C are occasional aberrant opaline claystone beds. Beds of silt are also found in unit C but not in unit A. Like unit A the wackes and muds of unit C are bioturbated and contain plant debris, have hummocky stratification, and display lenticular and wavy bedding. These features, especially bioturbation, are not observable in outcrop exposures but are most diagnostic in the cored sections (Figure 12). One unique but not a common feature seen in the wackes of unit C is that of storm surge bedding; highly contorted and disrupted bedding (Figure 10). Storm surge sands in the road cuts of 120 (Section C55) underly a massive 12 foot bed of zeolitic clay.

The fine to coarse-grained, glauconitic, densely fossiliferous, calcareous and ferruginous sand of the Winona Formation overlie unit C of the Tallahatta Formation. Exception to this is where Winona, Zilpha and to some extent Tallahatta unit C strata have been removed and replaced by nascent Neshoba delta plain fluvial and delta front sands. These sands are generally coarse to medium-grained, quartzose and stained red. The Neshoba Channel Sands can best be seen in the 120 road cuts near the Chunky interchange, the valley road exposures (E45) and in core MCH 8.

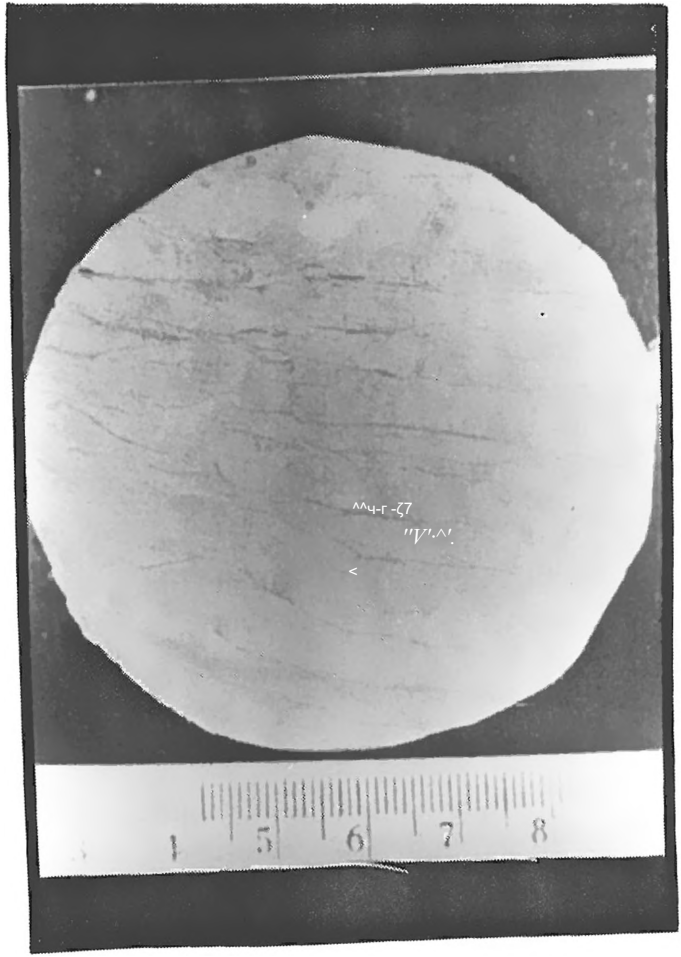
The contact between the Winona Formation and the Tallahatta unit C is



a



b



c

Figure 11: Sheet dewatering features:

- a) Petrographic thin section under plane polarized light of unit C clay. Dot scale is 25mμ.
- b) Same as a except from unit B claystone. Dot scale is 25mμ.
- c) Cross section of core from unit B claystone.

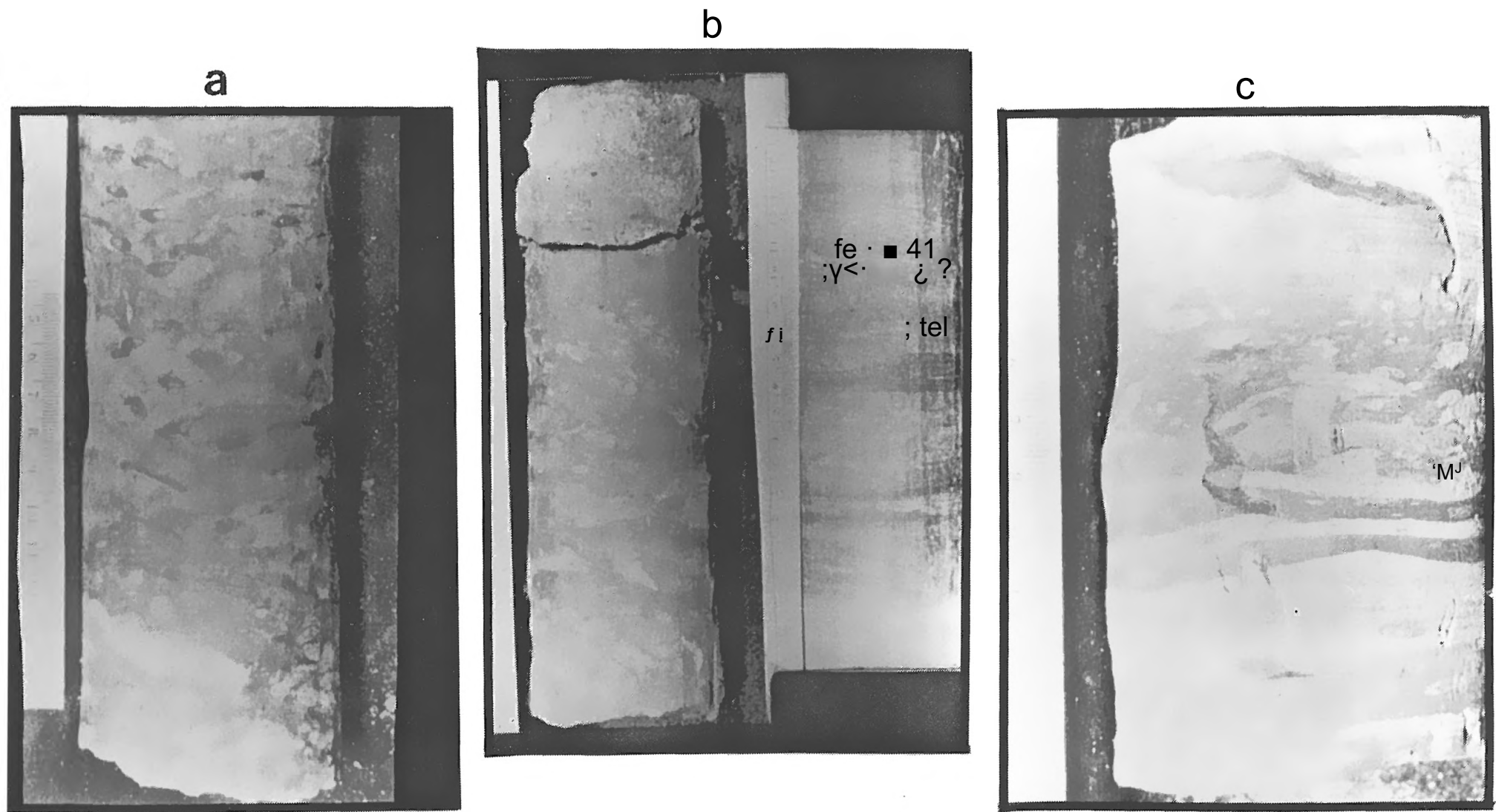


Figure 12: Examples of bioturbation seen in cores from units B and C.

everywhere conformable everywhere and is marked by a gradual change from clay or mud into glauconitic fossiliferous sand.

The Winona Formation in the study area is conformably overlain by the dark brown to black carbonaceous clays and silts of the Zilpha Formation which is a persistent unit throughout the study area. Often however, the Zilpha clays are lateral to the upper portion of the Winona Sand. These clays are massive, have a conchoidal to blocky fracture, contain mica and glauconite streaks, and down-dip are fossiliferous (MCH 7). These bentonitic clays of the Zilpha Formation which also contain minor amounts of clinoptilolite are in turn disconformably overlain by the delta front and delta plain sands of the Kosciusko Formation.

Mineralogy

Previous field investigation involved in part the sampling of all Tallahatta clay beds exposed in the study area for determination of mineral content. Mud strata and selected wackes and opaline claystone beds and selected Zilpha clays were also sampled and analysed. Samples were then analysed by x-ray diffraction and scanning electron microscopy (SEM) for mineral content, mineral quality, and an estimate of mineral quantity.

The bulk composition of exposed Tallahatta clay, mud, wacke and claystone strata was found to consist of, in varying proportion, the zeolite mineral clinoptilolite, smectite (predominantly montmorillonite), coarse-to fine-grained muscovite, some illite, opal-Ct, and coarse-to fine-grained quartz (Figures 13, 14, and 15).

Material sampled from the cores also analysed in the same manner had a bulk composition identical to that of exposure material (Appendix B). Minor amounts of potassium feldspar and gypsum were also identified in some of the core samples.

X-ray identification of clinoptilolite was based on the presence of the

m: MUSCOVITE
 c: CLINOPTILOLITE
 s: MONTMORILLONITE
 q: QUARTZ
 ct: OPAL CT

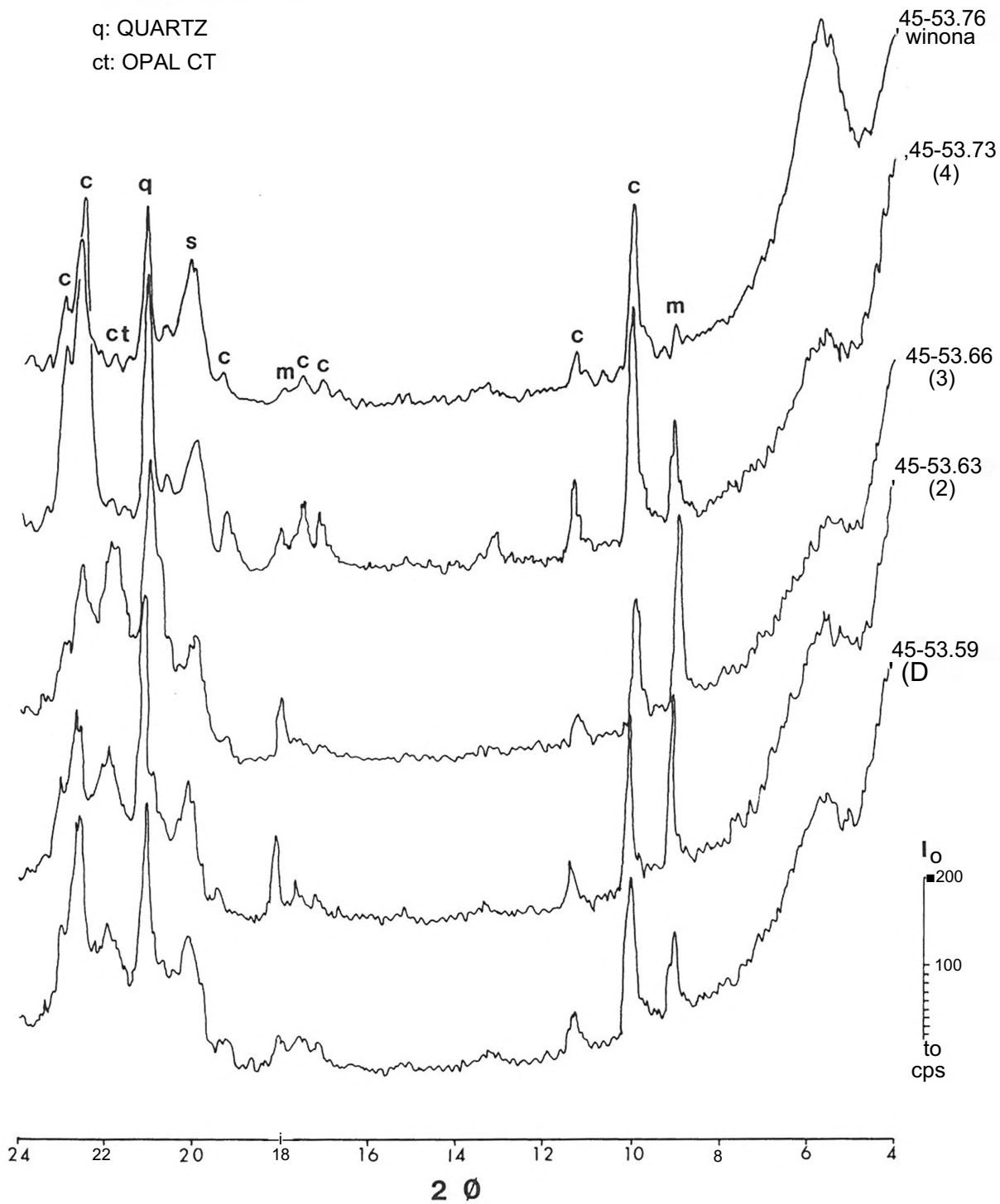


Figure 13: X-ray diffraction patterns of material sampled from clay beds exposed in section 45 (Valley Road).

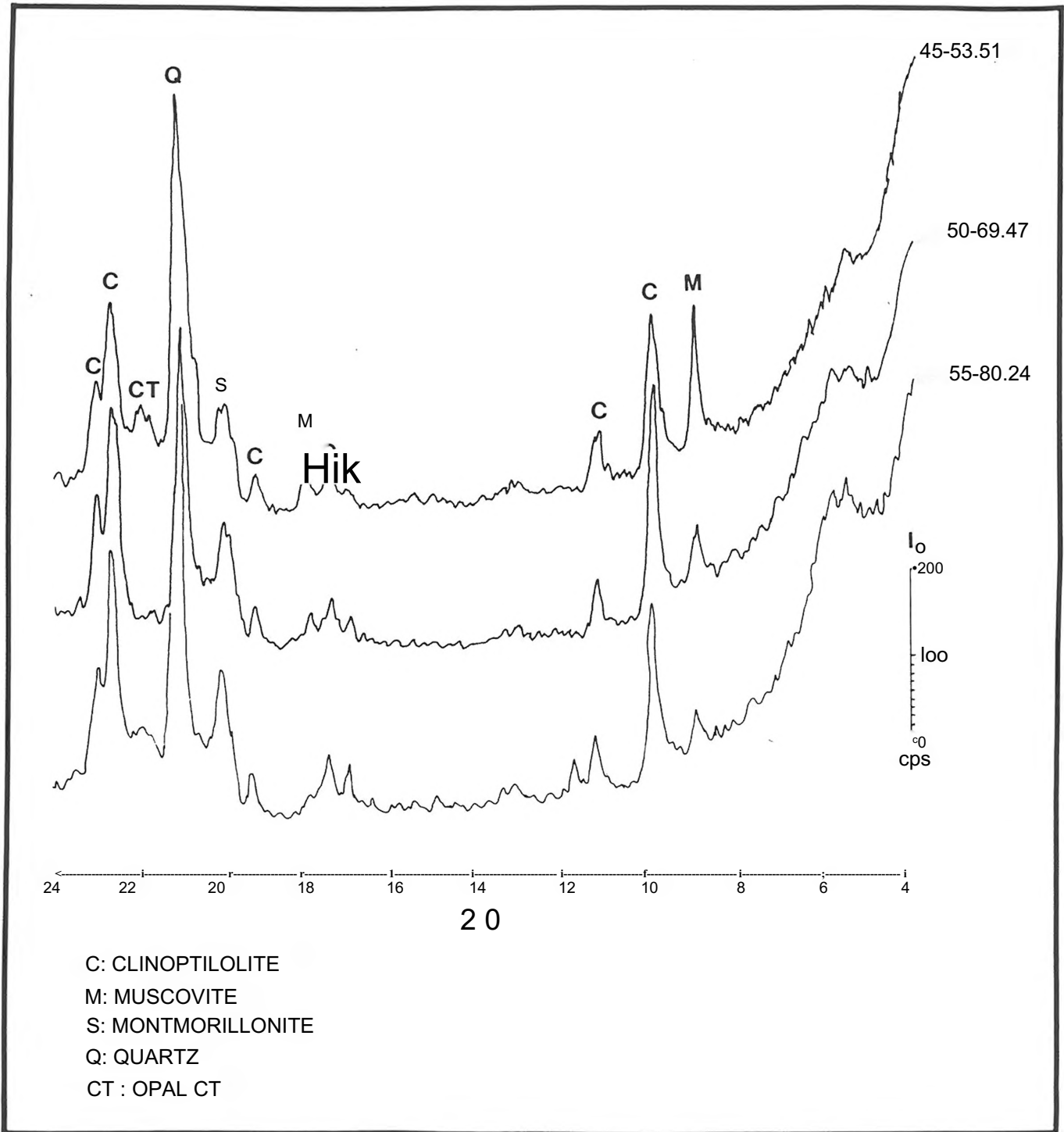


Figure 14: X-ray diffraction patterns of material sampled from Zilpha clay exposed in sections 45 (Valley Road), 50 (Savoy Road), and 55 (120).

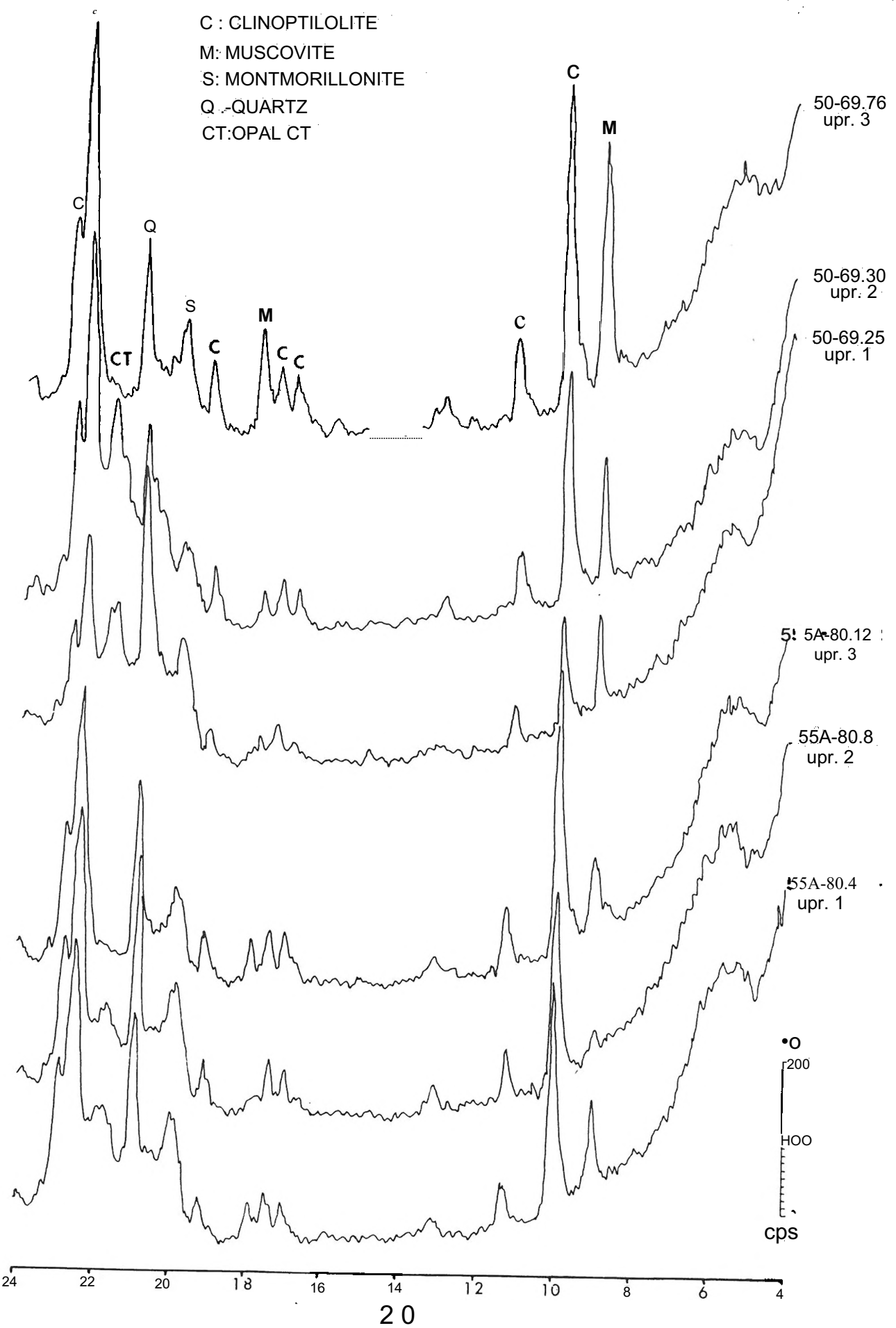


Figure 15: X-ray diffraction patterns of material sampled from selected clay beds i 50 (Savoy Road) and 55 (120).

020, 004, and 042 reflections at 8.92 \AA , 3.96 \AA and 3.89 \AA respectively.

Diffraction patterns of smectite minerals are placed into two categories: 1) basal 001 reflections from 12.4 \AA to 16 \AA , and 2) hk reflections principally from 4.5 \AA to 4.62 \AA , 2.43 \AA to 2.6 \AA , 1.69 \AA to 1.72 \AA , and 1.49 \AA to 1.54 \AA . Basal 001 reflections are often unpredictable to use in Smectite mineral identification due to the varying influence of interlayer water, cations in exchange positions, and interlayer organic complexes. Often the 001 reflections are not evident when smectite is present because of layer disruption and disorientation due to large organic molecules being "stuffed" into the interlayer positions. On the other hand, hk reflections indicate smectite form and therefore, species. Montmorillonite was found to be the dominant smectite identified by diffraction traces of hk reflections at 4.5 \AA and 1.5 \AA . There was also indication of minor amounts of montronite and mixed layered illite-montmorillonite.

Jones and Sinit (1971) have classified opaline silica into three structural groups designated as opal-A, opal-Ct, and opal-C. In an x-ray diffraction study of mixtures of opaline silica phases Tada and Iijima (1983) characterized and identified these structural groups using the (101) x-ray diffraction reflection. Diffraction patterns of siliceous clays from the Tallahatta Formation often had reflections from 4.06 \AA to 4.1 \AA indicating opal-Ct which is consistent with Tada and Iijima's results.

Muscovite was identified by its 002 and 004 reflections while quartz was identified by its 110 reflection.

Relative abundance of each of the dominant minerals per described exposure and cored section is shown as relative concentration in Zeta graphs coupled with lithology logs for each section - (Appendix C). Zeta graphs were constructed by assuming the sum of the selected x-ray diffraction peak intensities of the dominant minerals present in each sample would equal unity. Ratios of peak

height were derived for each mineral in a sample and a standard, and were summed for each sampled section. The mean and standard deviation were computed for each ratio sum. The peak ratios were then standardized using a Zeta transform which resulted in new values where each ratio of peak intensity has a zero mean and is expressed in units of standard deviation from the mean. This effectively allows a comparison of the relative mineral concentrations within a sample and between samples.

By examining the Zeta charts (bulk mineralogy) for each exposure and core logged section in Appendix C one can see some variance of clinoptilolite content within each section but less variance from section to section. The dominant occurrence of clinoptilolite in each section is in the upper clay bed of unit A and the one to three prominent clay beds of unit C. The variability of clinoptilolite content is shown more graphically in (Figure 16) which was constructed by determining the probability of occurrence of average relative mineral concentration between individual minerals within a stratigraphic unit (Figure 17) and plotting these values against stratigraphic position. This procedure subsequently enabled the construction of stratigraphic cross sections which are identical to Figures 7 and 8 except only the clinoptilolite-rich clay beds are correlated (Figures 18 and 19).

Clinoptilolite was detected in 88 percent of the samples examined by x-ray diffraction. Half of the samples taken from unit A have relative concentrations of clinoptilolite that are above average. Furthermore, clinoptilolite appears to be more concentrated in the muds and wackes than in the clays. Clinoptilolite occurs in 43 percent of the samples taken from unit B despite the fact that unit B composition is predominantly opal-Ct. In unit B above average relative concentration of clinoptilolite is found to correspond to above average relative concentration opal-Ct 26 percent of the time. This is probably due to the occurrence of extremely fine laminae of clinoptilolite clay alternating with

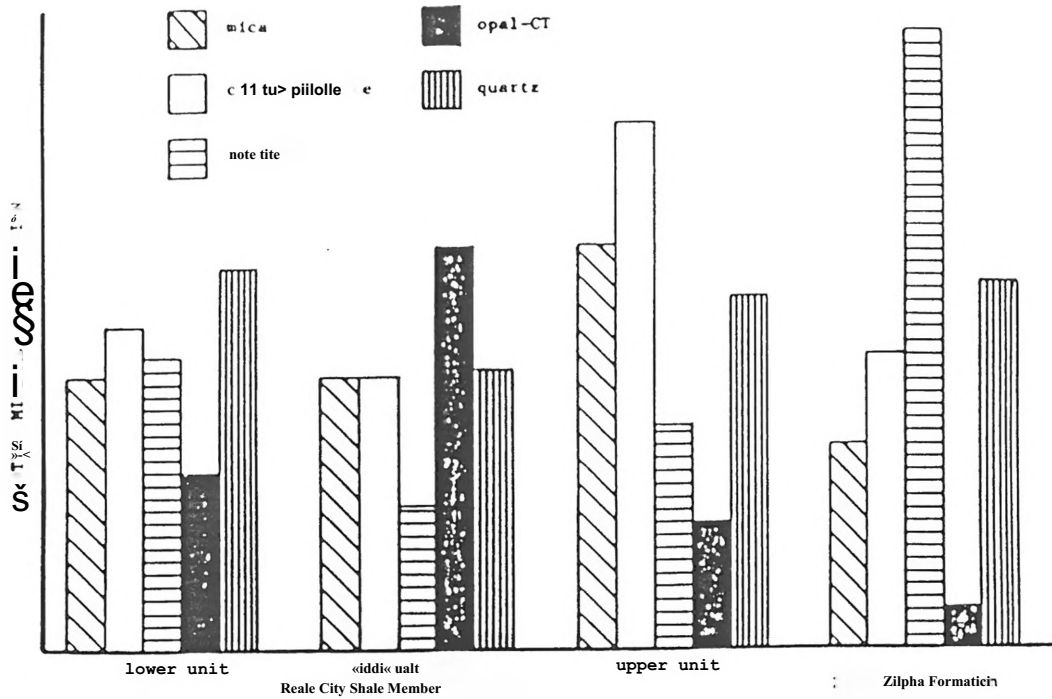


Figure 16: Relative mineral concentration of clays in units A, B and C of the Tallahatta Formation and the Zilpha Formation.

MICA CLINOPTILOLITE SMECTITE OPAL-CT QUARTZ

MICA	50	67	24	46
CLINOPTILOLITE		47	24	39
SMECTITE			28	29
OPAL-CT				18
QUARTZ				

Figure 17: Association probability of above average relative mineral concentration as determined by x-ray diffraction pattern analysis.

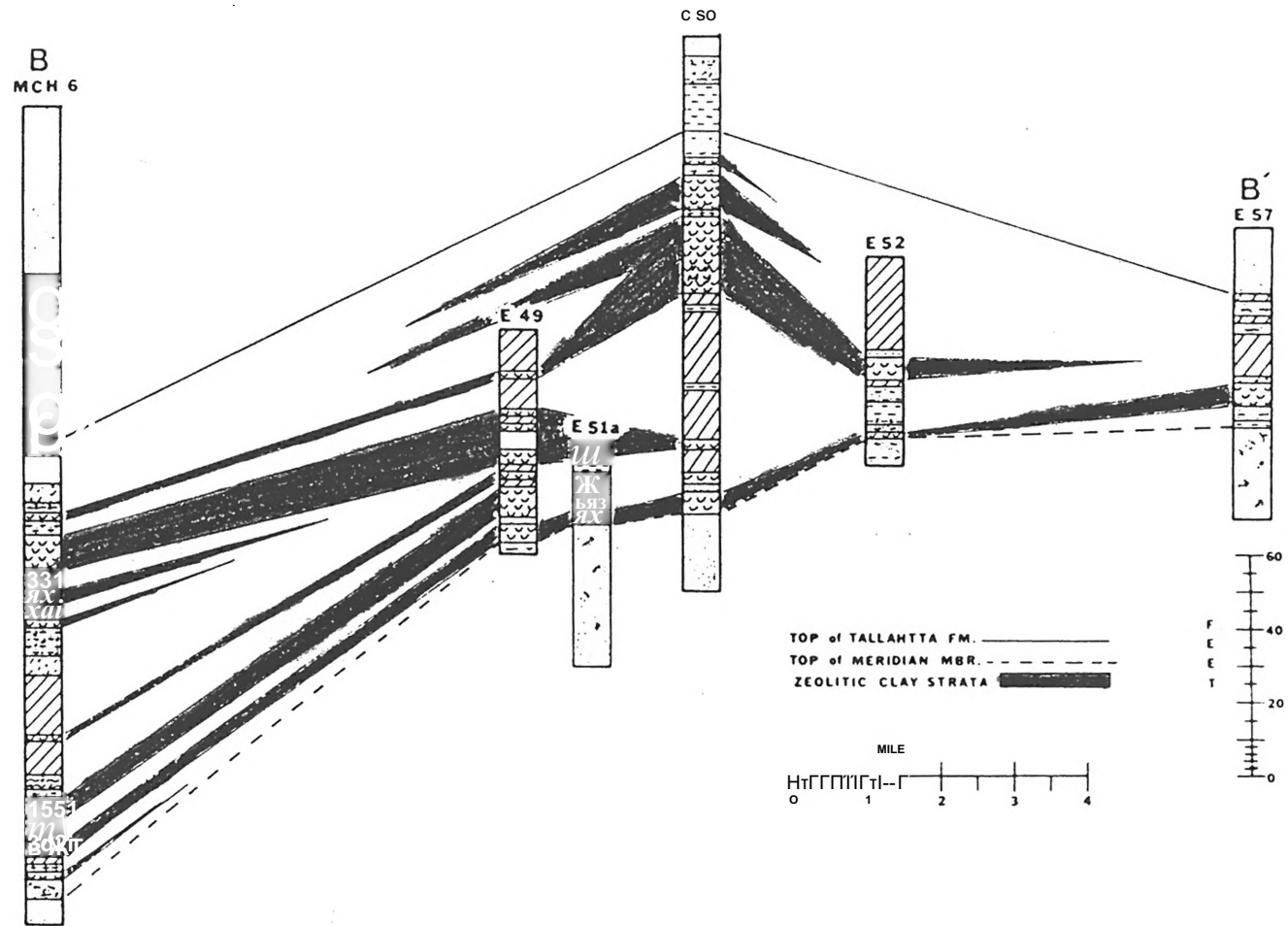


Figure 19: Concentration of clinoptililite-rich clay strata down dip: cross section BB' (see figure 7 for lithology key).

some regularity throughout unit B with thicker laminae and beds of opal-Ct. For a more complete and refined discussion of clinoptilolite occurrence refer to Roquemore, 1984.

SEM analysis of selected sample material known to contain an above average relative concentration of clinoptilolite revealed this mineral to be cryptocrystalline with well formed monoclinic crystals (Figures 20 and 21) enclosed in what appears to be a pyroclastic matrix (Figure 20a).

Upon closer examination it can be seen that the matrix is composed of authigenic montmorillonite (Figures 20b and 21a). Most often the submicroscopic crystals of clinoptilolite are nestled in clusters within vugs or pores which punctuate the matrix (Figure 21a and c). Clinoptilolite crystals and crystal clusters appear to grow either from the vug or pore wall or they seem to originate from the central portion of the vug or pore. These occurrences offer three alternative explanations concerning clinoptilolite formation: 1) clinoptilolite forms from a material that made up the vug itself such as a siliceous microfossil or volcanic glass, 2) the initial material was dissolved creating the pore space and clinoptilolite grew from a material introduced later, 3) or clinoptilolite precipitated from connate pore fluid.

The form of clinoptilolite crystals in the Mississippi materials is more like a potassium feldspar rather than henlandite (Reynolds, 1983). Often one can observe twinning of clinoptilolite crystals of either the carlsbed or manebach type. Furthermore, it appears that soon after a crystal has formed it begins to deteriorate (Figure 21a, c and d). It has recently been suggested that clinoptilolite deposits in humid areas such as the Coastal Plain of Southeastern United States are comprised of crystals formed in fluid filled pores which may or may not be relict bubble structures. Crystal growth proceeds to a point when there is a change in pore fluid chemistry at which time the fluids attack the crystals producing crystal degradation (Reynolds, 1983).

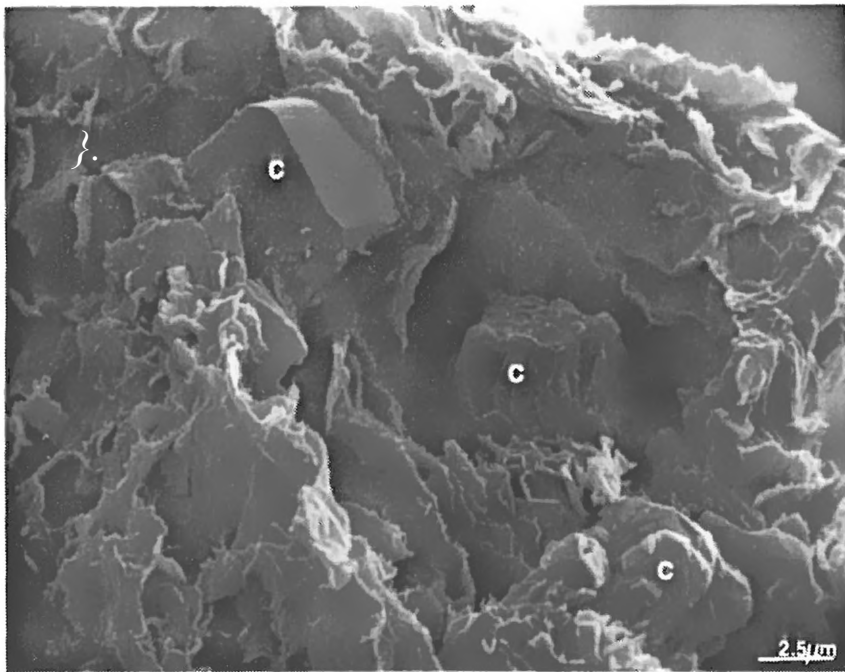
Figure 20

- a. Section 55A (Interstate 20)
Sample 80.10
320x Magnification
Low Magnification SEM surface
scan of material from the
upper zeolitic clay bed.
Surface appears to have a
relic pyroclastic texture.

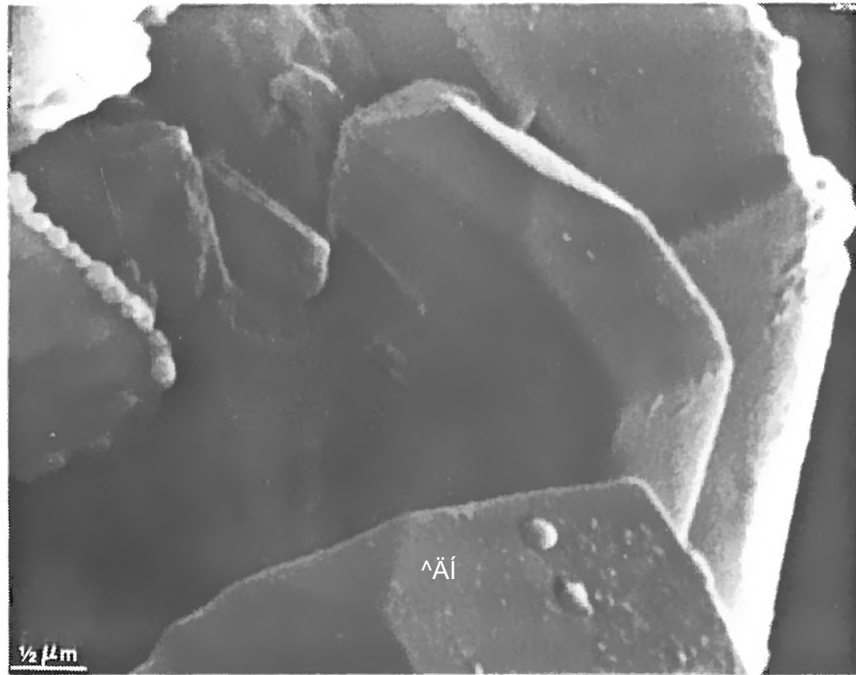
- b. Section 55A (Interstate 20)
Sample 80.10
7780x Magnification
High magnification SEM surface
scan of authigenic
montmorillonite.

- c. Section 45 (Valley Road)
Sample 53.33
5238x Magnification
SEM identification of a well
formed clinoptilolite crystal
with no indication of crystal
deterioration.

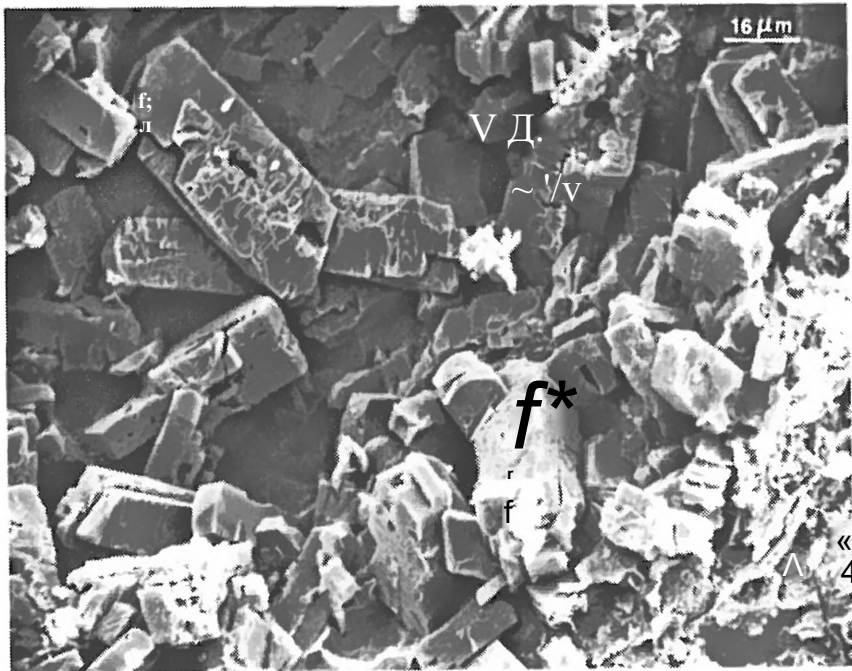
- d. Section 55A (Interstate 20)
Sample 80.10
21400x Magnification
SEM identification of a clinoptilolite
crystal showing well formed 010,
110, 101, and 100 faces.



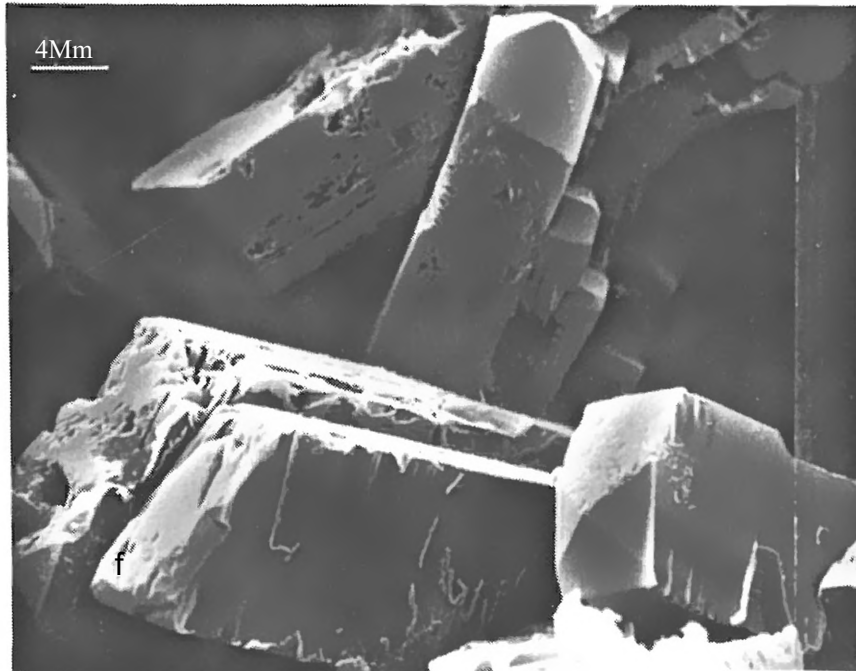
a



b



c



d

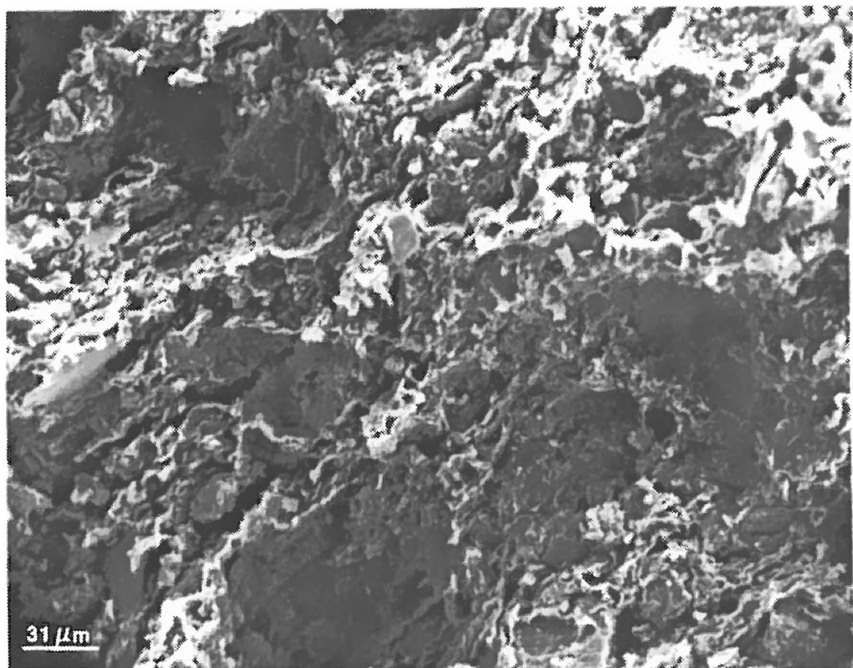
Figure 21

- a. Section 55A (Interstate 20)
Sample 80.10
4000x Magnification
SEM micrograph showing different states of clinoptilolite crystal deterioration. The three crystals of interest, marked with c, are encased in authigenic montmorillonite. The Crystal at the upper left shows little alteration, the central crystal shows the effects of severe leaching, and the crystal in the lower right has undergone almost total deterioration .

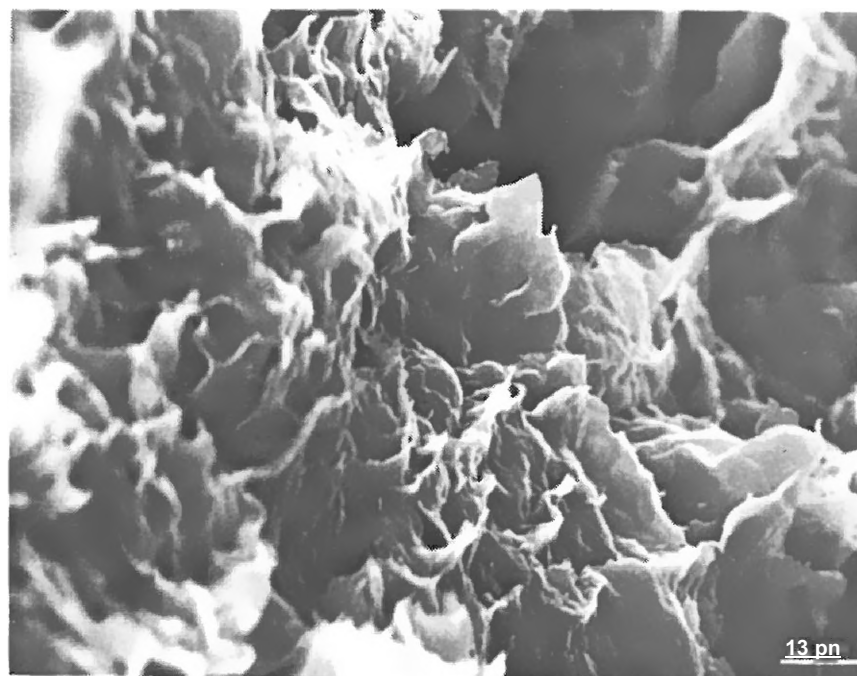
- b. Section 50 (Savoy Road)
Sample 69.76
22470x Magnification
SEM micrograph of well formed clinoptilolite crystals. Note at left side of photo the beads of incipient montmorillonite along a crystal face boundary.

- c. Section 52 (Arndel)
Sample 76.1
644x Magnification
SEM micrograph showing a cluster of clinoptilolite crystals in various stages of deterioration.

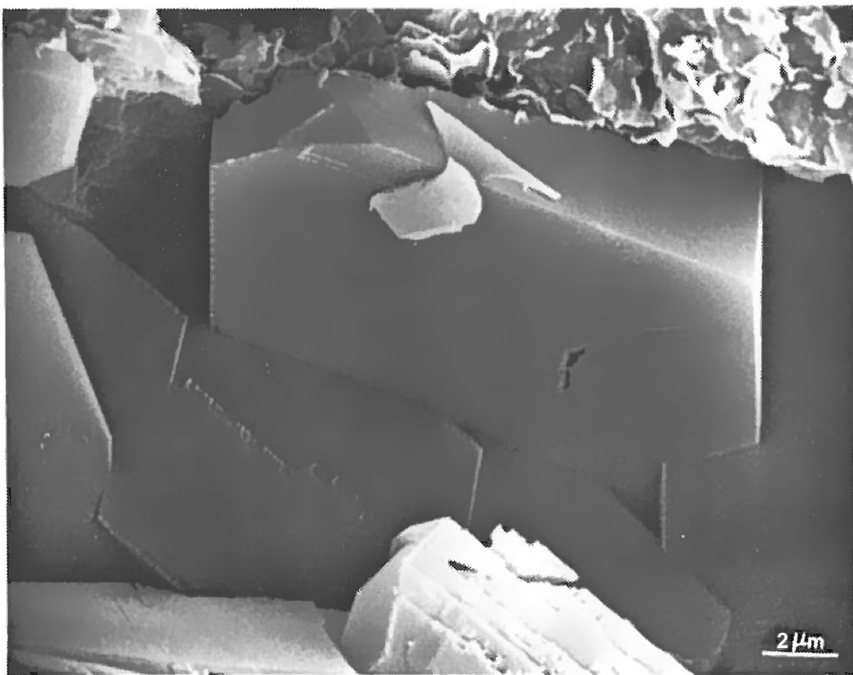
- d. Section 52 (Arndel)
Sample 76.1
2600x Magnification
SEM micrograph of c above at increased magnification to show incipient montmorillonite in the form of "tooth-paste" and "sheet" structure along cleavage planes.



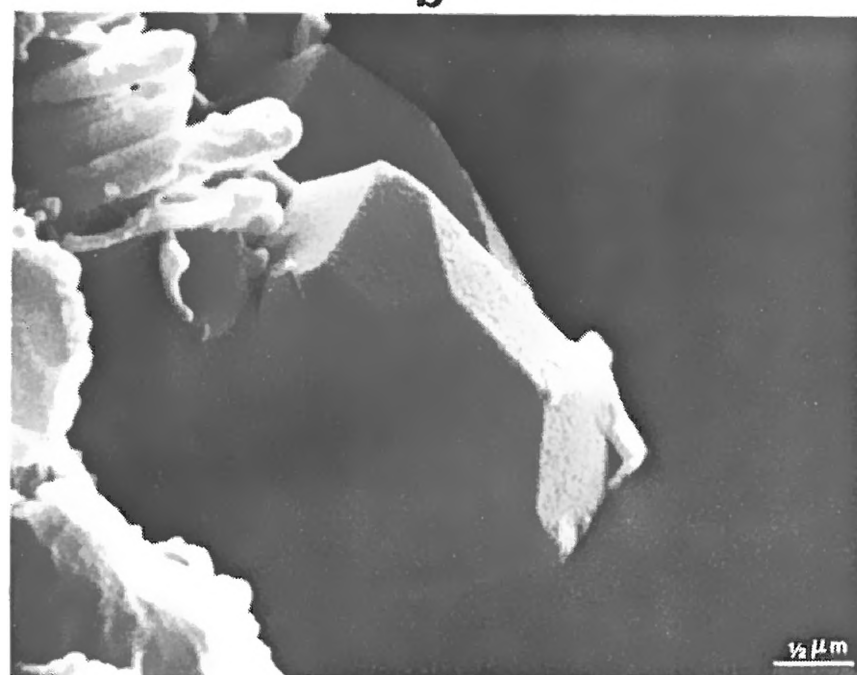
a



b



c



d

It is not known presently whether or not the Tallahatta and Mississippi is produced from the alteration of a volcanic precursor. The montmorillonite observed occurring with the clinoptilolite is possibly an initial authigenic product from the alteration of volcanic ash. If this is the case, clinoptilolite then is a later formed product growing in pore spaces provided by relic bubble structures. On the other hand, close examination of clinoptilolite crystals in various stages of deterioration reveals incipient montmorillonite in the forms of "beads" (Figure 21a) or as "toothpaste" lines (Figure 21a and c) and "sheets" (Figure 21d) along either crystal face boundaries or cleavage plane junctures.

M I N E R A L O C C U R R E N C E

X-ray and SEN investigations were significant in determining the existence of clinoptilolite besides crystal morphology and to some extent mineral quantity in material sampled from wackes, muds and clays of the Tallahatta Formation. These analytical methods however did not lend much insight into the modes of mineral occurrence or mineral genesis. Therefore, for this phase of investigation it was decided that in addition to x-ray and SEIM analysis there should be a return to the "basics"; petrography.

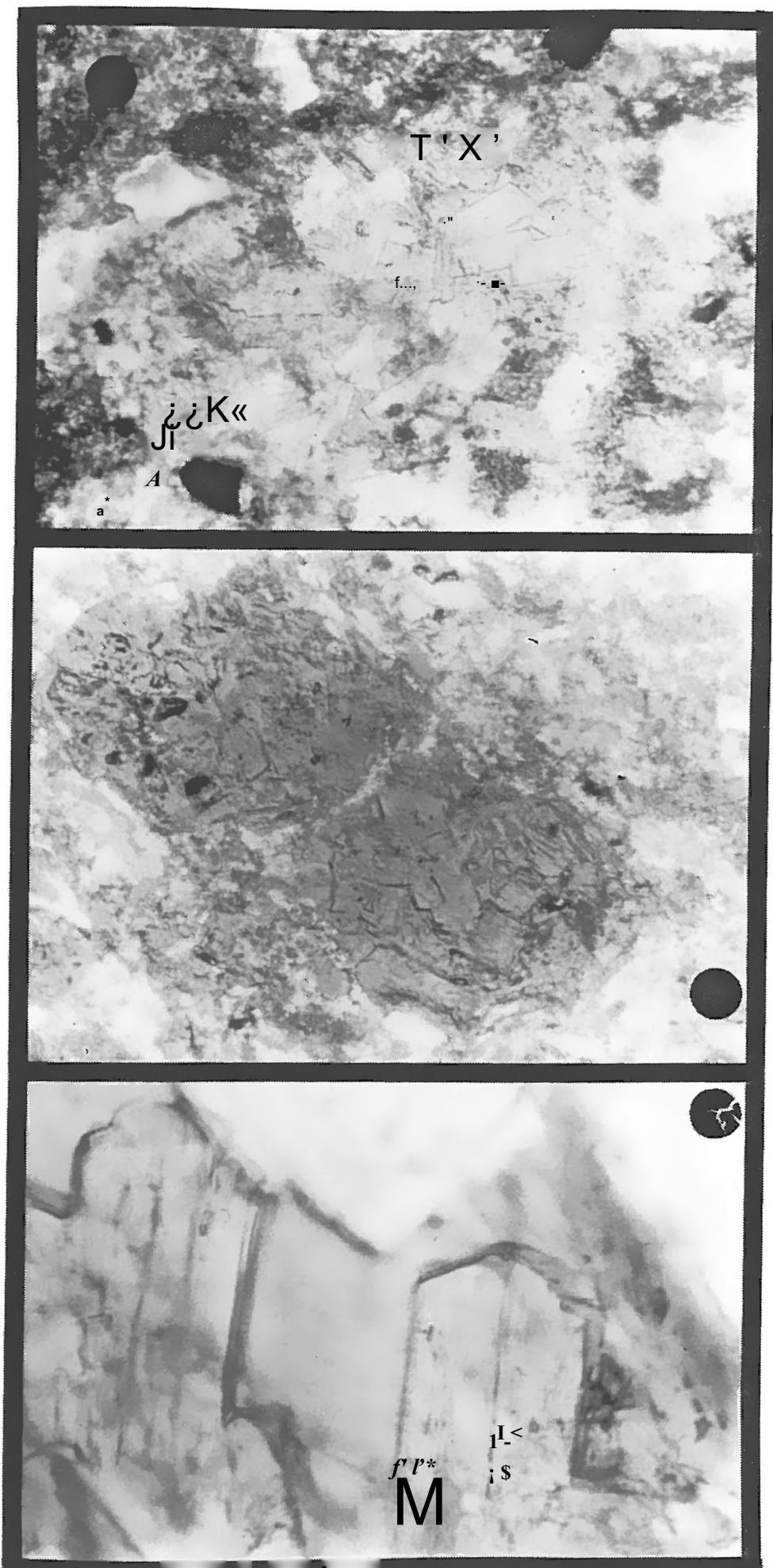
Petrographic characterization of clinoptilolite was based upon optical examination of thin-sections prepared using outcrop exposure and core samples both the Tallahatta and Zilpha Formations. To complement the thirty samples were disaggregated, separating the coarse fraction (62 urn) for optical examination in immersion oils with refractive indices of 1.54. Samples were selected for thin-section examination based on mineral content as revealed by examination of x-ray data. The samples were selected to represent different combinations of zeolite concentration and mineral association, and minerals were identified using standard optical methods.

Detailed petrographic description of each thin-section and grain mount was

beyond the scope and purpose of this study. Rather, a summary of the general characteristics of both thin-sections and grain mounts is presented here, with this petrographical character of clinoptilolite receiving a more detailed

The detrital component of the thin-sections studied consisted mostly of angular silt-sized quartz grains, crudely oriented laths of white mica, and more rarely alkali feldspar. The ground mass consisted of smectite and opal-CT (verified by x-ray diffraction). Texturally the samples are muds, silts and clays, as material coarser than 62 microns was not common. Bright green glauconite grains occurred in all thin-sections and most grain mounts. Usually these grains were elipsoidal to spherical in shape and of uniform size. Rare subhedral glauconite grains were also observed. Occasionally the elipsoidal and spherical glauconite grains are with cracks filled with a matrix material, probably opal-CT. Glauconite was also found to replace organic remains such as the central canals of sponge spicules. Pyrite was found in most all the thin-sections and grain mounts, and was usually associated with organic material and often occurred as single cubes or framboidal masses. Completely pyritized microfossils of diatoms, sponge spicules were observed. Opaque to semi-opaque organic material was common in the smectite-rich samples. Microfossils are abundant in all samples and consist mostly of diatoms, sponge spicules and more rarely radiolarians. Calcareous microfossils, mostly chambered foraminiferans and some calcareous algae were observed in a few samples. The most common accessory heavy minerals observed included rounded zircon, hornblende and staurolite, and rarely phosphategrains.

In both thin-sections and grain mounts clinoptilolite exhibits prismatic and tabular crystals having a monoclinic outline (Figure 22c). These crystals range in size from barely discernible under highest magnification to well-formed crystals up to a maximum of 40 microns. Average crystal size was about 15 to 20 micrometers. Observed clinoptilolite has a refractive index of approximately 1.48



a

b

c

Figure 22 : $\text{pSt}^{\wedge}\text{irapdiSFniIIS}$ graphs of large clinoptilolite crystals filling large pore spaces. Dot scale for a and b is 50m and for c is 25m/-..

which is in agreement with the index given by Boles (1972) and Mumpton (1960).

Under plane light clinoptilolite is colorless to light violet and has a strong negative relief. Under crossed polarizers clinoptilolite shows dark to pale grey

first-order interference colors. This tendency for a dark interference

the small size makes optical determination difficult in thin-section though a

well-formed biaxial figure can be obtained with difficulty from some crystals.

Clinoptilolite crystals were usually euhedral, commonly twinned and inclusion free. Corrosion of individual crystals is apparent, in some samples, though it is not common.

Clinoptilolite observed in thin section and grain mounts from the operational units in southeast Mississippi has several different petrographic modes of occurrence, which are classified into the following groups.

(1) Clinoptilolite occurs as matrix-cement of silt to sand sized particles, an occurrence which could only be observed in thin-section (Figure 23). The clinoptilolite in this category appears to grow within the pore spaces between angular particles of quartz, occasionally mica, and rarely feldspars. Other particles making up approximately 5 to 10 percent of the coarse fraction include abundant sponge spicules and diatoms and more rarely radiolarians. Glauconite grains and opaque organic particles were also present in the coarse fraction. Where other matrix material was associated with clinoptilolite, opal-CT was more common than was smectite. One should note in Figure 23 the sharp angularity and embayment of quartz particles. These particles more often than not exhibit straight extinction. Both of the above aspects suggest the quartz to be volcanic. Also, in Figure 23 note the wavy or undulose structure of the clinoptilolite matrix which appears as a pyroclastic fabric similar to authigenic montmorillonite.

(2) Clinoptilolite occurs as a mineralization product within dewatering veins and sheets (Figure 11) where it either fills the veins or sheets or only

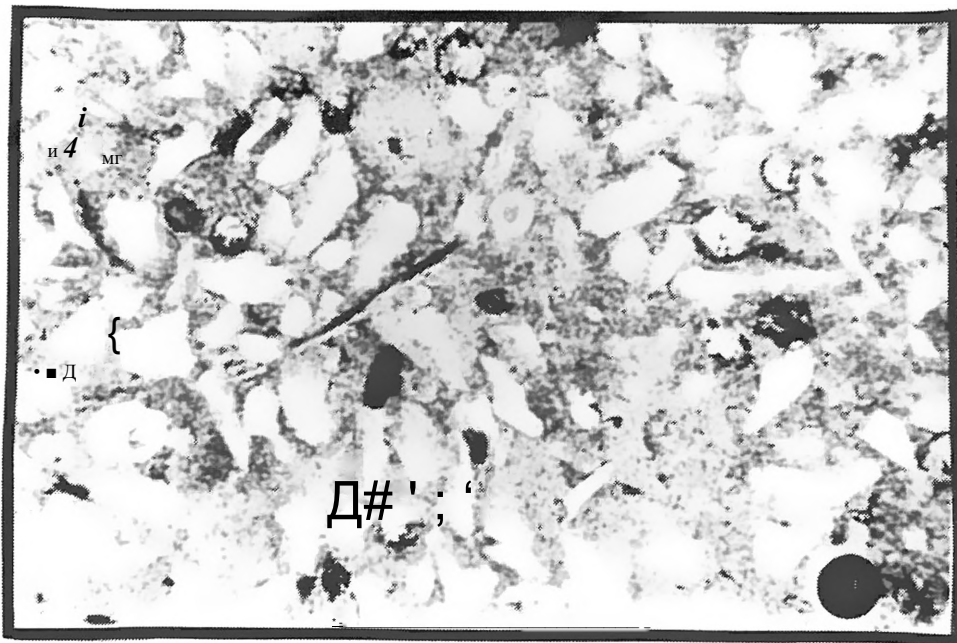
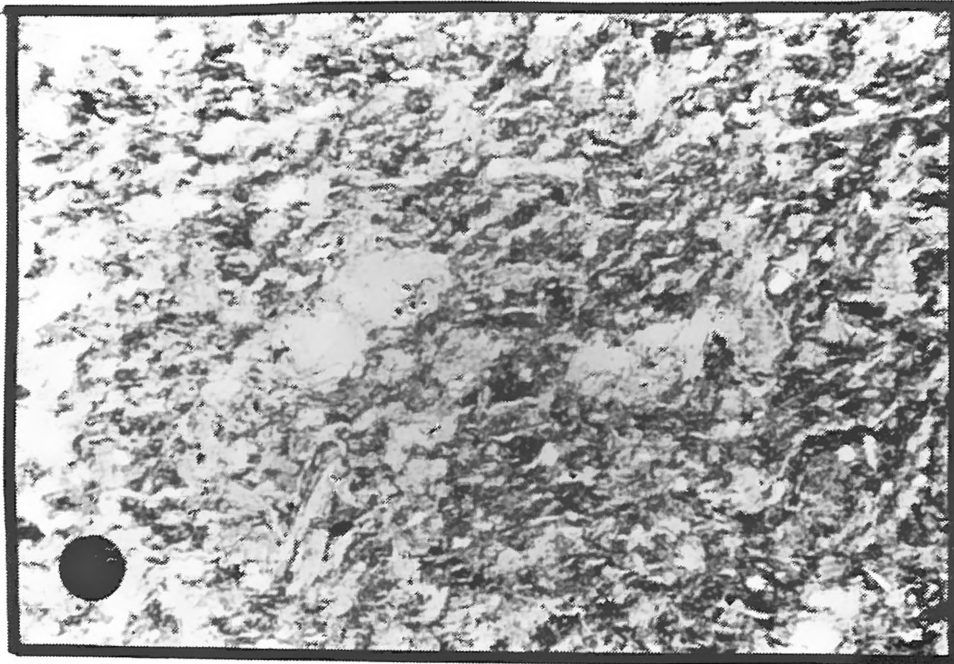


Figure 23: Petrographic micrographs showing pyroclastic fabric and clinoptilolite infilling of microfossils (upper) and clinoptilolite as a cement (lower). Dot scale is equivalent to 100μ.

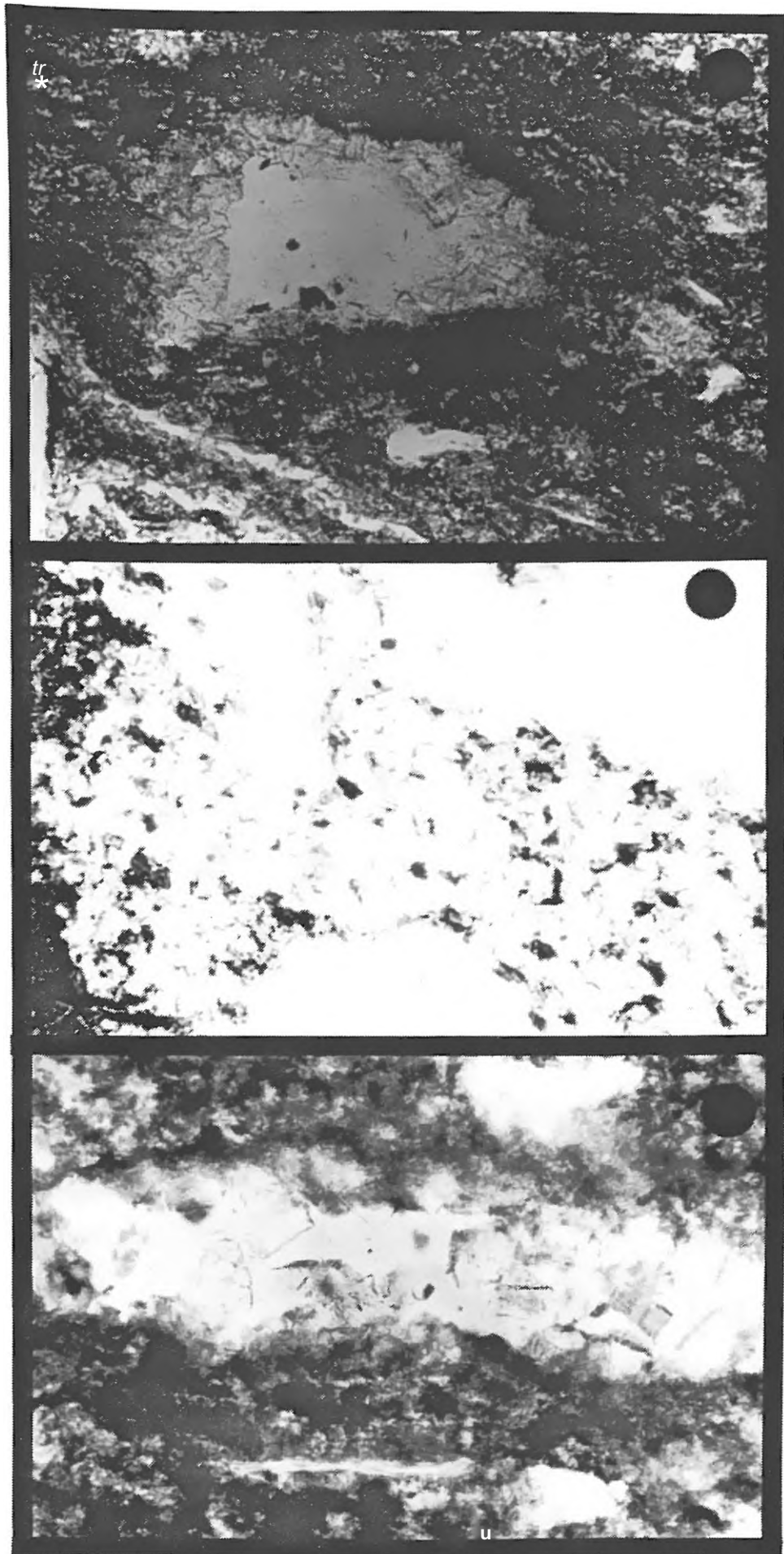
lines the perimeter (Figure 24c). It appears; that clinoptilolite growth proceeds from the vein or sheet wall inward which suggest precipitation from fluids moving not only through but into the veins and sheets.

(3) . Clinoptilolite occurs as a replacement material in voids of microfossil! and shell fragments. These voids are formed by the dissolution of diatoms, spongi spicules, foraminiferans and radiolarians are often filled by blocky crystals of clinoptilolite whereas others seemly have converted to opal-CT (Figure 23). Replacement involves dissolution and reprecipitation which destroys most of the textural aspects of the microfossils even though the relative size and shape remain the same. Grain mounts offer a better means of observing the replacement. type of clinoptilolite growth which seems to be toward the center of such voids Pyrite is nearly always found associated with clinoptilolite within these voids.

(4) . Clinoptilolite occurs as a direct transformation product of siliceous microfossils. This mode of zeolite occurrence involving siliceous microfossils was very apparent with optical examination of grain mounts. Clinoptilolite occurrence in this manner suggests the apparent direct transformation of microfossils to the zeolite without involving dissolution since the external structural integrity of the microfossil is retained (Figure 25c). This also may suggest material packed into the microfossil test after death and subsequently converted to clinoptilolite.

(5) ., The prominent occurrence of clinoptilolite is in large pore spaces (Figure 24a and b) where crystal clusters are seen growing from the walls or the central portions of the pore spaces. This occurrence like that in dewatering vients and sheets suggests clinoptilolite precipitated from fluids either that have moved through a buffering matrix into the pore spaces or were already occupying the pore spaces and responded to a physical stimulus such as temperature change and/or compaction pressure.

(6) . Clinoptilolite occurs as an encrusting material on detrital grains.



a

b

c

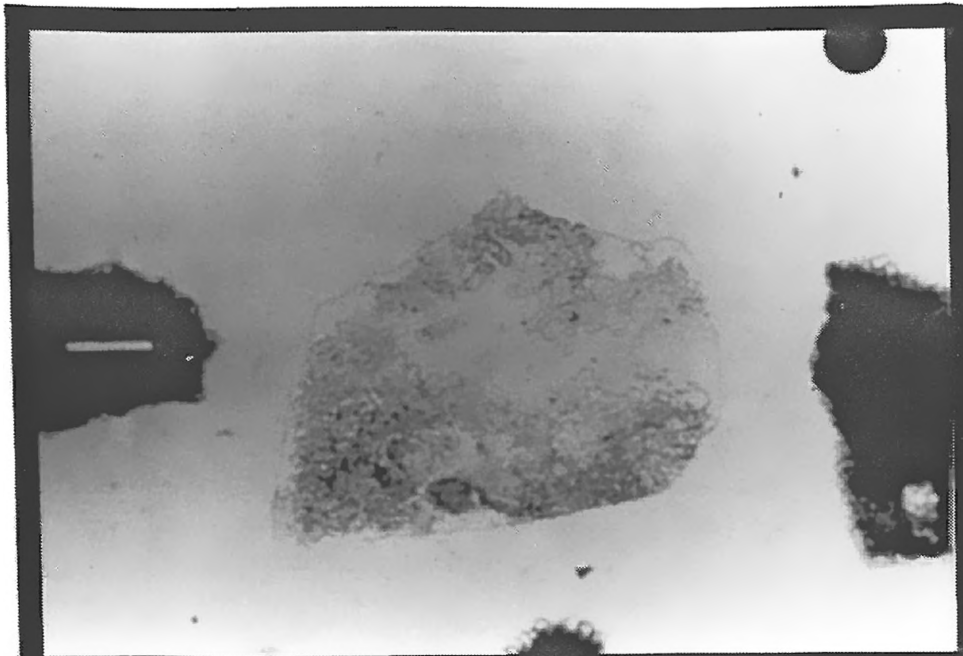
Figure 24: Petrographic micrographs showing clinoptilolite infilling large vugs (a and b) and dewatering veins (c).

This final category is most obvious observed in grain mounts rather than thin section. Here, clinoptilolite crystals encrust, quartz, mica and possibly feldspar grains, and there appears to be no dissolution, alteration or transformation involved between the clinoptilolite and the detrital mineral grain (Figure 25a and b). This association indicates clinoptilolite probably grew into pore spaces surrounding the detrital material from the grain surfaces thus becoming the grain to grain cement of the lithified wackes and muds (Figure 26).

This thin-section and grain mount, examination revealed no conclusive textural evidence to suggest a precursor pyroclastic material ever being present in the Lower Claiborne sediments of southeast Mississippi. According to Ross (1928) and Ross and Smith (1961) pyroclastic sediments have characteristic structures produced by the fragmentation of globular bubbles which produce curved plates, cusp and lunate shaped, and Y and U shaped shard particles. In addition, a definite mineral association is often present including: idiomorphic zircon, euhedral brown biotite, euhedral quartz with embayed structure, subhedral sanidine with irregular embayed fractures, hornblende and pyroxene.

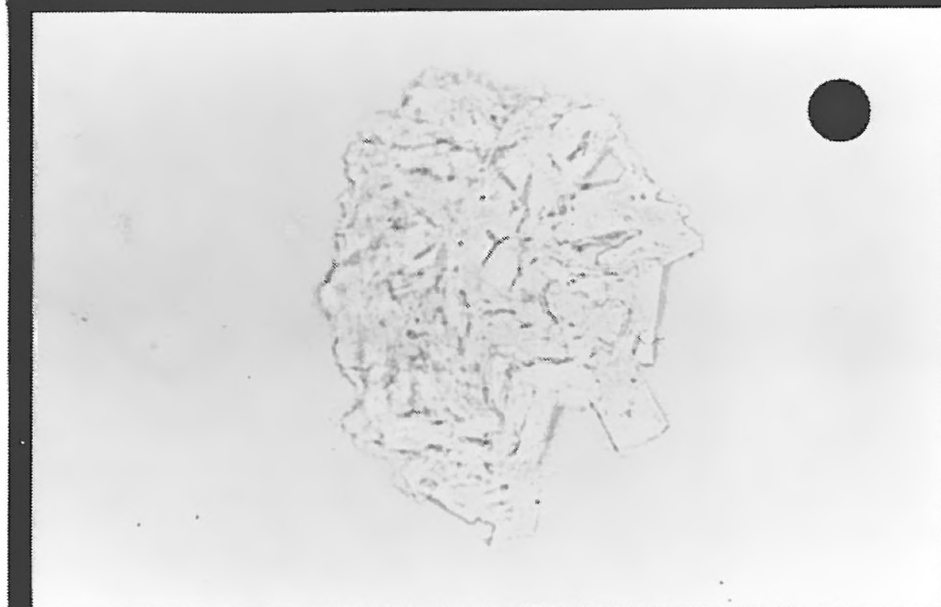
Authigenic feldspar was identified in some samples, usually first revealed by analysis of x-ray patterns.. A cursory examination of fine sand from various positions in the Basic City showed a surprising abundance of sponge spicules and diatom frustules associated with zeolite. Other, perhaps unusual, noted in this aggregated Zirconophane is some Tallahalla silt. These aggregates of sponge spicules surrounded by matrix of light brown (clay mineral) material are commonly observed. These aggregates also contain bright green glauconite part, mica, quartz grains and opaque organic materials. Disaggregation of samples containing a high opal-CT content also revealed this same aggregate feature. Close inspection of individual "grains" in grain mounts indicated they were composed of skeletal fragments of diatoms and or radiolarians in a pale brown cement.

Figure 25 : Photomicrograph of grain mounts showing.



a

Clinoptilolite encrusting a mica grain. Dot scale is equivalent to 50mμ.



b

Clinoptilolite encrusting a quartz grain. Dot scale is equivalent to 50m/x.

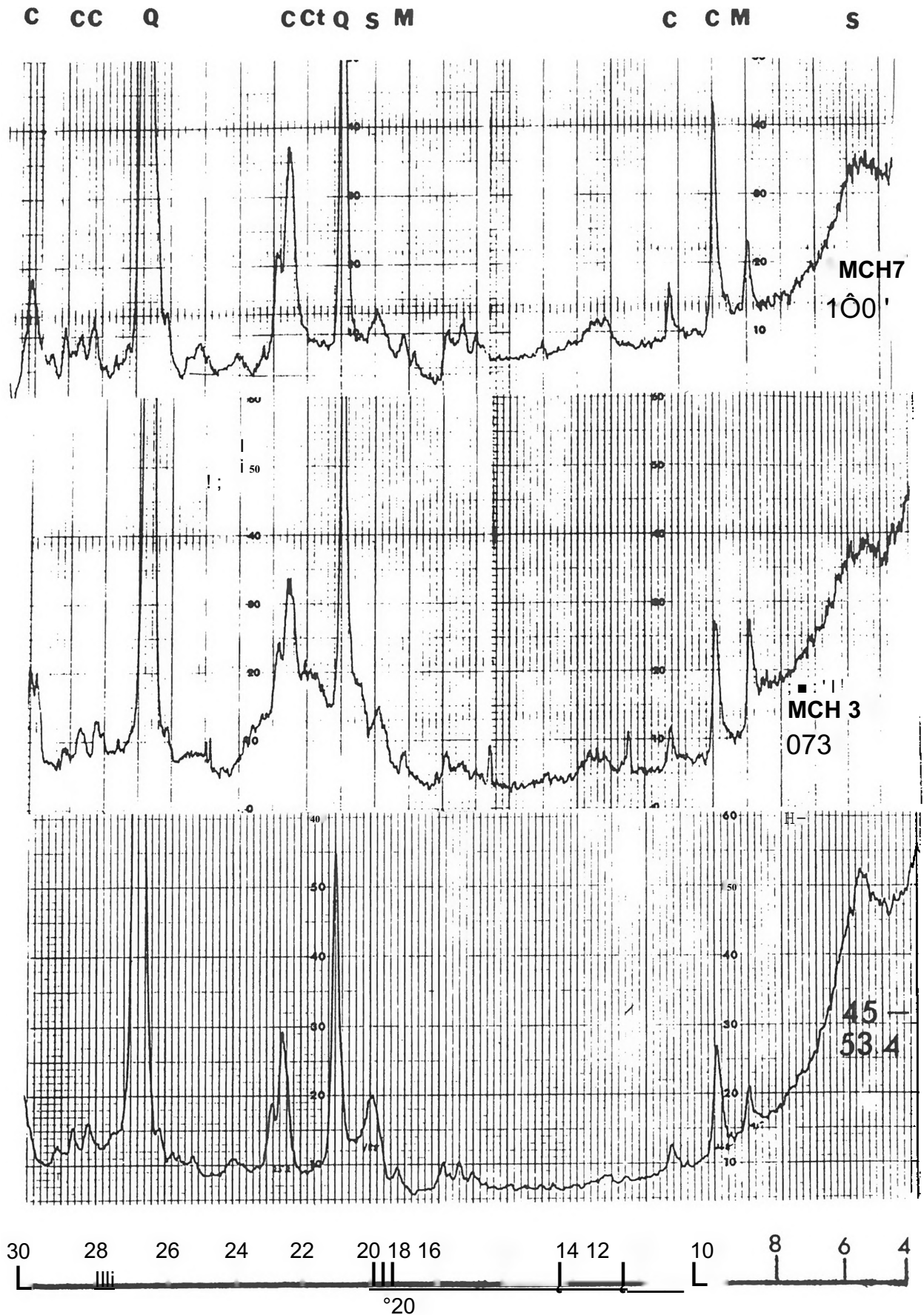


c

Clinoptilolite completely enclosed within a radiolaria test. Dot scale is equivalent to 25mμ.

Figure 26 : X-ray diffraction patterns of selected sand strata which contain clinoptilolite as a matrix cement.

CLINOPTILOLITE AS A CEMENT



D X. E? V. Y s S A Q D

Even though the ancient Mississippi embayment was generally characterized by fine sedimentation on the coast-ocessess and reefs found along the mesotidal coast of a shelf sea with incorporate depositional environments as tidal flats, barred coastal areas, open beaches and nascent deltas. During Wilcox and early Claiborne time the western and northwestern portions of the embayment were lined with large coalescing delta complexes (Duplantis 1975). On the other hand, along the eastern and southeastern portion smaller Wilcox deltas easily gave way to wave dominated coasts which seaward bordered a broad shallow marine shelf.

The lithologic units of the Tallahatta Formation in the area of Meridian, Mississippi reflect, a marine transgression cycle, beginning in the upper Meridian Sand and continuing into the Koscisko Formation. Mainland beach, barrier beach, delta front and tidal flat sands of the Meridian Formation give way to transitional wackes and muds of an early Tallahatta marine transgression from the southwest and extending beyond Meridian, Mississippi. The transgressive processes abated during the middle tallahatta with the deposition, under low energy conditions, of siliceous clays over a broad tidal flat shelf. During this time however were numerous short periods of coastal progradation and retrogradation represented by sediment distribution characteristic of numerous localized transgressions and regressions.

The lithofacie associations observed in the upper tallahatta suggest this time to be a period of marine regression. This was a time when coastal nearshore and foreshore plus nascent delta environments moved seaward to the southwest over the previous broad tidal flat shelf. The thickness of unit ft strata indicates the regressive phase to have occupied more time than the transgressive phase.

However, there is little evidence in unit ft strata that suggests rapid transgression. The difference must lie in the aspect that more terrigenous

material was supplied to the deposition area during the transgressive phase-

C1. D. 9 P. t i L Q1 í. t æ E C! L Φ É t .L Q Π

Obviously the tal .1 ahat, t a sediments represent a period of extensive silica deposition. The initial deposition of silica would have been in the form of opal-C (Carver 1980) which presently is undergoing transformation to quartz through the opal-Ct phase. Deposition of material eventually altered to clinoptilolite was apparently concomitant in time to the deposition of silica. Sites of clinoptilolite precursor deposition appear to have been segregated subenvironments on the shelf and along the coastal regions. Such segregated sites include a variety of entrapment depocenters, mainly nearshore runnels, lagoonal troughs, and back barrier intertidal zones.

Cryptocrystalline clinoptilolite crystals disseminated in argillaceous sediments consequent with the occurrence of clinoptilolite as much larger euhedral crystals in-filling various microfossil voids, sponge spicules and anomalous vugs and pores suggest clinoptilolite to be an authigenic mineral formed through precipitation from interstitial solutions. Furthermore, clinoptilolite growth in dewatering veins and sheets and as a cement, matrix suggest, post-burial migration of pore solutions prior to clinoptilolite formation. Growth of clinoptilolite within diatom and other siliceous fossils could be evidence for direct, in situ transformation with no apparent dissolution and reprecipitation phase (Curtis and Cornelius, 1972; Fan and Zimmels, 1972; Burger and van Rad, 1972; Lancelot, 1979; Houghton, et. al. 1979; and Riech, 1979).

There is only scanty petrographic evidence that volcanic ash was a major source of silica in the Tallahatta and Zilpha sediments. This may be due the fact that in nearshore environments strong currents and high production of biogenic material may have rework, redistribute and dilute pyroclastic material so that it is less easily recognizable in these types of deposits (Hathaway et al, 1970).

Boles and Wise (1978, p» 239), discuss the occurrence of clinoptilolite in deep-sea sediments and suggest, that if clinoptilolite is formed only from glass then the majority of clinoptilolite occurrences should be associated with ash beds, and concluded that the majority of deep-sea clinoptilolite is not associate! with volcanic glass. Furthermore, Kastner and Stonecipher (1978) report that onix twenty to twenty-five percent of the deep-sea clinoptilolite occur in sediments that are prdominantly volcanic.

The presence of abundant siliceous microfossils in various stages of dissolution somewhat supports the hypothesis that they contributed to the vast, amount of silica deposited during Tallahatta time. Hein et al. (1978), in a study of sediments from the Berincj Sea, derived a similar hypothesis for a biogenic contribution to the formation of clinoptilolite in those sediments. .pa The absence of petrographic evidence of pyroclastic material in Tallahatta sediments does not however preclude the existence of such. Perhaps a cause-and-effect relationship between volcanic activity and biogenic deposition is possible. Reynolds (1970) has pointed out that the clinoptilolite-rich strata in the fall ahatta Formation of Alabama may have had a volcanic precursor, but also suggested that volcanic ash could not have been the precursor of the opal-CT.

In this study it was found that clinoptilolite is more likely* to be associated with detritial sediments than with large amounts of opal.....CT. This relationship suggests that clinoptilolite formation is more favorable in sediments with some terrigenous input while? opal-CT formation is favored when there is a minimum of terrigenous input. Kastner et al., (1977) has shown that the rates of dissolution of opal-A (biogenic) and recrystallization of opal-CT is inhibited by the presence of clay minerals. Houghton et al. (1979), reports that high carbonate content prohibits clinoptilolite growth and even pr dissolution. Nathan and Flexer (1977) have noted the negative correlation between opal-CT and clinoptilolite and suggest, that clinoptilolite formation is favored by

higher than normal concentrations of magnesium.

Traditionally Zeolite formation is considered as an alteration process of volcanic, glass; a concept well documented for most categories; of zeolite occurrence in a variety of sedimentary environments (Hay, 1978). In this study however field and laboratory investigation failed to produce strong evidence of a volcanic ash precursor for clinoptilolite formation. This does not suggest, however, that the volcanic precursor was not there. Alternatively, results of petrographic study show that a biogenic contribution of silica was possible as clinoptilolite has been observed in void spaces provided by dissolution of siliceous as well as calcareous microfossils. Therefore, it seems plausible to suggest that clinoptilolite in Tallahatta sediments may owe its origin, at least in part, to silica derived from the dissolution of siliceous organisms.

Stratigraphic positioning and mineralogic relationships by the simplest of interpretation indicate clinoptilolite formation is more favorable when a clastic component has diluted biogenic sediments, whereas opal-CT formation is more likely in sediment having a greater proportion of biogenic silica.

The major source of silica is thought to be the same for both clinoptilolite and opal-CT formation, and depositional environment is thought to have played a significant role in influencing the formation of either mineral. The absence of opal-CT in the zeolitic beds of both unit A and unit C is thought, to have resulted from a number of factors. First, in the lower and upper beds of the Tallahatta a greater content of coarse-grained material produces higher porosity and permeability which could have enhanced the formation of clinoptilolite by allowing easier migration of reactive ions in silica-rich fluids. The upper and lower units are also highly bioturbated, which suggests organic activity may have been an effective agent for clinoptilolite formation. Finally, pyritized organic material such as plant remains and diatom frustules indicate reducing post-depositional conditions.

The one discrepancy concerning clinoptilolite formation from siliceous biogenic material is the lack of an apparent aluminum source. In the case where clinoptilolite forms from a volcanic precursor this source is readily apparent. However, diatom frustules and other siliceous microorganisms are reported to contain only a minor amount of aluminum (0.5 ppm). Hein, et al. (1978) support a biogenic source of silica for clinoptilolite formation, but suggest that the reacting system in which clinoptilolite forms must derive its necessary aluminum through the dissolution of amorphous clays.

Their work suggests that diatom debris, already covered with clay-like minerals, might serve as nucleus for authigenic mineral formation such as clinoptilolite. Smectite has been reported to be present in living diatoms the frustules of which are reported to contain up to 1.5 percent aluminum (Van Bennekum and Vander Gaast, 1976). This may suggest diatom debris, already covered with clay-like material, might serve as a nucleus for authigenic mineralization such as clinoptilolite formation.

When considering all of the evidence it seems highly unlikely that dissolution of siliceous microorganisms would provide an adequate amount of necessary ion constituents to form clinoptilolite. Evidence is strong however for the precipitation of clinoptilolite from interstitial fluids. From where do these fluids incorporate, to a state of saturation, the necessary ions? Detrital clay has been one suggestion. Unfortunately most of the smectite occurs clinoptilolite is also authigenic. Clay and zeolite can form from the same precursor material which is evident in the recent Mt. St. Helens ash falls (Revier 1982) ..

Mol for mol clinoptilolite is composed of the same ions found in rhyolitic ash however, montmorillonite requires only half the silica and some magnesium (Reynolds, 1970). Therefore, montmorillonite could be produced by the deterioration of the first formed clinoptilolite which originated by precipitation

+ r om pare waters enriched by the dissolution o(v o l c a n i c a s h .

REFERENCOES

- Boles, J. R., 1972, Composition, Optical Properties, Cell Dimensions, and Thermal Stability of Some Heulandite Group Minerals: *American Mineralogist*, V. 57, p. 1463-1493.
- Boles, J. R. and Wise, W. S., 1978, Nature and Origin of Deep-Sea Clinoptilolite, in Sand, L. B. and Mumpton, F. A., eds., *Natural Zeolites, Occurrence, Properties, Use*: New York, Pergamon Press, p. 235-243.
- Burger R. and Von Rad W. H., 1972, Cretaceous and Cenozoic Sediments from the Atlantic Ocean, In Hayes, D. E. , Primm, A. C. , et al. , eds. , *Initial Reports of the Deep Sea Drilling Project, V. XIV*: Washington (U. S. Government Printing Office) p. 787-955.
- Carver, R. E. , 1980, Petrology of Paleocene-Eocene and Miocene opaline Sediments, Southeastern Atlantic Coastal Plain: *Journal of Sedimentary Petrology*, V. 50, p. 569-582.
- Chamberline, K. C. , 1978, Recognition of Trace Fossils in Cores, In Basin, P. B. , ed. , *Trace? Fossil Concepts: Society Economic Paleontologist Mineralogist Short Course No. 5*, 201 p.
- Curtis, C. D. and Cornelius, W. C. , 1972, Unusual Occurrence of Clinoptilolite, Fresno County, California: *Geo. Soc. America Bull.*, V. 83, p. 833-838.
- Dockery, D. T. , Ill, 1981, *Stratigraphic Column of Mississippi*: Mississippi Bureau of Geology.
- Duplantis, M. J. (1975) *Depositional Systems in the Midway and Wilcox Groups North Mississippi*: Masters thesis, The University of Mississippi, University, MS, 82 p.
- Fan, P. , and Zemmels, I. , 1972, X-ray Mineralogy Studies-Leg 12, In Laughton, A. S., Beggren, W. A., et al., eds., *Initial Reports of the Deep-Sea Drilling Project, V. XII*: Washington (U.S. Government Printing Office) p. 1127-1143.
- Hathaway, J. C., McFarlin, P. F. and Ross, D. A., 1970, *Mineralogy and Origin of Sediments from Drill Holes in the Continental Margin of Florida*: U.S. Geological Surv. Prof. Paper 581-E, 26 pp.
- Hein, J. R., Scholl, D. W., Barron, J. A., Jones, M.G. and Miller J., 1978, Diagenesis of Late Cenozoic Diatomaceous Deposits and the Bottom Simulating Reflectors in the Bering Sea: *Sedimentology* v. 25, p. 115-181.
- Houghton, R. L., Roth, P. and Galehouse, J. S., 1979, Distribution and Chemistry of Phillipsite, Clinoptilolite, and Associated Zeolites at DSDP Sites 382, 385 and 386 in the Western North Atlantic, In Tochoke, B. E. , Vogt, P. R. , et al. , eds. , *Initial Reports of the*

Deep-Sea Drilling Project, Vol. 43: Washington (U.S. Government Printing Office), p. 463-484.

Jones, J. B. , and Segnit, E. R., 1971, The Nature of Opal: 1. Nomenclature and Constituent Phases: Jour., of Geol. Soc. of Australia, V. 18, p. 57-68.

Kastner, M. , Keene, J. B. , and Gieskes, J. M. . , 1977, Diagenesis of Siliceous Oozes: I. Chemical Controls on the Rate of Opal-A Diagenesis-an Experimental Study: Goochem, et Cosmoch. Acta, V. 41, p. 1041-1059.

Kastner, M. and Stonecipher, S. A., 1978, Zeolite in Pelagic Sediments of the Atlantic, Pacific and Indian Oceans, In Sand, L. B., and Mumpton, F. A., Natural Zeolites, Occurrence, Properties and Use: New York, Pergamon Press, p. 199-220.

Lancelot, Y. 1979, Evidence of the Direct Transformation of Radiolarians into Zeolites in Mid-Cretaceous Deep-Sea Clays (abs): Geol. Soc. America Abstract. Prog. V. 11, No. 7, p. 462.

Lundegard, P. D. and Samuels, N. D. (1980) Field Classification of Fine-Grained Sedimentary Rocks: Jour. Sed. Petrology, V. 50, p. 781-786.

Milliman, J. S. and Boyle, E. , 1975, Biological Uptake of Dissolved Silica in the Amazon River Estuary: Science, V. 189, p. 995-997.

Mumpton, F. A., 1960, Clinoptilolite Redefined: American Mineralogist, V. 45, p. 351-369.

Mumpton, F. A., 1978, Natural Zeolites: A New Industrial Mineral Commodity, In Sands L. B., and Mumpton, F. A., eds., Natural Zeolites, Occurrence, Properties, use: New York, Pergamon p. 3-27.

Nathan, Y. and Flexer, A., 1977, Clinoptilolite, Paragenesis and Stratigraphy. Sedimentology, V. 24, p. 845-855.

Pevear, D. R., Dethier, D. P., and Frank, D. (1982) Clay Minerals in the 1980 Deposits from Mount St. Helens: Clays and Clay Minerals, Vol. 30, p. 241-252.

Raybon, S. O. , 1982, Lithology and Clay Mineral Variation in the Middle Phase of the Paleocene Porters Creek Formation of Mississippi (M.S. thesis): University, Mississippi, University of Mississippi, 100 p..

Reynolds, W. R., 1966, Formation of Cristobalite, Zeolite and Clay Minerals in the Paleocene and Lower Eocene of Alabama (Ph.D. dissertation): Tallahassee, Florida, Florida State University, 301 p.

Reynolds, W. R., 1970, Mineralogy and Stratigraphy of Lower Tertiary Clays and Claystones of Alabama: Jour, of Sed. Petrology, V. 40, p. 829.....838.

Reynolds, W. R., 1983, Crystal Form and Deterioration of Clinoptilolite in the Tallahatta Formation of Alabama and Mississippi (abs): Meeting abstracts of the 6th Annual International Zeolite Conference, Reno,

Nevada.

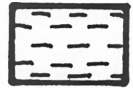
- Riech, V. , 1979, Diagenesis of Silica, Zeolites and Phyl osi licates at Sites 397 and 398» , In Von Rad, U. , Ryan, W.B.F. , et al. , eds. , Initial Reports of the Deep-Sea Drilling Project., V. 47, F. 1: Washington (U. S. Government Printing ūf-fice), p. 741-761.
- Roquemore, S. K. (1984) Clinoptilolite Occurrence in the Tallahatta Formation of Sout. h e a s t. M i. s s i s s i p p i : M a s t e r s T h e s i s , t h e U n i v e r s i t y o f M i s s i s s i p p i , H S. , 106 p.
- Ross, C. S., 1928, Altered Volcanic Material and their Recognition. Bull. Amer. Assoc. of Petrol . Geol. V.. 12, p. 143-164.
- Ross, C. S. , and Smith, R. L. , 1961, Ash-Flow Tuffs: Their Origin, Geologic Relationships and Identification. U.S. Geological Survey Professional Paper 366, 81 p.
- Sims, J. D. (1972) Petrographic Evidence for Volcanic Origin of Part of the Porter s Cree k C lay, J a c k s o n F u r c h a s e r e g i o n , W e s t e r n K e n t u c k y Prof. Paper 800-C , p. 39-51.
- Tada, R. and Ijima, A., 1983, Identification of Opaline Silica Phases and its Implication for Silica Diagenesis, In Iijima, A., Hein, J.R. and Sei ever, R. , eds. , Siliceous deposits in the Pacific Regions Developments in Sedimentology, V. 36, p. 229-246.
- T o u l m i n , , L. D. , 1966 , S u m m a t " y o f t h e T e r t i a r y S t r a t i g r a p h y o f t h e S o u t h - W e s t A l a b a m a , I n C o p e l a n d , C. W. , e d. , F a c i e s C h a n g e s i n t h e A l a b a m a T e r t i a r y : G u i d e b o o k f o r t h e F o u r t h A n n u a l F i e l d T r i p o f t h e A l a b a m a G e o l o g i c a l S o c i e t y , p. 6.
- Van Bennekam, A. J. and Van der Gaast , S. J. , 19 76, Possible Clay Structures in the Frustules of Living Diatoms: Geochim. Cosmochim. Acta, V. 40, p. 1149-1152.
- Visher, G. S., 1969, Grain Size Distribution and Depositional Processes: Jour. of Sed. Petrology, V. 39, p. 1074-1106.
- Wermond, E. G. and Moila, R. J., 1966, Opal, Zeolites and Clays in an Eocene Neritic Bar Sand. Jour, of Sed. Petrology, V. 36, p. 248-253.

APPENDIX A

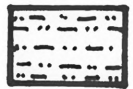
CORE LOGS

CORE LOG KEY

LITHOLOGY



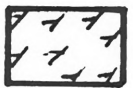
CLAY



SAND (WACKE)



SAND (ARENITE)



OPALINE CLAY



CLAYSTONE OPAL CT



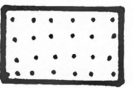
SILT & SILTSTONE



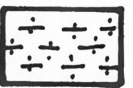
CHERT



MUD



SANDSTONE



MUDSTONE

ALPHA NUMERIC

A1	MICACEOUS	G13	CLAY PEBBLES
A1a	SLIGHTLY MICACEOUS	G14	SILT BLEBS
A2	GLAUCONITIC	G15	SILTY
A2a	SLIGHTLY GLAUCONITIC	G16	OPALINE BLEBS
A3	PYRITE		
A4	OPALINE	H1	SAND FLASERS
A5	OPALINE CEMENT	H2	LENTICULAR BEDDING
A6	CHERTY	H3	WAVY BEDDING
A7	GYPNUM	H4	SAND BLEBS
A8	FERRUGENOUS	H5	SANDY
A9	ARGILLACEOUS		
A10	CALCAREOUS		
B	FOSSILIFEROUS		
B1	BIOTURBATED		
B2	PLANT REMAINS		
CI	MASSIVE BEDDING		
C2	LAMINAR BEDDING		
C3	TRANSITIONAL		
C4	DENSE		
DI	BLOCKY		
D2	CHONCOIDAL		
D2a	SEMI-CHONIOIDAL		
D3	FRONDESCENT OR VEIN STRUCTURE		
D4	MOTTLED		
D5	CROSS LAMINATION		
D6	FISSIL		
E	SECONDARY SULFATES		
F	LIGNITIC		
G1	COURSE TEXTURE		
G2	MEDIUM TEXTURE		
G3	FINE TEXTURE		
G4	PLASTIC		
G5	WAVY		
G6	SILT LAMINAE OR STREAKS		
G7	SAND LAMINAE		
G8	CLAY LAMINAE		
G9	BRITTLE		
G10	SHARP		
G11	CLAY BLEBS		
G12	QUARTZ PEBBLES		

SECTION NO. 1001 REPUBLIC OF KENYA
 COUNTY, NAKURU
 DISTRICT, NAKURU
 SHEET NO. 1001
 SCALE 1:50,000
 PROJECT NO. 1001
 SHEET NO. 1001

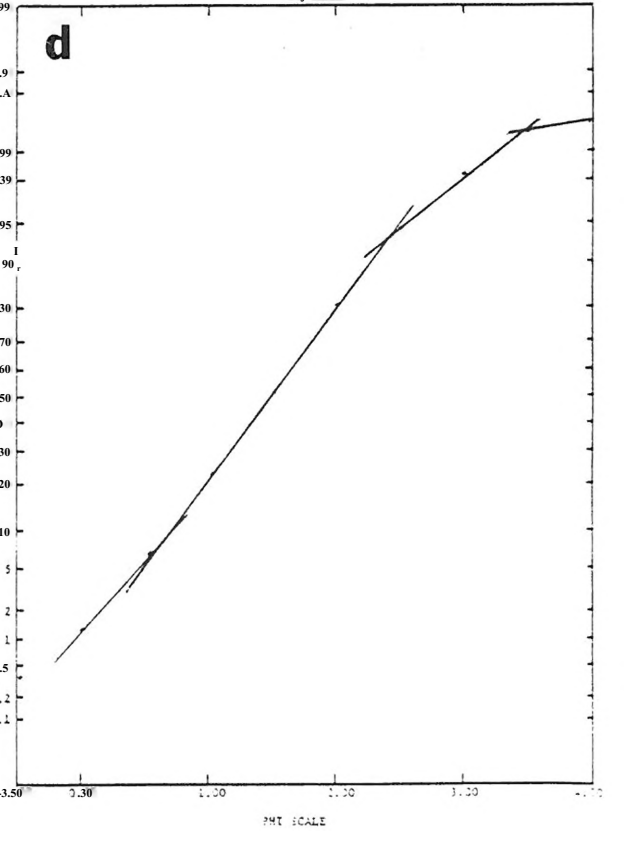
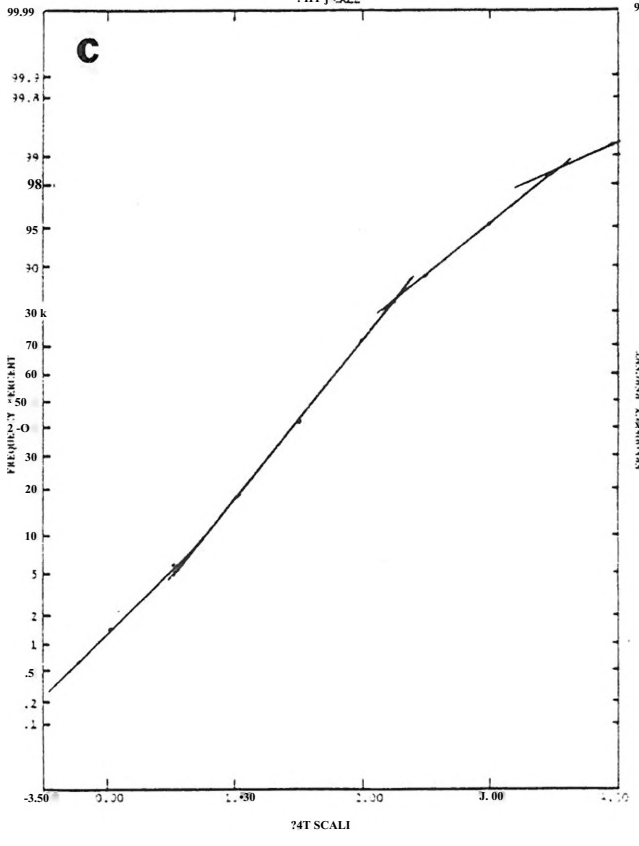
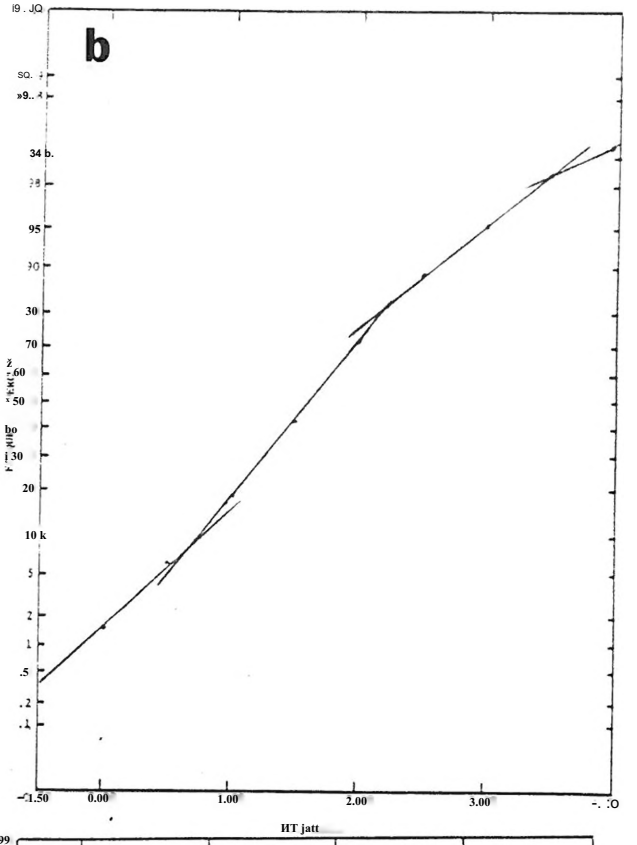
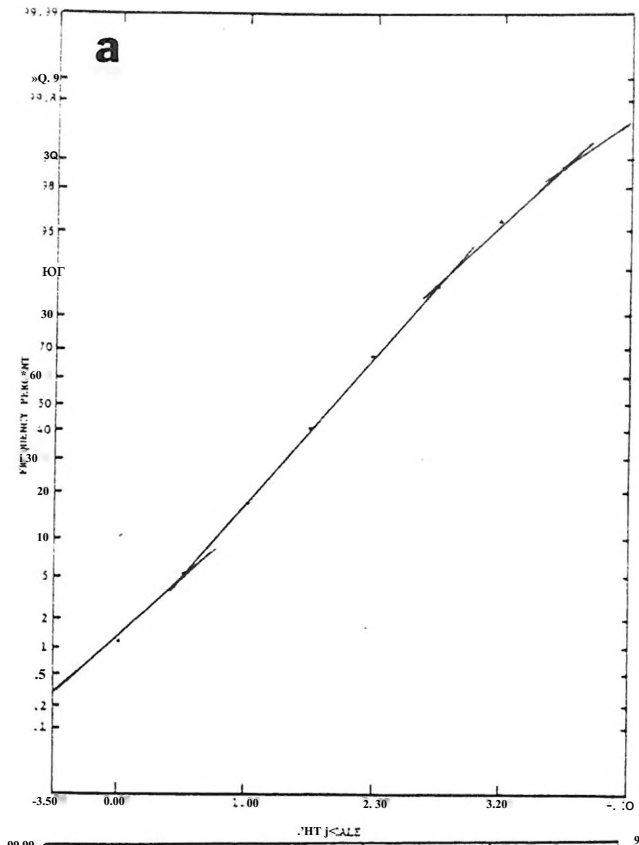
DEPTH FT./M	SAMPLE	LOG	LITHOLOGY	COLOR	ACCOMpany INFORMATION
10					→ 100 out 9 feet
10-20	001-002		CLAY	Ochre	Mixed, prob. Vienna Sand
20-25					Massive; blocky; silty; micaceous; plant
25-30			SAND (weak)	Ochre	Mixed, prob. sand below
30-35					Quartz, ore. to med.; glass; clay & fts. pebbles
35-40			SAND (weak)	Ochre	Mixed, prob. above sand
40-45	003-004		CLAY	Ochre	As above
45-50			CLAY	Ochre	Massive; blocky; silty; micaceous; plant
50-55			CLAY	Ochre	Mixed, prob. above sand
55-60			CLAY	Ochre	As above
60-65			CLAY	Ochre	Massive; blocky; silty; micaceous; plant
65-70			CLAY	Ochre	Mixed, prob. above sand
70-75			CLAY	Ochre	As above
75-80			CLAY	Ochre	Massive; blocky; silty; micaceous; plant
80-85			CLAY	Ochre	Mixed, prob. above sand
85-90			CLAY	Ochre	As above
90-95			CLAY	Ochre	Massive; blocky; silty; micaceous; plant
95-100			CLAY	Ochre	Mixed, prob. above sand
100-105			CLAY	Ochre	As above
105-110			CLAY	Ochre	Massive; blocky; silty; micaceous; plant
110-115			CLAY	Ochre	Mixed, prob. above sand
115-120			CLAY	Ochre	As above
120-125			CLAY	Ochre	Massive; blocky; silty; micaceous; plant
125-130			CLAY	Ochre	Mixed, prob. above sand
130-135			CLAY	Ochre	As above
135-140			CLAY	Ochre	Massive; blocky; silty; micaceous; plant
140-145			CLAY	Ochre	Mixed, prob. above sand
145-150			CLAY	Ochre	As above
150-155			CLAY	Ochre	Massive; blocky; silty; micaceous; plant
155-160			CLAY	Ochre	Mixed, prob. above sand
160-165			CLAY	Ochre	As above
165-170			CLAY	Ochre	Massive; blocky; silty; micaceous; plant
170-175			CLAY	Ochre	Mixed, prob. above sand
175-180			CLAY	Ochre	As above
180-185			CLAY	Ochre	Massive; blocky; silty; micaceous; plant
185-190			CLAY	Ochre	Mixed, possible sand
190-195			CLAY	Ochre	(Matchlight)
195-200			CLAY	Ochre	Mixed
200-205			CLAY	Ochre	(Matchlight)

SECTION CO. 10. 1 CORE 1. REVERSE SAMPLE SERIES: PAGE 07
 STATE MISSISSIPPI COUNTY CLAY COUNTY CLAY
 SEC. 24 T. 48 N. 16E R. 16E GRID COORD. NAD 83
 UTM ZONE 17Q UTM EASTING 110 UTM NORTHING 578 ELEVATION 578

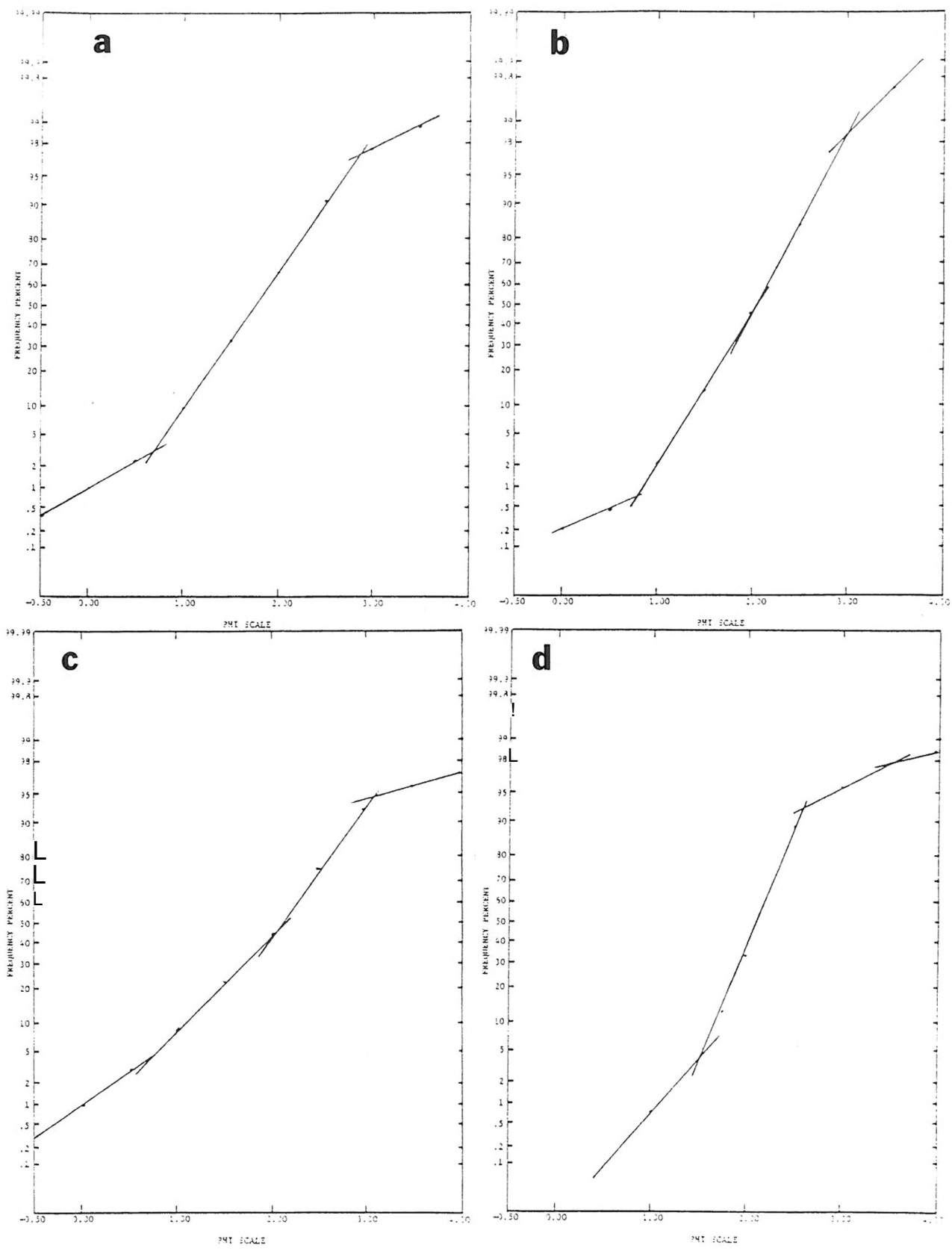
DEPTH FEET	SAMPLE NO.	LOG	LITHOLOGY	CODE	ACCRETION INFORMATION
60	160		Mixed		Drilled out 44 feet to set core barrel. Drilled through 36 feet sand; orange m. grt. quartz arenite
61	161		SAND(weak)	Green	Quartz, sub-ang. A1, A2, G19
70	162		MUD	OLIVE-GRN	As above
71	163		CLAY	OLIVE-GRN	As above
			MUD	OLIVE-GRN	As above
			MUD	OLIVE-GRN	As above
			MUD	OLIVE-GRN	As above
80	164		CLAY(opal)	OLIVE-GRN	G2, G1, A1, A2, G15
81.5	165		SLTSPHRE	As above	G1-G2, G1, A1, P, B1
90	166		CLAY(opal)	OLIVE-GRN	G2, G2, U6, 1, A1, A2a, B2
91.5	167		MUD	As above	
			MUD	As above	
			MUD	As above	
			MUD	As above	
100	168		CLAY(opal)	OLIVE-GRN	G1, G1, G17, G10, A6, B2, A1, B4
101.5	169		CLAY(opal)	OLIVE-GRN	G2, G1, P, B2, A1, B2a
110	170		CLAY(opal)	OLIVE-GRN	As above
111	171		CLAY(opal)	OLIVE-GRN	As above
112	172		CLAY(opal)	OLIVE-GRN	G2, G3, U7, O9, U7, O8
113	173		CLAY(opal)	OLIVE-GRN	G2, C: G: G1, G10, G6(omitted), A1, G: B1, B2
114	174		CLAY(opal)	OLIVE-GRN	Quartz, weak, fr. sub-ang. A2, G15
115	175		CLAY(opal)	OLIVE-GRN	G2, G3, G10, A6, U4, B2
116	176		CLAY(opal)	OLIVE-GRN	G1, G1, A1, G: B1, B2
117	177		CLAY(opal)	OLIVE-GRN	G2, G1, G15, U, 1, 4, N: 4
118	178		CLAY(opal)	OLIVE-GRN	G2, G1, G15, G17, G1, B
119	179		CLAY(opal)	OLIVE-GRN	G2, G2, A1, A2, B
120	180		CLAY(opal)	OLIVE-GRN	As above
121	181		CLAY(opal)	OLIVE-GRN	Quartz, weak, sub-ang. G1, A1
122	182		CLAY(opal)	OLIVE-GRN	G2, G2, G: 1, A2, B1
123	183		CLAY(opal)	OLIVE-GRN	G2, U, G: 5, A1, A2, G, P, U, U1
124	184		CLAY(opal)	OLIVE-GRN	G1, G: 1, A2, G12
125	185		CLAY(opal)	OLIVE-GRN	G2, G2, G: 1, A1, P, G
126	186		CLAY(opal)	OLIVE-GRN	As above
127	187		CLAY(opal)	OLIVE-GRN	As above
128	188		CLAY(opal)	OLIVE-GRN	As above
129	189		CLAY(opal)	OLIVE-GRN	As above
130	190		CLAY(opal)	OLIVE-GRN	As above
131	191		CLAY(opal)	OLIVE-GRN	As above
132	192		CLAY(opal)	OLIVE-GRN	As above
133	193		CLAY(opal)	OLIVE-GRN	As above
134	194		CLAY(opal)	OLIVE-GRN	As above
135	195		CLAY(opal)	OLIVE-GRN	As above
136	196		CLAY(opal)	OLIVE-GRN	As above
137	197		CLAY(opal)	OLIVE-GRN	As above
138	198		CLAY(opal)	OLIVE-GRN	As above
139	199		CLAY(opal)	OLIVE-GRN	As above
140	200		CLAY(opal)	OLIVE-GRN	As above
141	201		CLAY(opal)	OLIVE-GRN	As above
142	202		CLAY(opal)	OLIVE-GRN	As above
143	203		CLAY(opal)	OLIVE-GRN	As above
144	204		CLAY(opal)	OLIVE-GRN	As above
145	205		CLAY(opal)	OLIVE-GRN	As above
146	206		CLAY(opal)	OLIVE-GRN	As above
147	207		CLAY(opal)	OLIVE-GRN	As above
148	208		CLAY(opal)	OLIVE-GRN	As above
149	209		CLAY(opal)	OLIVE-GRN	As above
150	210		CLAY(opal)	OLIVE-GRN	As above
151	211		CLAY(opal)	OLIVE-GRN	As above
152	212		CLAY(opal)	OLIVE-GRN	As above
153	213		CLAY(opal)	OLIVE-GRN	As above
154	214		CLAY(opal)	OLIVE-GRN	As above
155	215		CLAY(opal)	OLIVE-GRN	As above
156	216		CLAY(opal)	OLIVE-GRN	As above
157	217		CLAY(opal)	OLIVE-GRN	As above
158	218		CLAY(opal)	OLIVE-GRN	As above
159	219		CLAY(opal)	OLIVE-GRN	As above
160	220		CLAY(opal)	OLIVE-GRN	As above
161	221		CLAY(opal)	OLIVE-GRN	As above
162	222		CLAY(opal)	OLIVE-GRN	As above
163	223		CLAY(opal)	OLIVE-GRN	As above
164	224		CLAY(opal)	OLIVE-GRN	As above
165	225		CLAY(opal)	OLIVE-GRN	As above
166	226		CLAY(opal)	OLIVE-GRN	As above
167	227		CLAY(opal)	OLIVE-GRN	As above
168	228		CLAY(opal)	OLIVE-GRN	As above
169	229		CLAY(opal)	OLIVE-GRN	As above
170	230		CLAY(opal)	OLIVE-GRN	As above
171	231		CLAY(opal)	OLIVE-GRN	As above
172	232		CLAY(opal)	OLIVE-GRN	As above
173	233		CLAY(opal)	OLIVE-GRN	As above
174	234		CLAY(opal)	OLIVE-GRN	As above
175	235		CLAY(opal)	OLIVE-GRN	As above
176	236		CLAY(opal)	OLIVE-GRN	As above
177	237		CLAY(opal)	OLIVE-GRN	As above
178	238		CLAY(opal)	OLIVE-GRN	As above
179	239		CLAY(opal)	OLIVE-GRN	As above
180	240		CLAY(opal)	OLIVE-GRN	As above
181	241		CLAY(opal)	OLIVE-GRN	As above
182	242		CLAY(opal)	OLIVE-GRN	As above
183	243		CLAY(opal)	OLIVE-GRN	As above
184	244		CLAY(opal)	OLIVE-GRN	As above
185	245		CLAY(opal)	OLIVE-GRN	As above
186	246		CLAY(opal)	OLIVE-GRN	As above
187	247		CLAY(opal)	OLIVE-GRN	As above
188	248		CLAY(opal)	OLIVE-GRN	As above
189	249		CLAY(opal)	OLIVE-GRN	As above
190	250		CLAY(opal)	OLIVE-GRN	As above
191	251		CLAY(opal)	OLIVE-GRN	As above
192	252		CLAY(opal)	OLIVE-GRN	As above
193	253		CLAY(opal)	OLIVE-GRN	As above
194	254		CLAY(opal)	OLIVE-GRN	As above
195	255		CLAY(opal)	OLIVE-GRN	As above
196	256		CLAY(opal)	OLIVE-GRN	As above
197	257		CLAY(opal)	OLIVE-GRN	As above
198	258		CLAY(opal)	OLIVE-GRN	As above
199	259		CLAY(opal)	OLIVE-GRN	As above
200	260		CLAY(opal)	OLIVE-GRN	As above
201	261		CLAY(opal)	OLIVE-GRN	As above
202	262		CLAY(opal)	OLIVE-GRN	As above
203	263		CLAY(opal)	OLIVE-GRN	As above
204	264		CLAY(opal)	OLIVE-GRN	As above
205	265		CLAY(opal)	OLIVE-GRN	As above
206	266		CLAY(opal)	OLIVE-GRN	As above
207	267		CLAY(opal)	OLIVE-GRN	As above
208	268		CLAY(opal)	OLIVE-GRN	As above
209	269		CLAY(opal)	OLIVE-GRN	As above
210	270		CLAY(opal)	OLIVE-GRN	As above
211	271		CLAY(opal)	OLIVE-GRN	As above
212	272		CLAY(opal)	OLIVE-GRN	As above
213	273		CLAY(opal)	OLIVE-GRN	As above
214	274		CLAY(opal)	OLIVE-GRN	As above
215	275		CLAY(opal)	OLIVE-GRN	As above
216	276		CLAY(opal)	OLIVE-GRN	As above
217	277		CLAY(opal)	OLIVE-GRN	As above
218	278		CLAY(opal)	OLIVE-GRN	As above
219	279		CLAY(opal)	OLIVE-GRN	As above
220	280		CLAY(opal)	OLIVE-GRN	As above
221	281		CLAY(opal)	OLIVE-GRN	As above
222	282		CLAY(opal)	OLIVE-GRN	As above
223	283		CLAY(opal)	OLIVE-GRN	As above
224	284		CLAY(opal)	OLIVE-GRN	As above
225	285		CLAY(opal)	OLIVE-GRN	As above
226	286		CLAY(opal)	OLIVE-GRN	As above
227	287		CLAY(opal)	OLIVE-GRN	As above
228	288		CLAY(opal)	OLIVE-GRN	As above
229	289		CLAY(opal)	OLIVE-GRN	As above
230	290		CLAY(opal)	OLIVE-GRN	As above
231	291		CLAY(opal)	OLIVE-GRN	As above
232	292		CLAY(opal)	OLIVE-GRN	As above
233	293		CLAY(opal)	OLIVE-GRN	As above
234	294		CLAY(opal)	OLIVE-GRN	As above
235	295		CLAY(opal)	OLIVE-GRN	As above
236	296		CLAY(opal)	OLIVE-GRN	As above
237	297		CLAY(opal)	OLIVE-GRN	As above
238	298		CLAY(opal)	OLIVE-GRN	As above
239	299		CLAY(opal)	OLIVE-GRN	As above
240	300		CLAY(opal)	OLIVE-GRN	As above
241	301		CLAY(opal)	OLIVE-GRN	As above
242	302		CLAY(opal)	OLIVE-GRN	As above
243	303		CLAY(opal)	OLIVE-GRN	As above
244	304		CLAY(opal)	OLIVE-GRN	As above
245	305		CLAY(opal)	OLIVE-GRN	As above
246	306		CLAY(opal)	OLIVE-GRN	As above
247	307		CLAY(opal)	OLIVE-GRN	As above
248	308		CLAY(opal)	OLIVE-GRN	As above
249	309		CLAY(opal)	OLIVE-GRN	As above
250	310		CLAY(opal)	OLIVE-GRN	As above
251	311		CLAY(opal)	OLIVE-GRN	As above
252	312		CLAY(opal)	OLIVE-GRN	As above
253	313		CLAY(opal)	OLIVE-GRN	As above
254	314		CLAY(opal)	OLIVE-GRN	As above
255	315		CLAY(opal)	OLIVE-GRN	As above
256	316		CLAY(opal)	OLIVE-GRN	As above
257	317		CLAY(opal)	OLIVE-GRN	As above
258	318		CLAY(opal)	OLIVE-GRN	As above
259	319		CLAY(opal)	OLIVE-GRN	As above
260	320		CLAY(opal)	OLIVE-GRN	As above
261	321		CLAY(opal)	OLIVE-GRN	As above
262	322		CLAY(opal)	OLIVE-GRN	As above
263	323		CLAY(opal)	OLIVE-GRN	As above
264	324		CLAY(opal)	OLIVE-GRN	As above
265	325		CLAY(opal)	OLIVE-GRN	As above
266	326		CLAY(opal)	OLIVE-GRN	As above
267	327		CLAY(opal)	OLIVE-GRN	As above
268	328		CLAY(opal)	OLIVE-GRN	As above
269	329		CLAY(opal)	OLIVE-GRN	As above
270	330		CLAY(opal)	OLIVE-GRN	As above
271	331		CLAY(opal)	OLIVE-GRN	As above
272	332		CLAY(opal)	OLIVE-GRN	As above
273	333		CLAY(opal)	OLIVE-GRN	As above
274	334		CLAY(opal)	OLIVE-GRN	As above
275	335		CLAY(opal)	OLIVE-GRN	As above
276	336		CLAY(opal)	OLIVE-GRN	As above
277	337		CLAY(opal)	OLIVE-GRN	As above
278	338		CLAY(opal)	OLIVE-GRN	As above
279	339		CLAY(opal)	OLIVE-GRN	As above
280	340		CLAY(opal)	OLIVE-GRN	As above
281	341		CLAY(opal)	OLIVE-GRN	As above
282	342		CLAY(opal)	OLIVE-GRN	As above
283	343		CLAY(opal)	OLIVE-GRN	As above
284	344		CLAY(opal)	OLIVE-GRN	As above
285	345		CLAY(opal)	OLIVE-GRN	As above
286	346		CLAY(opal)	OLIVE-GRN	As above
287	347		CLAY(opal)	OLIVE-GRN	As above
288	348		CLAY(opal)	OLIVE-GRN	As above
289	349		CLAY(opal)	OLIVE-GRN	As above
290	350		CLAY(opal)	OLIVE-GRN	As above
291	351		CLAY(opal)	OLIVE-GRN	As above
292	352		CLAY(opal)	OLIVE-GRN	As above
293	353		CLAY(opal)	OLIVE-GRN	As above
294	354		CLAY(opal)	OLIVE-GRN	As above
295	355		CLAY(opal)	OLIVE-GRN	As above
296					

AFFEND I X B

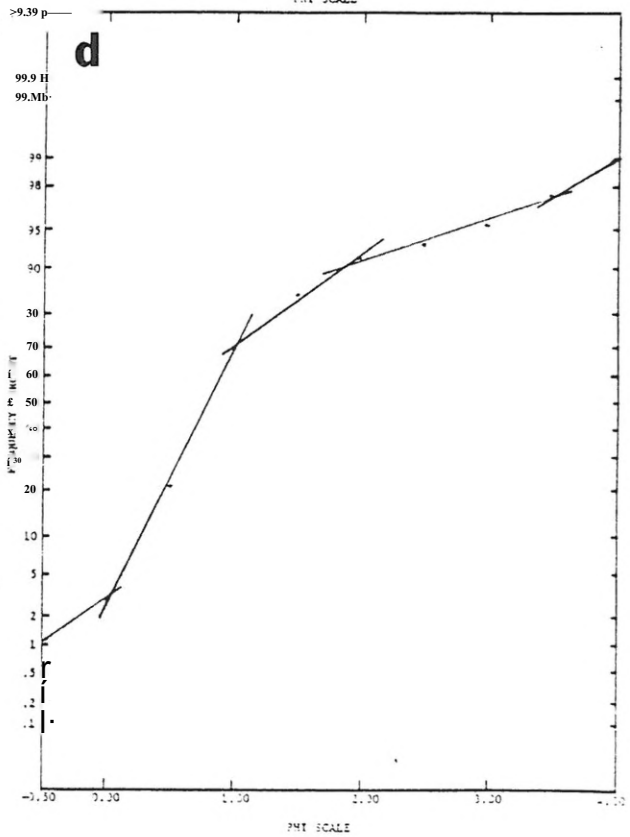
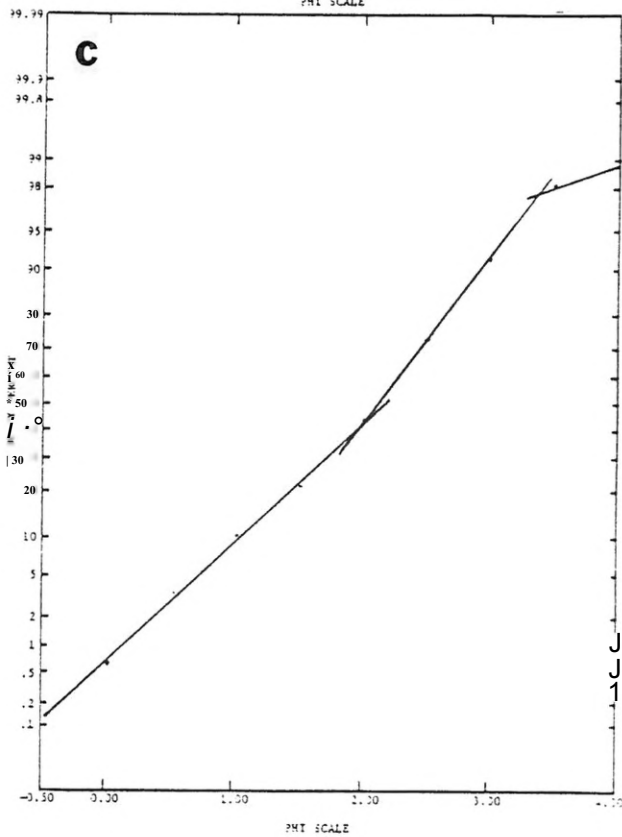
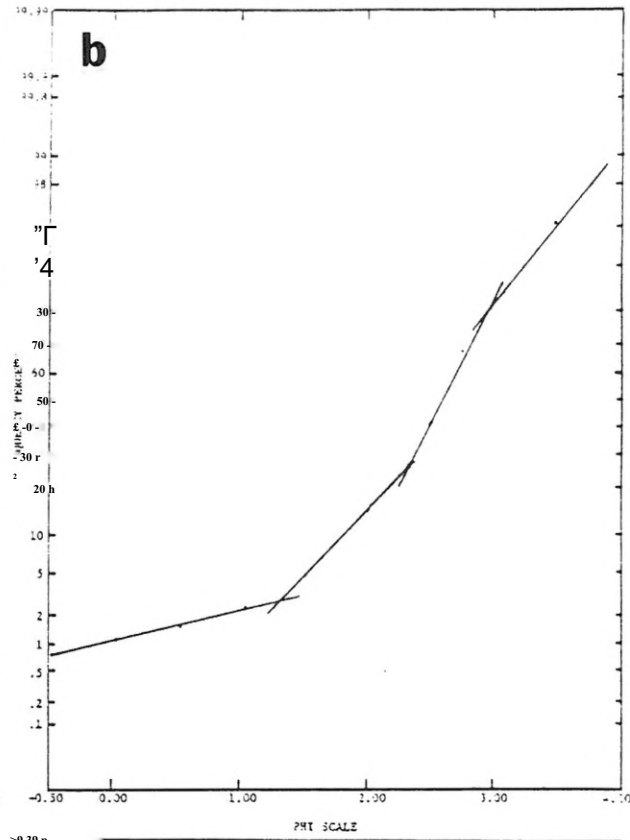
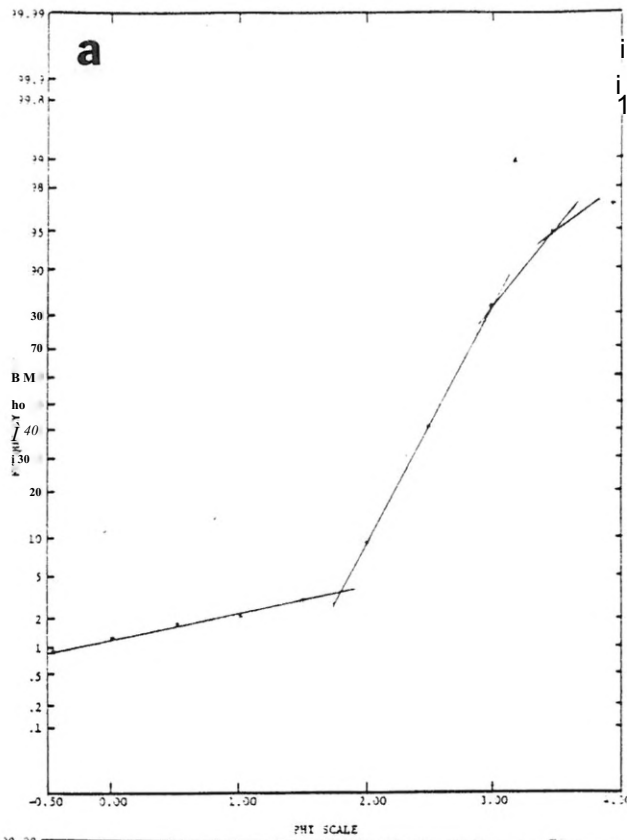
FRODABILITIES ÜF SAND-SIZE POPULATIONS



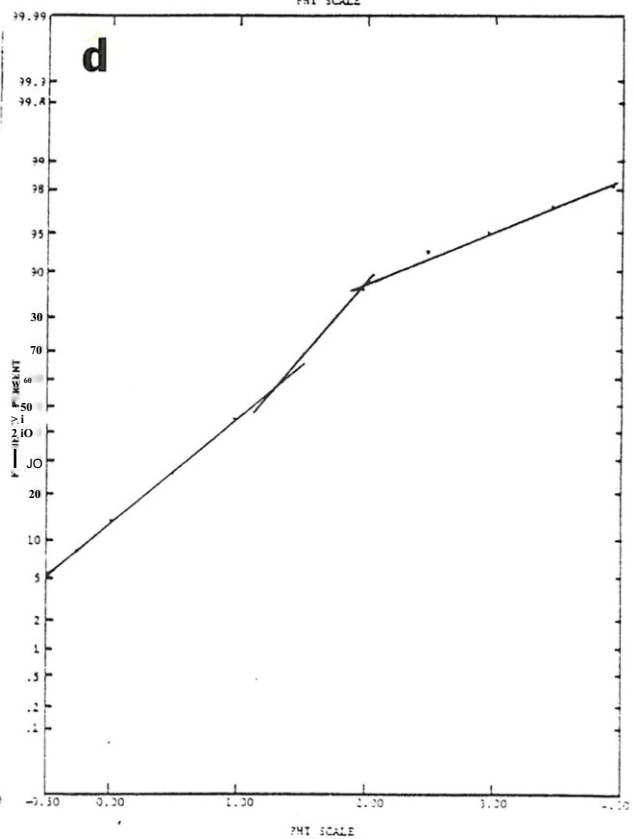
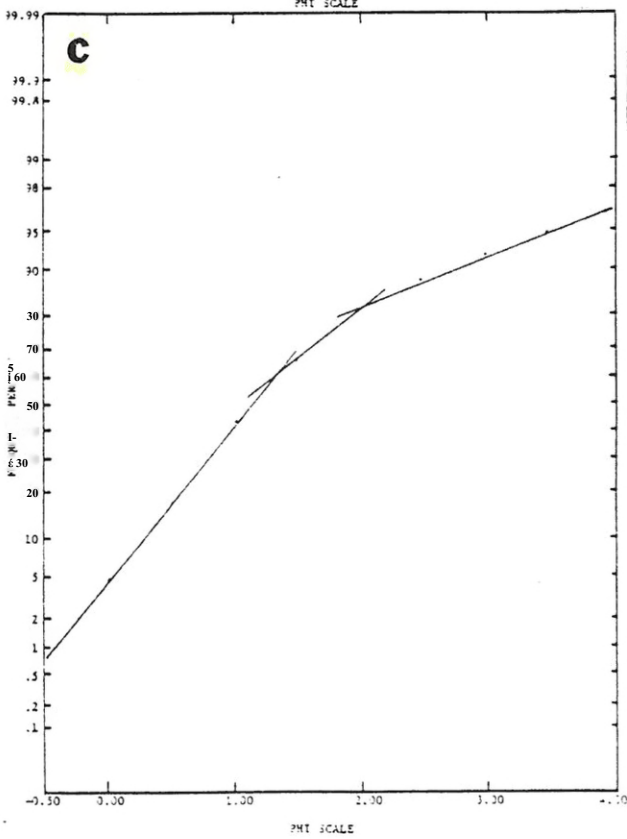
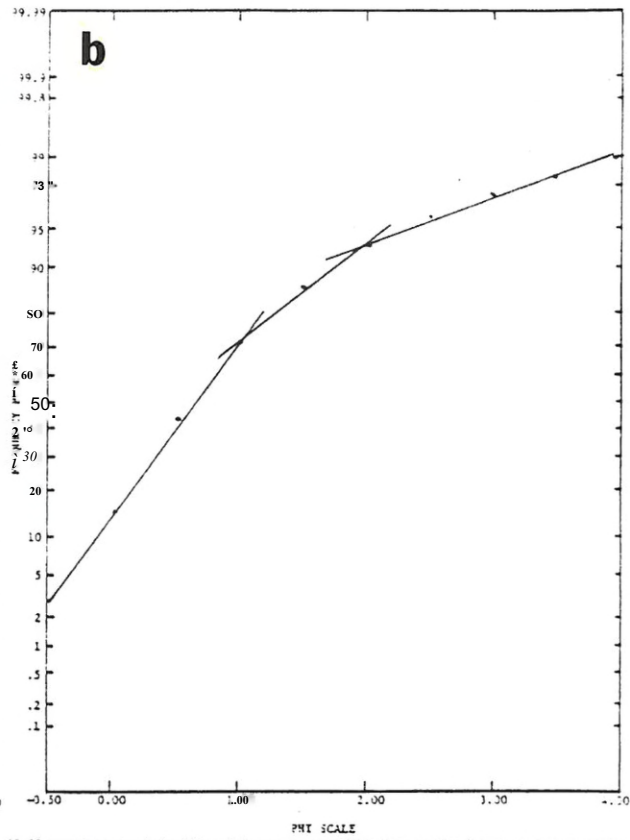
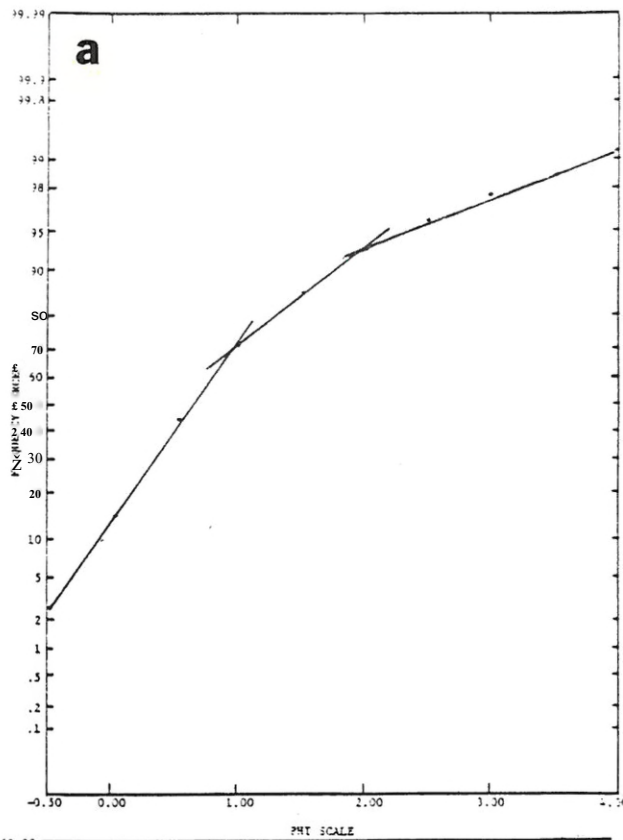
Cumulative probabilities of sand-size populations of the Upper Meridian Formation.
 Section 57 (Mt. Barton): a, b, c
 Section 55 (l 20): d



Curamulative probabilities of sand-size populations of the Upper Meridian Formation.
 Section 45 (Valley Road): a, b
 Section 50 (Savoy Road): c, d



Cummulative probabilities of sand-size populations of the Upper Meridian Formation (section 51 Highway 111 a, b, c) and of the Lower Tallahatta Formation (section 55? 120; d).

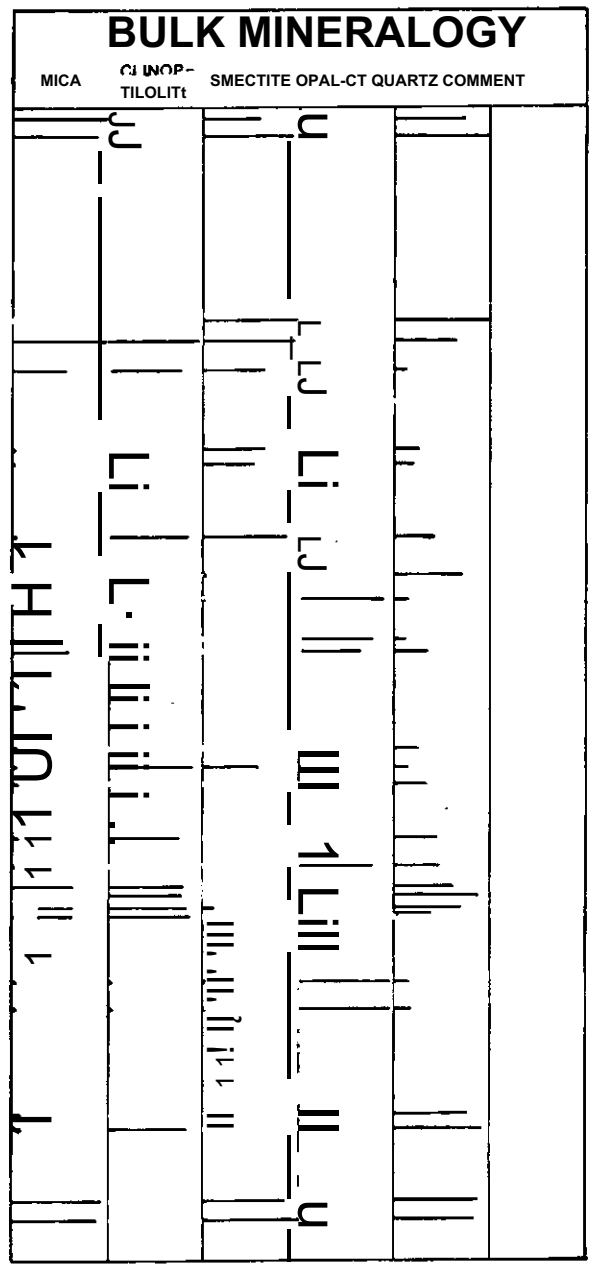
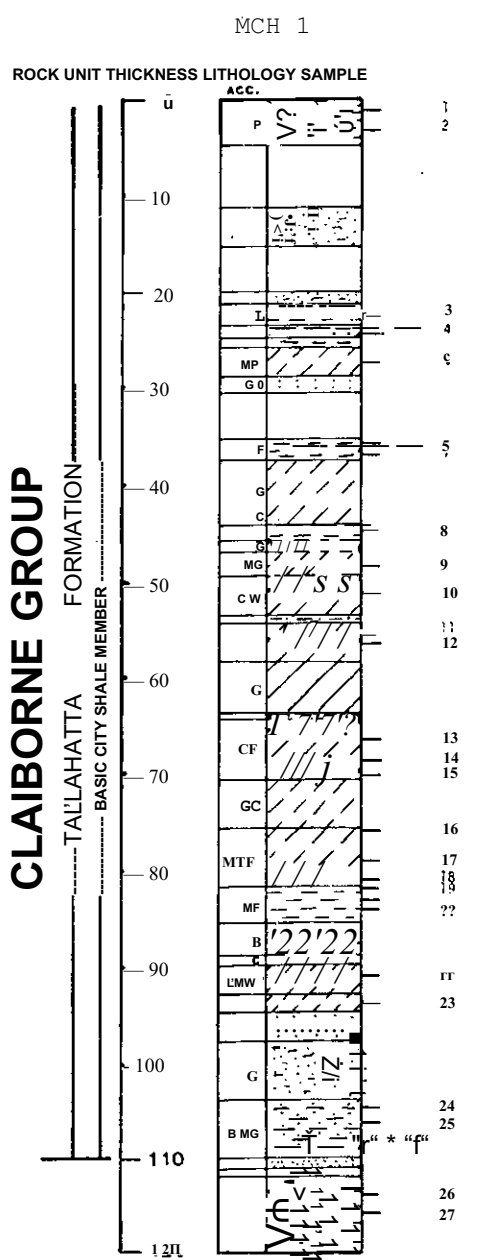


Cummulative probabilities of sand-size populations of the Lower Tallahatta Formation (section 49; Basic City: a, b) and of the Winona Formation (section 45; Valley Road: c, d)

APPENDIX C

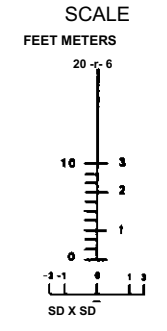
MINERAL DULK COMPOSITION

CLAIBORNE GROUP
 TALLAHATTA FORMATION
 BASIC CITY SHALE MEMBER



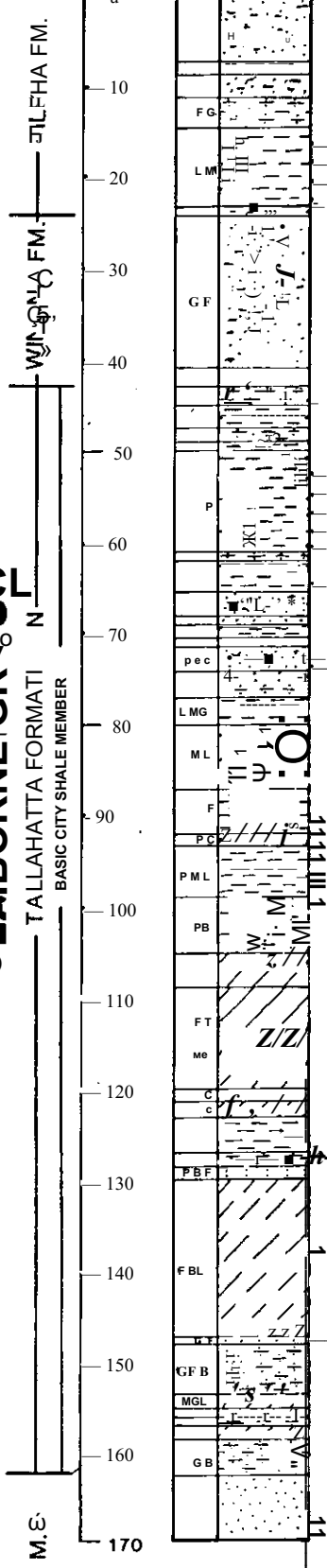
- EXPLANATION
- SANDSTONE
 - SAND/WACKE
 - SAND/ARENITE
 - SILT/STONE
 - MUD/STONE
 - CLAYSTONE
 - CLAYSTONE/CLAY
 - CLAY
 - MISSING/COVERED

- ACCESSORY
- G GLAUCONITIC
 - M MICACEOUS
 - F FOSSILIFEROUS
 - P PLANT FRAGMENT
 - B BIOTURBATED
 - T TRACE FOSSILS
 - W DEWATERING VEIN
 - X CROSS LAMINATIONS
 - L LAMINATED
 - C CHERTY
- COMMENT
- FD FELDSPAR
 - TS THIN SECTION
 - GM GRAIN MOUNT
 - PH PHOTO



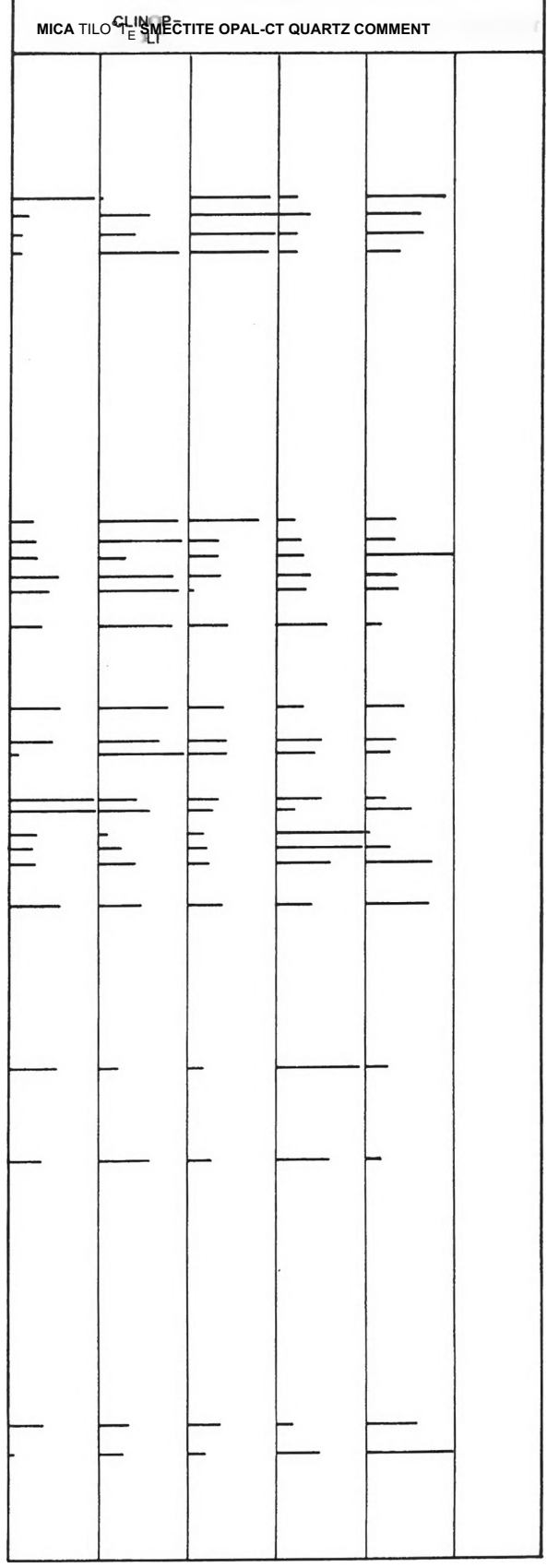
LAIBORNE GR₂U₀

ROCK UNIT THICKNESS LITHOLOGY SAMPLE ACC.



BICH 2

BULK MINERALOGY



EXPLANATION

- SANDSTONE
- SAND/WACKE
- SANDIARENITE
- SILT/STONE
- MUD/STONE
- CLAYSTONE
- CLAYSTONE/CLAY
- CLAY
- MISSING/COVERED

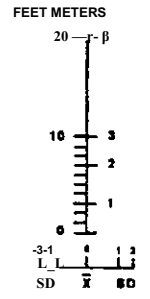
ACCESSORY

- G GLAUCONITIC
- M MICACEOUS
- f FOSSILIFEROUS
- P PLANT FRAGMENTS
- o ROTUNGATED
- T TRACE FOSSILS
- W DEWATERING VEIN
- X CROSS LAMINATIONS
- L LAMINATED
- C CERTY

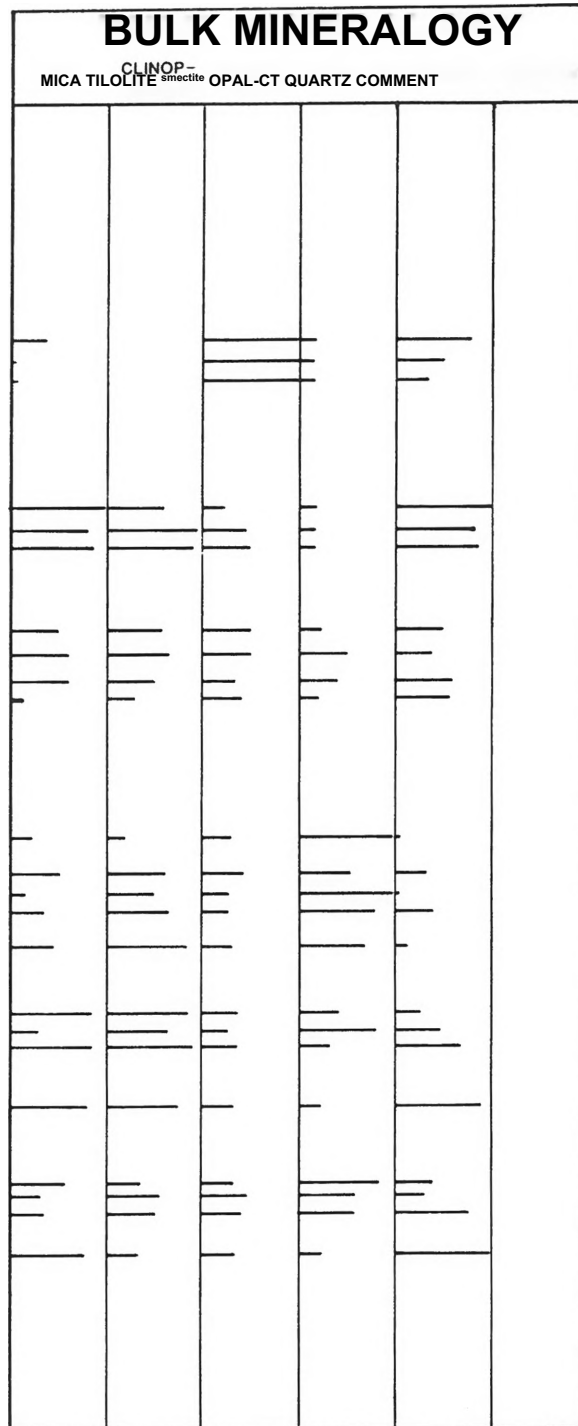
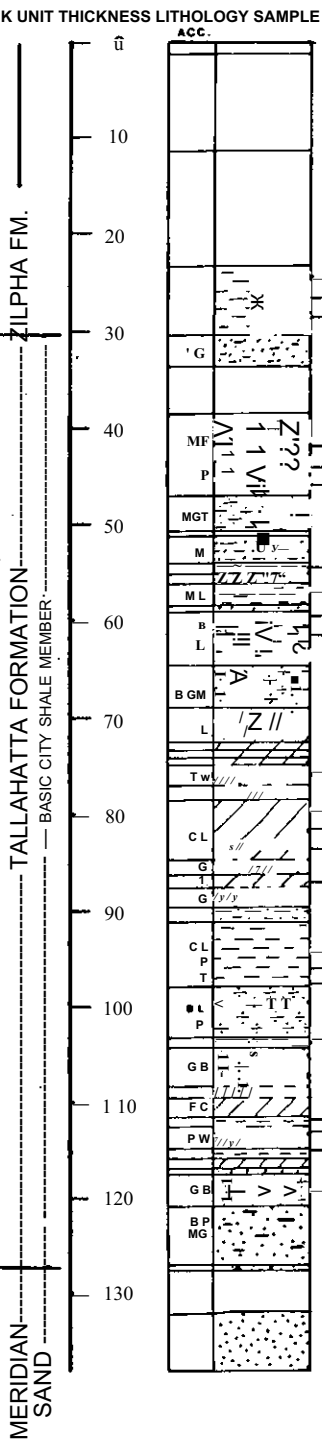
COMMENT

- FD FELDSPAR
- TS TH SECTION
- GM GRAIN MOUNT
- PH PHOTO

SCALE



CLAIBORNE GROUP



EXPLANATION

- SANDSTONE
- SAND/WACKE
- SAND/ARENITE
- SILT/STONE
- MUD/STONE
- CLAYSTONE
- CLAYSTONE/CLAY
- CLAY
- MISSING/COVERED

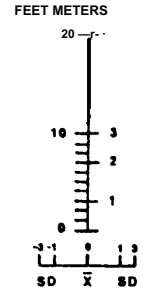
ACCESSORY

- G GLAUCOMITIC
- M MICACEOUS
- F PO & SI U FERUGS
- P PLANT FRAGMENT
- D BIOTWATED
- T TRACE FOSSILS
- W DE WATERING VEIN
- X CROSS LAMINATIONS
- L LAMINATED
- C CHENTY

COMMENT

- FD FELDSPAR
- TS THIN SECTION
- GM GRAIN MOUNT
- PH PHOTO

SCALE



CLAIBORNE CO. GA.

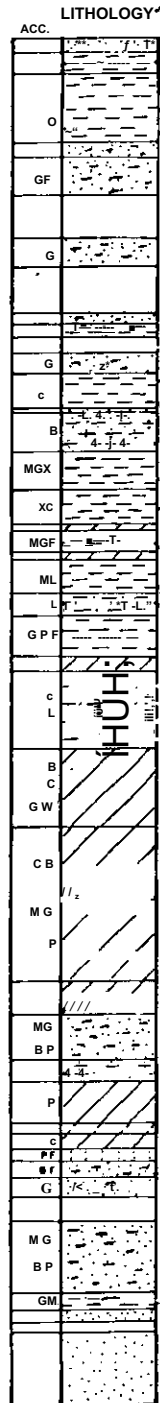
ROCK UNIT THICKNESS

WINONA F.M. ZILPHA

LLAHATTA FORMATION
BASIC CITY SHALE MEMBER

TA
MERIDIAN SAND

MCE 5



SAMPLE

99
100
101
102

103
104

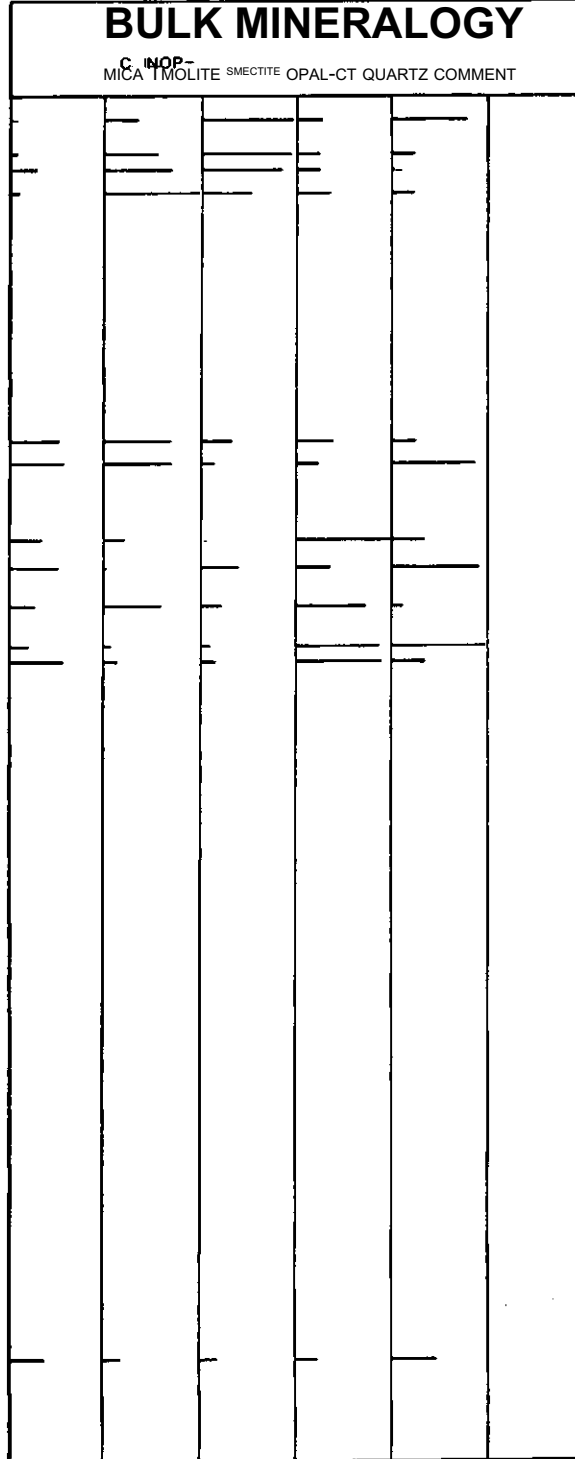
105
106

107
108
109

110

BULK MINERALOGY

C. INOP-
MICA T MOLITE SMECTITE OPAL-CT QUARTZ COMMENT



EXPLANATION

- SANDSTONE
- SAND/WACKE
- SANDIARENITE
- SILT/STONE
- MUD/STONE
- CLAYSTONE
- CLAYSTONE/CLAY
- CLAY
- MISSING/COVERED

ACCESSORY

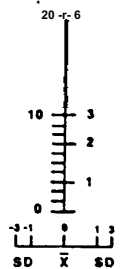
- G GLAUCONITIC
- M MICACEOUS
- F FOSSILIFEROUS
- P PLANT FRAGMENT
- o ROTURATED
- T TRACE FOSSILS
- W DEWATERING VEIN
- X CROSS LAMINATIONS
- L LAMINATED
- C CHERTY

COMMENT

- FD FELDSPAR
- TS THIN SECTION
- GM GRAIN MOUNT
- PH PHOTO

SCALE

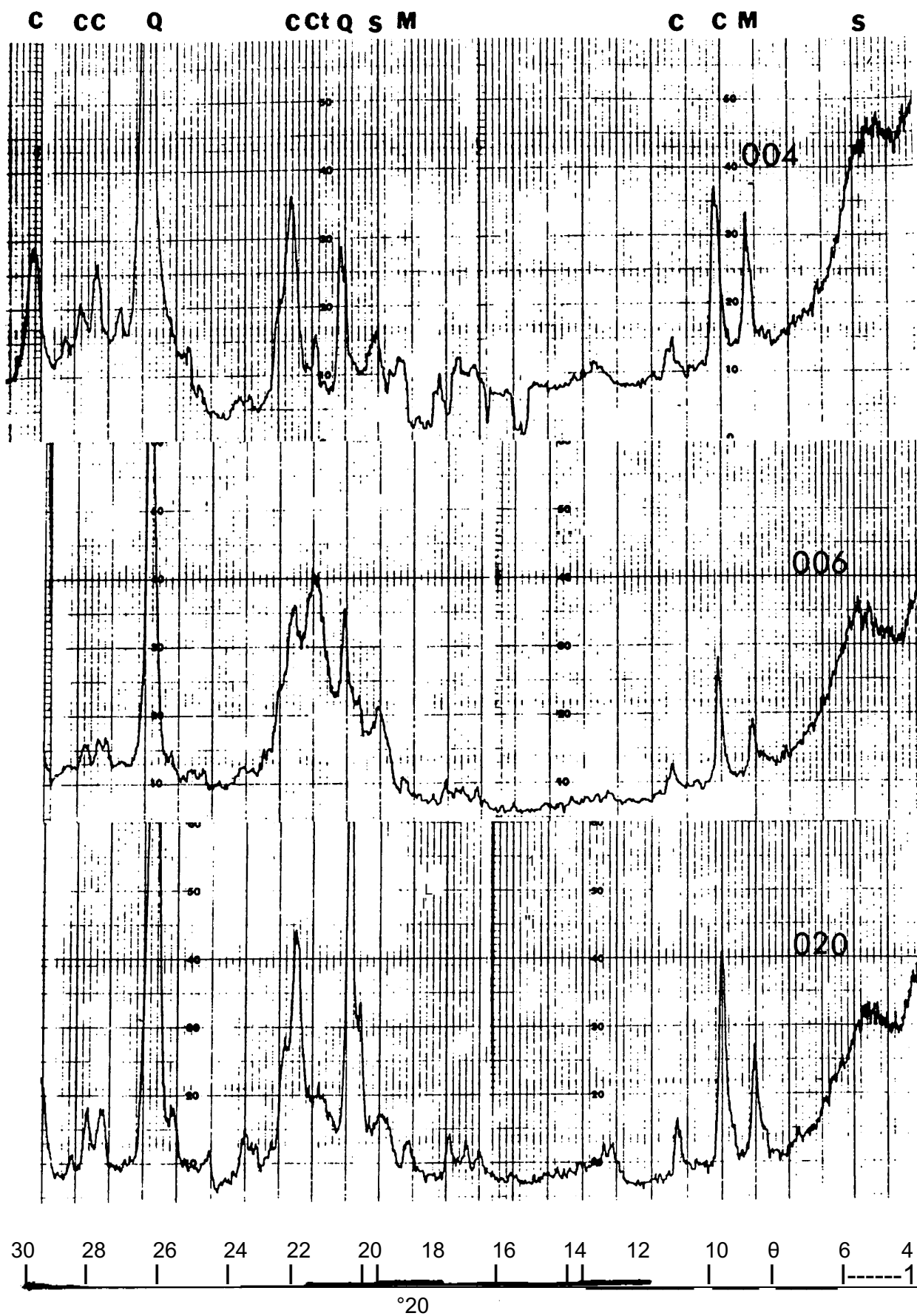
FEET METERS



APPENDIX D

X-RAY DIFFRACTOGRAMS OF CORE SAMPLI ES

MCH 1

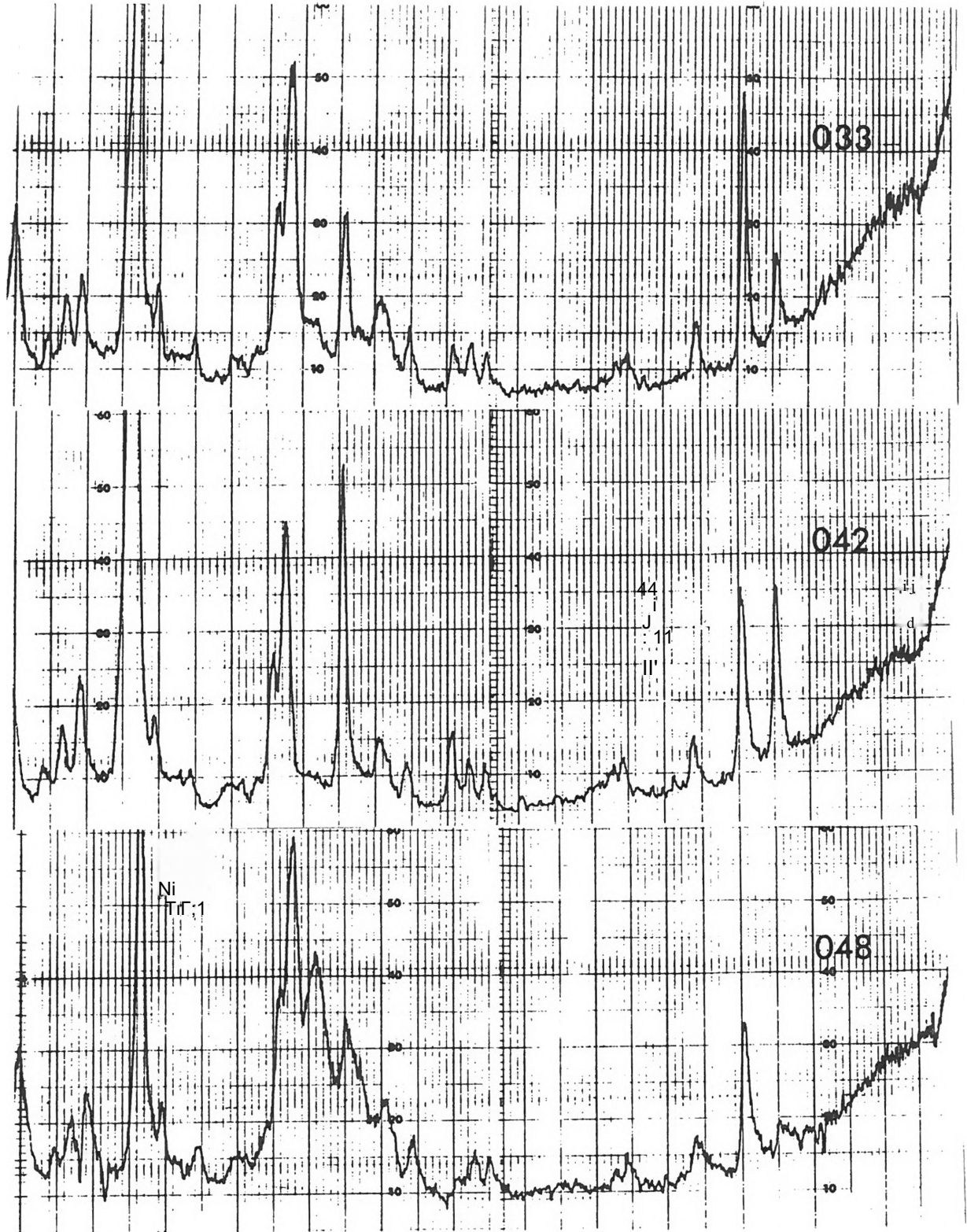


MCH 2

C CC Q

eet Q S M

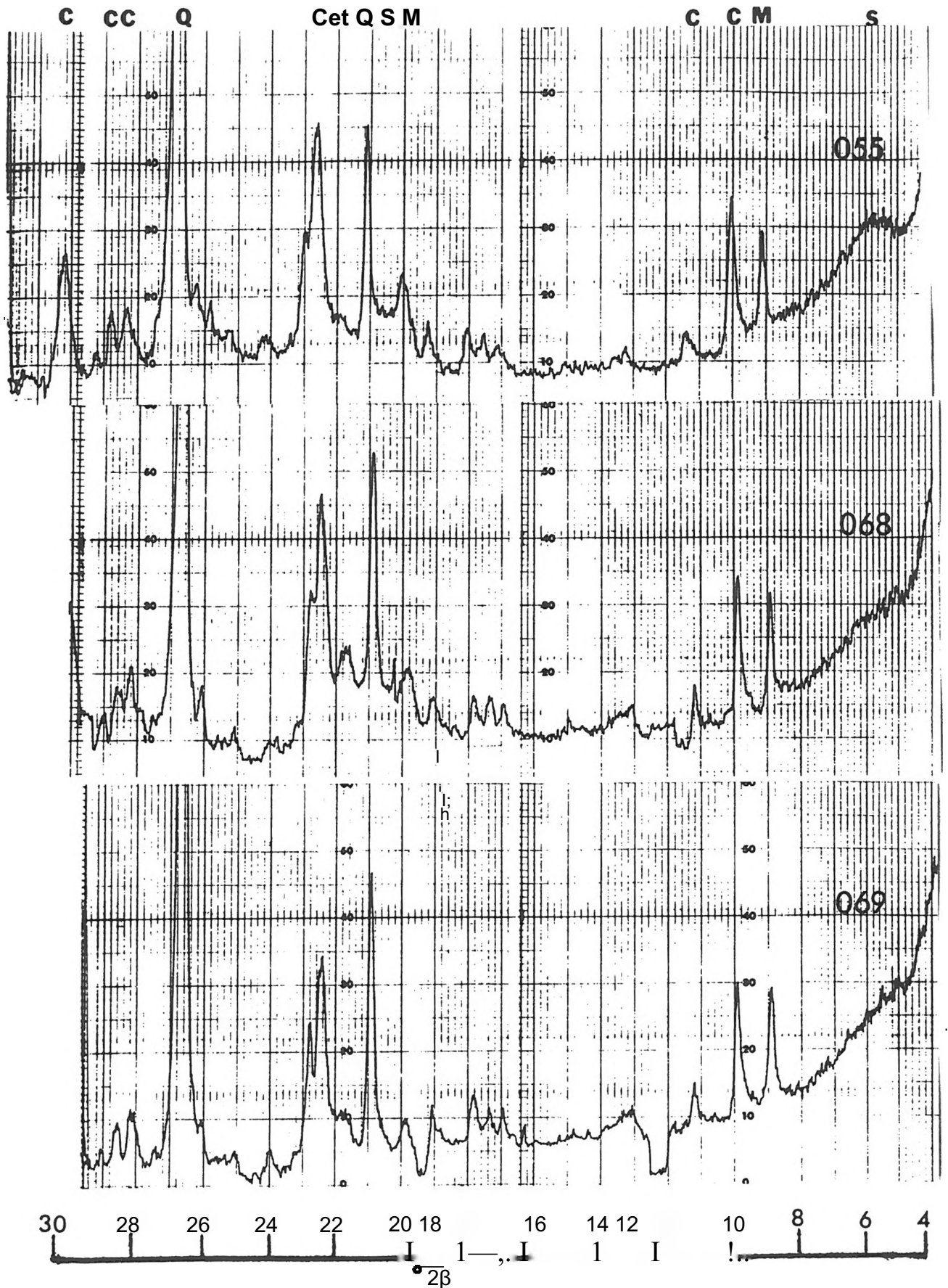
CCM s



30 28 26 24 22 20 18 16 14 12 10 6 4

2θ

MCH 3



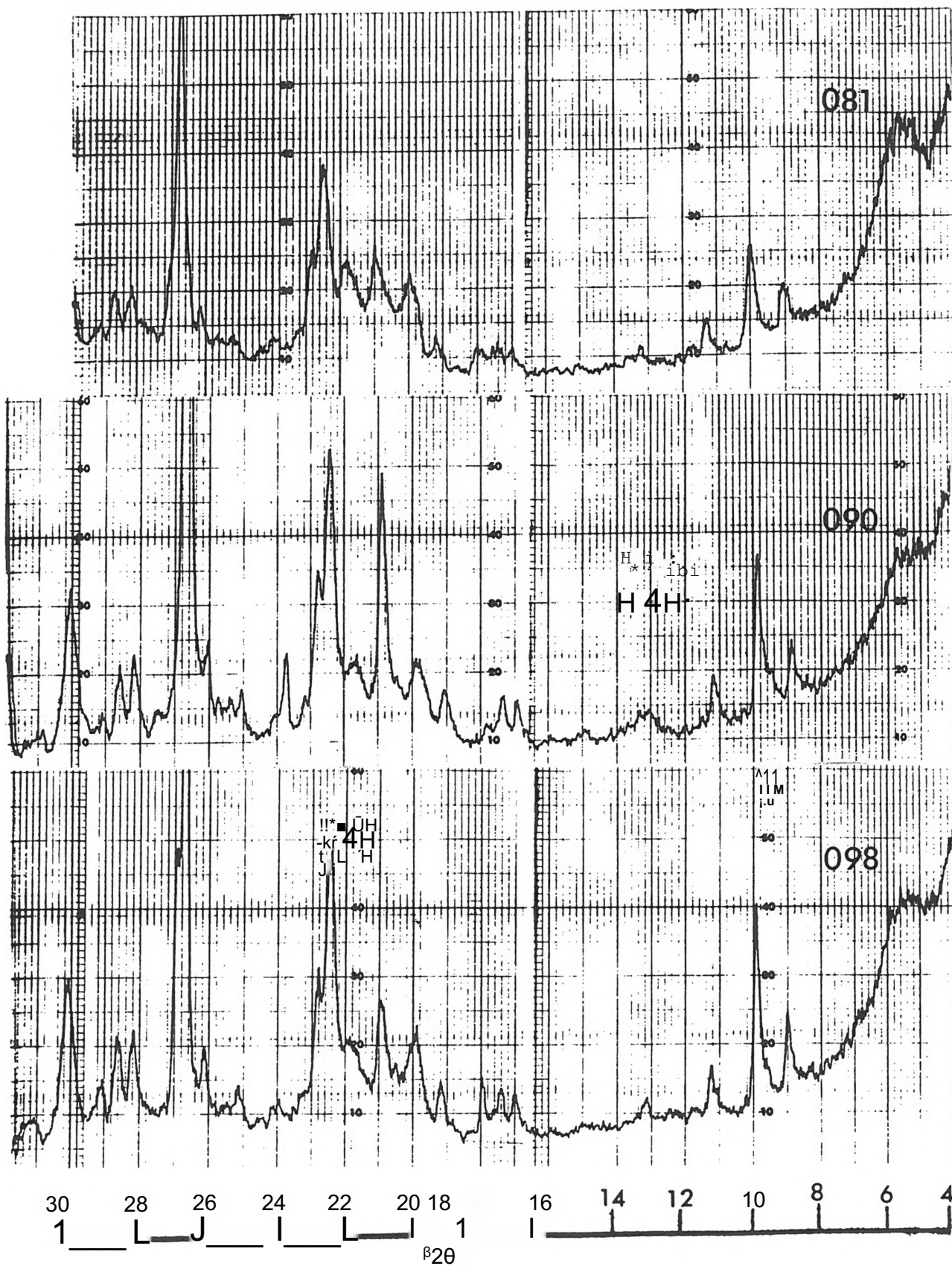
MCH 4

C CC Q

cct Q s M

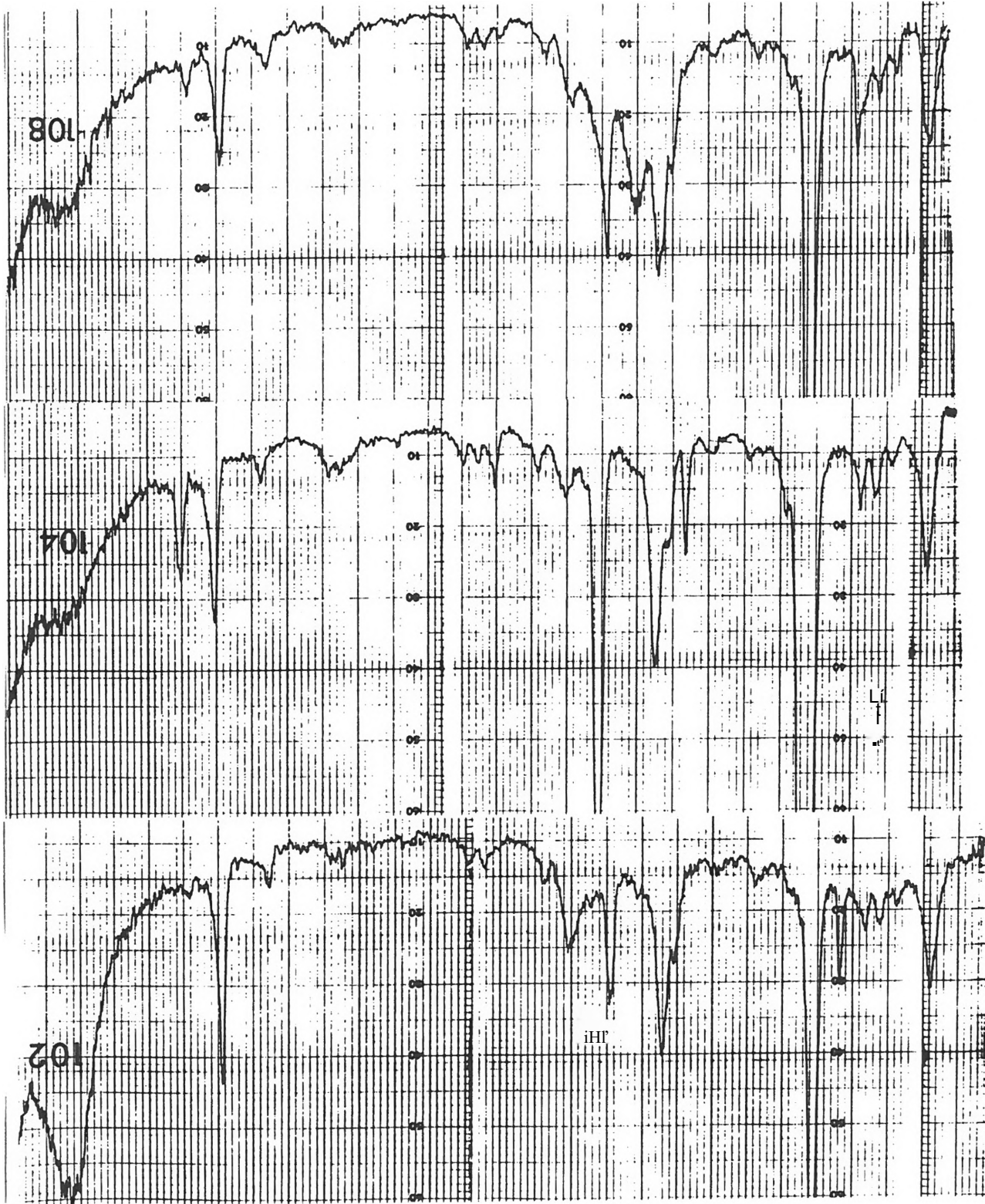
C CM

S



θz_0

I I П I I 7 П I I I I
r 9 8 01 M 91 81 02 ZZ, VZ 92 82 OC



S HOI I

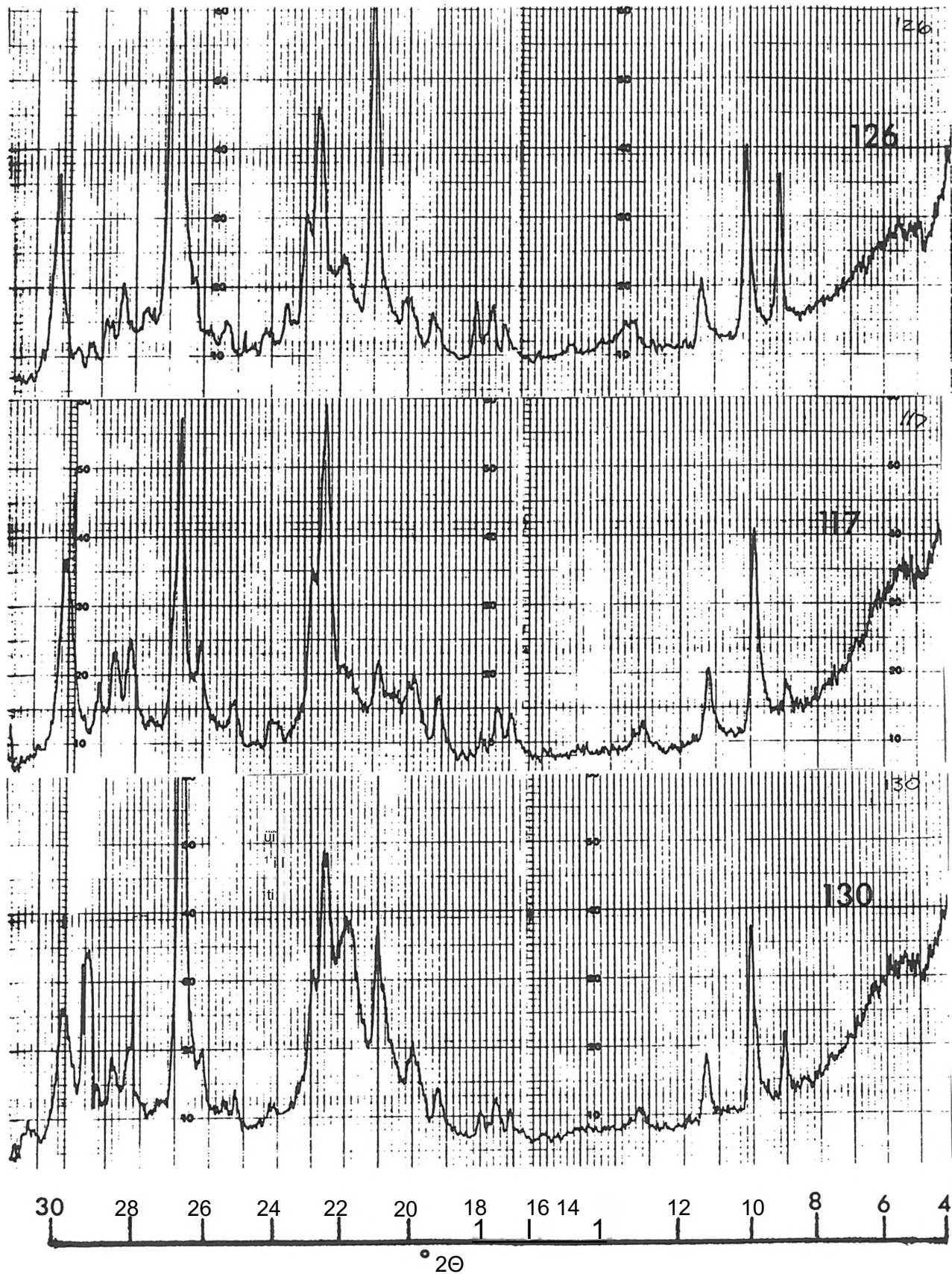
MCH 6

C CC Q

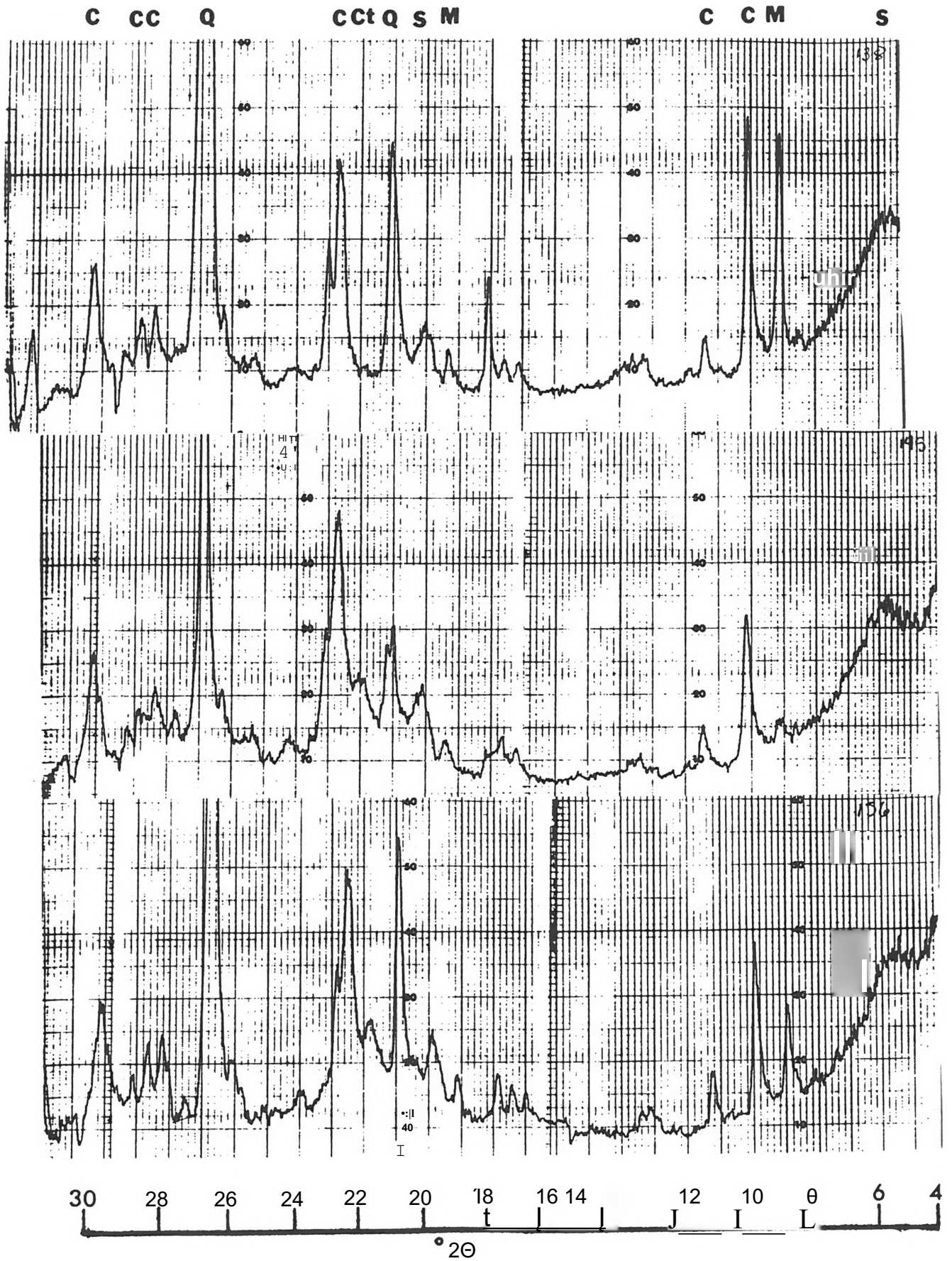
C C t Q s M

C C M

S



MCH 7



sr	EЭТ	143	jastel	6348	ASSUBA ВВМШЯ
1-13					ВШЫ Ш*o » fwt. MI m- M 40 Cwt
			HUMO		
			14Я («МК»)	ММ	teKirMI^il az(my).», Af
			U0 («МК»)	SUW	ВММ, ОмНН U» B- Af
1М			CUI	3m»Uw	01, Of, >, Ai, >1, OM
40			уома	IU	Bart: w«lw, «к«o<i Af, Olf, (Kve)
41-42			KUwA		
43			UXOtoate)	Mite	ВМУ. wboil Ai. U. B. Г. 00
44			RUMO		
45			ШВ (ММЙ)	Uto	Om«, B<M At, At, M
46			ОШ	^H	01, 01, Ai, Af, Mte «T
47			А С У Т (И М)	Olvw an	01, 01, At, BI, B1, M, A2
48			JO	Olvw gw	01, 01, If, At, At, Olf, OU
49			AZWOGAS	»w	01, 901 At, At, 14, >1
50			С С	IUWФi	И, 1, «i», *1, «, w, M
51			ОШ	»lw Y	M, 01, A1, off
52			С Л А У (о р а 1)	Olvw gw	01, 01, A1, 915
53			сиягав	SUw^MB	pt, 0t, 015, At, Oto, A4, M
54			С Л А У (о р а 1)	lauw cm	01, 01, 915, M, 04, M» At, Ai
55			ю	>TP	M, 01, 14, At, At, oto
56			ini	»w	И, as, Ai, 010
57			Я4Я0ЯВ	IMTR	BI, 01, 04, Ai, AO, M, »f, M, M, M, ote, oцmmb), oio
58			С Л А У (о р а 1)	Olvw gw	01, 01, 915, A1, A1, A1, 31
59			С Л А У (о р а 1)	nXw^n	te aheve
60			SUMI		
61			С Л А У (о р а 1)	IUw-Bi	u otaw
62			С Л А У (о р а 1)	Mчro	M-01, 05, At, Ai, >1, oto
63			Ш С Т	»w	Noif(i>iAh4) a
64			С U Z (e p a)	»w	N, 01, Olf, >1, Ai, AO, M
65			GlaXmz	Irmal	я, ci, At, u, an, ei, au, m
66			suitou)	niwo	Я, 01, Ai, AO, Otf
67			«ХИХВОЯК»	»w gw	M, at, at, k
68			Ш И М М	Olvw gw	01, 01, 915, A1, A1, A1, A1, A1
69			UBtoete)	B i Or > и	00M, MMOOI At, AO, It
70			У Ш	USMDL	»w
71			»w	niw B	n, 05, AS, At, AO, »1, M, It
72			UD(iraU4'	WC	OarU.ttefHi At, Г
73			SUMI		